AD

THE PREPARATION AND CHARACTERISATION OF OXYNITRIDE GLASSES AND GLASS-CERAMICS

Final Technical Report

by

Dr Stuart Hampshire

July, 1989

United States Army

EUROPEAN RESEARCH OFFICE OF THE U.S. ARMY

London, England

CONTRACT NUMBER DAJA45 - 85 - C - 0050

UNIVERSITY OF LIMERICK
(formerly NIHE, Limerick)
Ireland

Approved for Public Release; distribution unlimited

REPORT DOCUMENTATION PAGE

1a REPORT SECURITY CLASSIFICATION Unclassified	1b. RESTRICTIVE MARKINGS
2a. SECURITY CLASSIFICATION AUTHORITY	3. DISTRIBUTION / AVAILABILITY OF REPORT Approved for public release, distribution unlimited
2b. DECLASSIFICATION / DOWNGRADING SCHEDULE	
4. PERFORMING ORGANIZATION REPORT NUMBER(S)	5. MONITORING ORGANIZATION REPORT NUMBER(S) R&D 4881-MS-01
6a NAME OF PERFORMING ORGANIZATION The National Institute for Higher Education 6b OFFICE SYMBOL (If applicable)	7a NAME OF MONITORING ORGANIZATION USARDSG-UK
6c ADDRESS (City, State, and ZIP Code) Pl ssey Technological Park Limerick Ireland	7b ADDRESS (City, State, and ZIP Code) Box 65 FPO NY 09510-1500
8a. NAME OF FUNDING / SPONSORING ORGANIZATION USARDSG-UK 8b. OFFICE SYMBOL (If applicable)	9 PROCUREMENT INSTRUMENT IDENTIFICATION NUMBER DAJA45-85-C-0050
8c. ADDRESS (City, State, and ZIP Code) Box 65 FPO NY 09510-1500	10 SOURCE OF FUNDING NUMBERS PROGRAM ELEMENT NO: 61103A; PROJECT NO.: 1L161103BH57; TASK NO: 04; WORK UNIT ACCESSION NO: AR

11 TITLE (Include Security Classification)
(U) THE PREPARATION AND CHARACTERIZATION OF OXYNITRIDE GLASSES AND GLASS CERAMICS

12 PERSONAL AUTHOR(S)
Dr. S. Hampshire

13a. TYPE OF REPORT	13b TIME COVERED	14. DATE OF REPORT (Year, Month, Day)	15 PAGE COUNT
Final	FROM 25 Nov 85 TO 25 Nov 88		

16. SUPPLEMENTARY NOTATION

17 COSATI CODES			18 SUBJECT TERMS (Continue on reverse if necessary and identify by block number)
FIELD	GROUP	SUB-GROUP	

19 ABSTRACT (Continue on reverse if necessary and identify by block number)

The objective was to study the effect on properties (such as microhardness, glass transition, crystallisation temperature, viscosity, etc.) of replacing oxygen by nitrogen in sialon-based glasses containing rare-earth cations and to study the formation of glass-ceramics by controlled crystallisation of these oxynitride glasses and to assess the effects of this on properties.

Glasses were prepared by melting appropriate oxides and nitrides in boron nitride lined crucibles, melting at 1700°C under nitrogen and casting into preheated graphite moulds followed by annealing. Characterisation of the glasses was carried out by differential thermal analysis (DTA) to ascertain the glass transition and crystallisation temperatures and standard techniques used for microhardness and viscosity. Nitrogen increases the glass transition and crystallisation temperatures and standard techniques used for microhardness and viscosity. Nitrogen increases

20 DISTRIBUTION / AVAILABILITY OF ABSTRACT	21 ABSTRACT SECURITY CLASSIFICATION	
☒ UNCLASSIFIED UNLIMITED ☐ SAME AS RPT ☐ DTIC USERS	Unclassified	
22a NAME OF RESPONSIBLE INDIVIDUAL Dr. Wilbur C. Simmons	22b TELEPHONE (Include Area Code) 01-409-4423	22c OFFICE SYMBOL AMXSN-MC

(19) the glass transition, microhardness and viscosity for constant cation ratio glasses and also inhibits crystallisation. From DTA, suitable heat-treatment schedules were designed to produce fine-grain glass-ceramics. Optimisation of these heat treatments was by measuring the changes (increases) in microhardness.

Fully amorphous glasses can be prepared easily in large batches ($\sim$ 100g) in many M-Si-Al-O-N systems. Work concentrated on Nd- and Y-sialon glasses which undergo homogeneous nucleation at Tg+50 (^{o}C) followed by crystal growth at Tc-40 (^{o}C) each for 2.5 hours.

THE PREPARATION AND CHARACTERIZATION OF

OXYNITRIDE GLASSES AND GLASS-CERAMICS

Abstract

The objective was to study the effect on properties (such as microhardness, glass transition, crystallization temperature, viscosity, etc.) of replacing oxygen by nitrogen in sialon-based glasses containing rare-earth cations and to study the formation of glass-ceramics by controlled crystallization of these oxynitride glasses and to assess the effects of this on properties.

Glasses were prepared by melting appropriate oxides and nitrides in boron nitride lined crucibles, melting at 1700°C under nitrogen and casting into preheated graphite moulds followed by annealing. Characterization of the glasses was carried out by differential thermal analysis (DTA) to ascertain the glass transition and crystallization temperatures and standard techniques used for microhardness and viscosity. Nitrogen increases the glass transition, microhardness and viscosity for constant cation ratio glasses and also inhibits crystallization. From DTA, suitable heat-treatment schedules were designed to produce fine-grain glass-ceramics. Optimization of these heat treatments was by measuring the changes (increases) in microhardness.

Fully amorphous glasses can be prepared easily in large batches (≈ 100g) in many M-Si-Al-O-N systems. Work concentrated on Nd- and Y-sialon glasses which undergo homogeneous nucleation at Tg+50 (°C) followed by crystal growth at Tc-40 (°C) each for 2.5 hours.

Keywords

Glass, oxynitride-, sialon-
Glass-ceramics, oxynitride-, sialon-,

CONTENTS

List of Figures

List of Tables

THE PREPARATION AND CHARACTERIZATION OF OXYNITRIDE GLASSES AND GLASS-CERAMICS

Dr Stuart Hampshire

1. INTRODUCTION

The ease of shaping glasses, the possibility of producing glass-ceramics containing refractory oxynitride crystalline phases and the occurrence of oxynitride glasses as grain-boundary phases in silicon nitride based ceramics has given the impetus for a number of investigations (1 - 10) on oxynitride glass formation and properties. Originally, small concentrations of nitrogen in oxide glasses were reported to increase their softening temperature, viscosity and resistance to devitrification (11, 12).

Crystallization of selected oxynitride glasses has been investigated (6,8,9,13), principally to complement more extensive studies of phase equilibria in M-Si-Al-O-N systems and the effects of vitreous phases on high-temperature mechanical properties of silicon nitride based ceramics. So far, no study of the glass-ceramic process as applied to oxynitride glasses has been reported though a U.S. patent (14) describes a series of alumino-silicate glass compositions containing nitrogen that may have potential as glass-ceramics.

2. LITERATURE REVIEW

2.1 Solubility of nitrogen in glasses

Mulfinger (15,16) was one of the first investigators to study the solubility of nitrogen in glasses and found that the physical solubility of nitrogen in glasses was very low by bubbling nitrogen gas through the glass melt. However by bubbling ammonia gas through the glass melt for five hours at a temperature of 1400°C, the chemical solubility of nitrogen in the melt reached a value 10^3 times higher than that of the physical solubility. Using this method, 0.33w/o nitrogen was introduced into soda-lime-silica glass. Mulfinger suggested that the substitution of nitrogen for oxygen must lead to a higher than average coordination of non-metal atoms and that increased crosslinking should produce a more rigid glass network as follows:

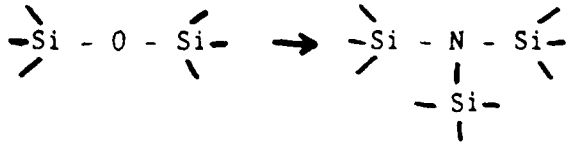

Elmer and Nordberg (11) observed that devitrification of certain glasses could be induced electrolytically. They showed that incorporation of nitrogen into these glasses inhibited the electrolytically induced devitrification which they attributed to increased viscosity, due to the presence of (=NH) and (=N-) groups in the glass structure and this was one of the first observations of an improvement in some physical property of a glass resulting from the incorporation of nitrogen into the glass structure. In this case, ammonia was again used as the nitriding agent and nitrogen contents of the order of 3w/o, or ten times that reported by Mulfinger, were obtained.

Davies and Meherali (17) concluded from their investigations that the solubility of nitrogen in glass melts was chemical rather than physical and they found that severe reducing conditions had to be imposed in order to dissolve significant amounts of nitrogen in the glass melts. They discovered that the solubility of nitrogen increased with increasing basicity, indicating that bridging rather than non-bridging oxygen atoms were involved in the dissolution reaction.

Dancy and Janssen (18) investigated the solubility of nitrogen in $CaO-SiO_2-Al_2O_3$ slags. They compared physical and chemical methods of dissolving nitrogen in these melts and found that under one atmosphere of nitrogen an equilibrium solubility of 0.25 to 2.5w/o nitrogen was achieved after 24hrs. By contrast when Si_3N_4 was added to the melt, again under an atmosphere of nitrogen, nitrogen incorporation was very rapid and reached significantly higher levels (4w/o). They suggested that most oxide melts would not be significantly reducing to dissolve N_2 or NH_3 to any great extent. Subsequently nitrogen additions to melts were mainly in the form of Si_3N_4 or AlN.

2.2 Si-Al-O-N Glasses

It is now well established (19-22) that both Si_3N_4 and β'-sialons require an oxide additive for liquid phase densification. The silicate liquid formed dissolves some nitrogen and cools to form a grain boundary glass, sometimes in conjunction with other oxynitride or sialon phases.

Jack (1) observed the close similarity between the building units for the structure of silicate glasses (SiO_4 tetrahedra) and those in silicon nitride (SiN_4 tetrahedra) and also the similarity between the lengths of Si-N, Si-O and Al-O bonds, and proposed that nitrogen could be incorporated in the network of silicate and alumino-silicate glasses.

Jack (2) reported preparing oxynitride glasses in the following

systems, Si_3N_4-Al_2O_3-SiO_2, Si_3N_4-MgO-SiO_2, and AlN-Y_2O_3-SiO_2, with nitrogen levels up to 10%. Changes in physical properties due to incorporation of nitrogen were not reported at this point. Subsequently, considerable investigation (6-10) has been carried out on glass formation and glass properties in a wide range of M-Si-O-N and M-Si-Al-O-N systems where M=Y, Mg, Ca, Al or Nd and the effects of increasing nitrogen content on properties of these glasses have also been reported.

Both Shillito et al (3) and Loehman (4,5) were among the first to report correlations between amounts of nitrogen incorporated into oxynitride glasses and changes in their physical properties. Shillito et al, reported a linear increase in the knoop hardness of a Y-Si-Al-O-N glass as the nitrogen content increased. Loehman produced more detailed results of changes in physical properties due to incorporation of nitrogen when he prepared glasses in the same system with up to 7a/o nitrogen. He reported that glass transition temperature (Tg), microhardness and relative fracture toughness, all increased with increasing nitrogen content, while the thermal expansion coefficient decreased. IR spectroscopic analysis carried out by Loehman indicated that the incorporated nitrogen became chemically bonded to silicon in the glass network, and by substitution for oxygen, produces a more tightly and highly linked structure. Loehman reported that typical glass forming systems for oxynitride glasses were the M-Si-O-N and M-Si-Al-O-N systems where M=Ca, Li, Mg or Y, and that glasses with up to 10a/o nitrogen had been prepared from these compositions. However, while these results did indicate improvements in properties of glasses related to incorporation of nitrogen, these property changes could not be attributed solely to the incorporation of nitrogen, since it is well known that viscosities of glasses may increase or decrease depending on field strength, polarizability and size and coordination requirements of the added cation. Thus for glasses with a constant nitrogen:oxygen ratio, changes in Al or M concentration may cause changes in viscosity, Tg and hardness and these variances remained unaccounted for.

Drew et al (6,8) carried out extensive systematic studies on nitrogen-containing glasses in M-Si-O-N and M-Si-Al-O-N systems. Glasses with a fixed cation composition, with varying nitrogen:oxygen ratios were prepared, to allow direct comparison between different M-Si-Al-O-N systems and the effect of replacing oxygen by nitrogen within each system. This was the first and most extensive investigation of its kind revealing the true effect of nitrogen on properties.

2.3 Representation of M-Si-Al-O-N glass forming systems

Convenient methods of representing both Si-Al-O-N and M-Si-Al-O-N systems have been developed (23). Five component metal sialon systems can be represented by Janecke's triangular prism (24). The Nd-Si-Al-O-N prism is shown in figure 1. The basal plane of the prism is a square which, in this case, represents the Si_3N_4-AlN-Al_2O_3-SiO_2 system ie. the oxides and nitrides of silicon and aluminium. The bottom right hand corner is Si_3N_4 ($3Si^{4+}$ and $4N^{3-}$) and, maintaining 12 positive and 12 negative valency units throughout, the other corners are then Si_3O_6, Al_4O_6 and Al_4N_4. Addition of a fifth component such as Nd, produces a prism with the back triangular face being a ternary oxide system and the front face the nitrides. The concentrations of all components are expressed in equivalent units so that any point in the prism again represents a combination of 12 positive and 12 negative valencies. As shown by figure 1, the distance, x, of any point P from the front face represents the concentration (in equivalent units) of oxygen, and the distance y represents the equivalent concentration of nitrogen ie. the equivalent concentration ratio of nitrogen = $y/(x+y) = (3N)/(20+3N)$ where O and N are, respectively, the atomic concentrations of oxygen and nitrogen within any composition. The edge of the prism is scaled such that $x+y = 12$. The vertical plane is scaled such that each division is two valency units. The point P thus has a composition $Nd^{0.6+}Si^{4+}Al^{2+}O^{6.6-}N^{5.4-}$ in valency units and hence $Nd_{2.0}Si_{1.0}Al_{0.67}O_{3.3}N_{1.8}$ in atomic units.

This representation was adopted by various investigators (8-10,25)to describe the limits of glass formation in different metal sialon systems. The limits of the metal alumino-silicate glass regions were plotted on the oxide face of the prism and it was possible to observe how the glass region extended into the M-Si-Al-O-N prism on replacing oxygen by nitrogen and they produced the three dimensional representation of the complete glass forming regions in both the Mg- and Y-Si-Al-O-N systems (see figures 2 and 3 respectively). Prior to this, investigation of these systems had been carried out by Jack (2) and Loehman (4) but adequate exploration of the full extent of these systems was not completed. Hampshire and Jack (22) showed that nitrogen lowers the eutectic temperatures in metal oxide-silica systems and increases the tendency to form glass. Drew et al (6) again showed this more clearly and from figure 2 it can be seen that the extent of the glass forming region in the Mg-Si-Al-O-N system expands away from the oxide face with increasing replacement of oxygen by nitrogen. This increase continues until 10e/o nitrogen is incorporated, after which the glass forming region contracts with a simultaneous shift towards slightly more Mg-rich compositions (25), which shows

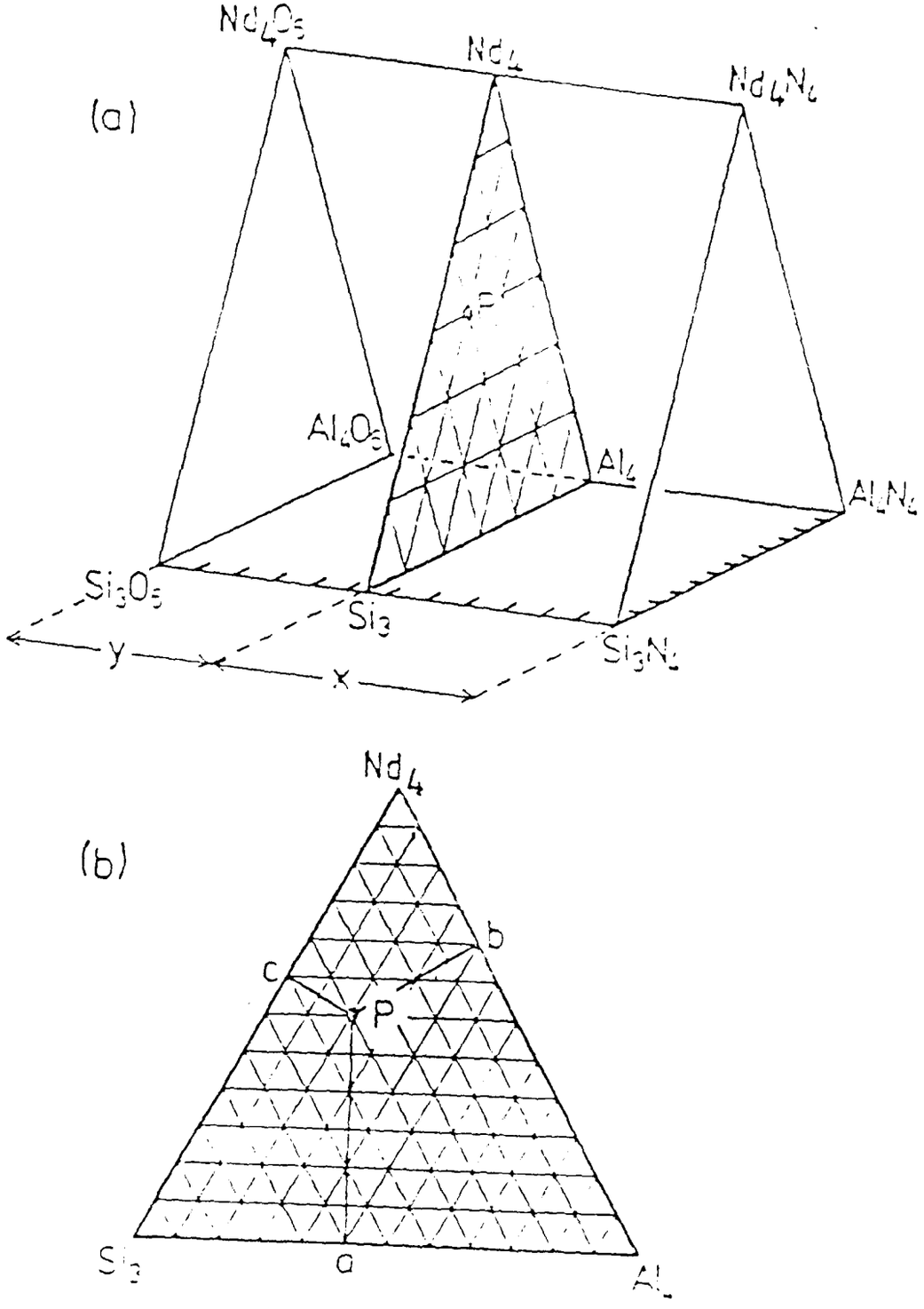

FIGURE 1 Janecke prism representation of the Nd-Si-Al-O-N system.

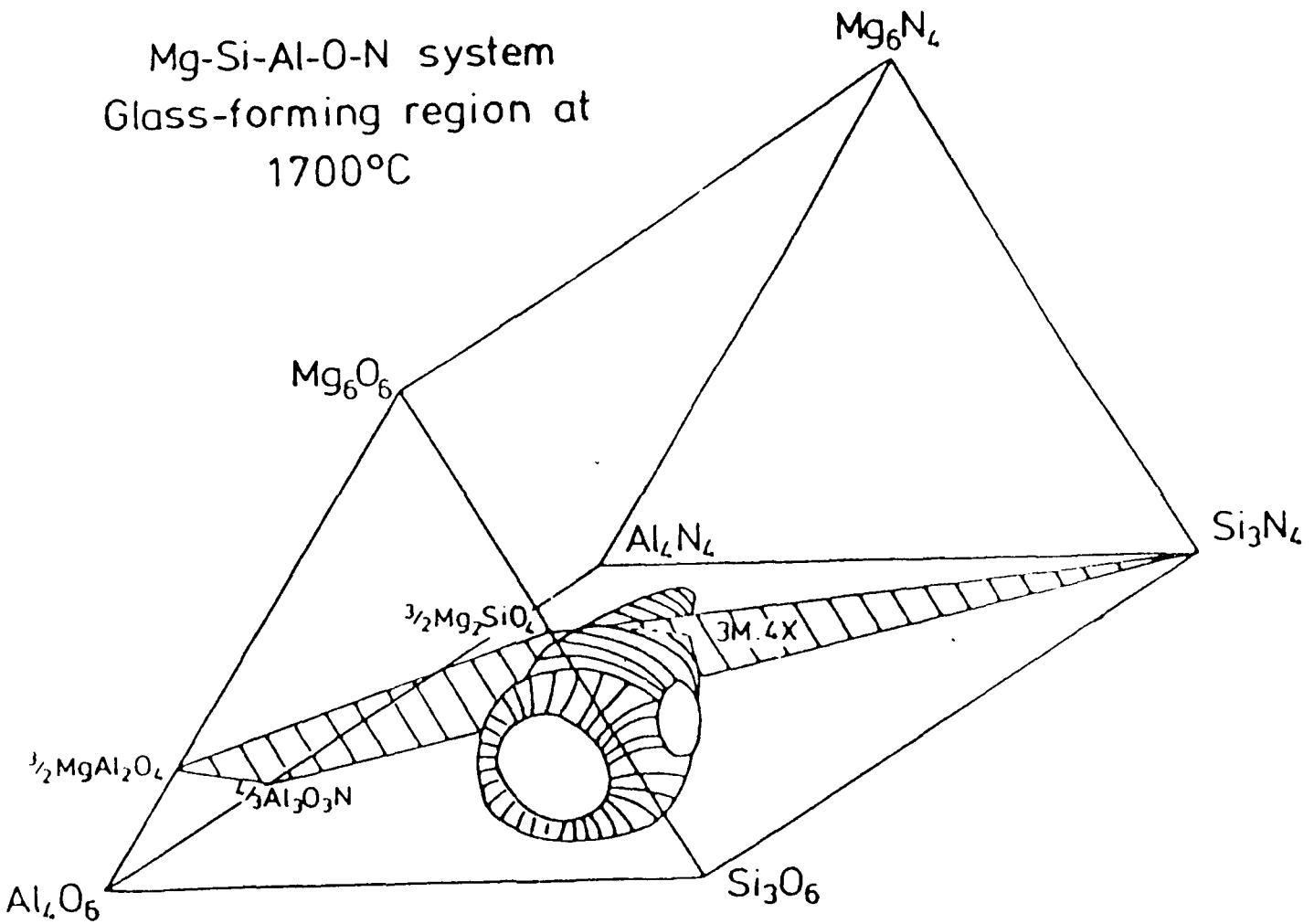

FIGURE 2 Glass formation region in the Mg-Si-Al-O-N Janecke prism.

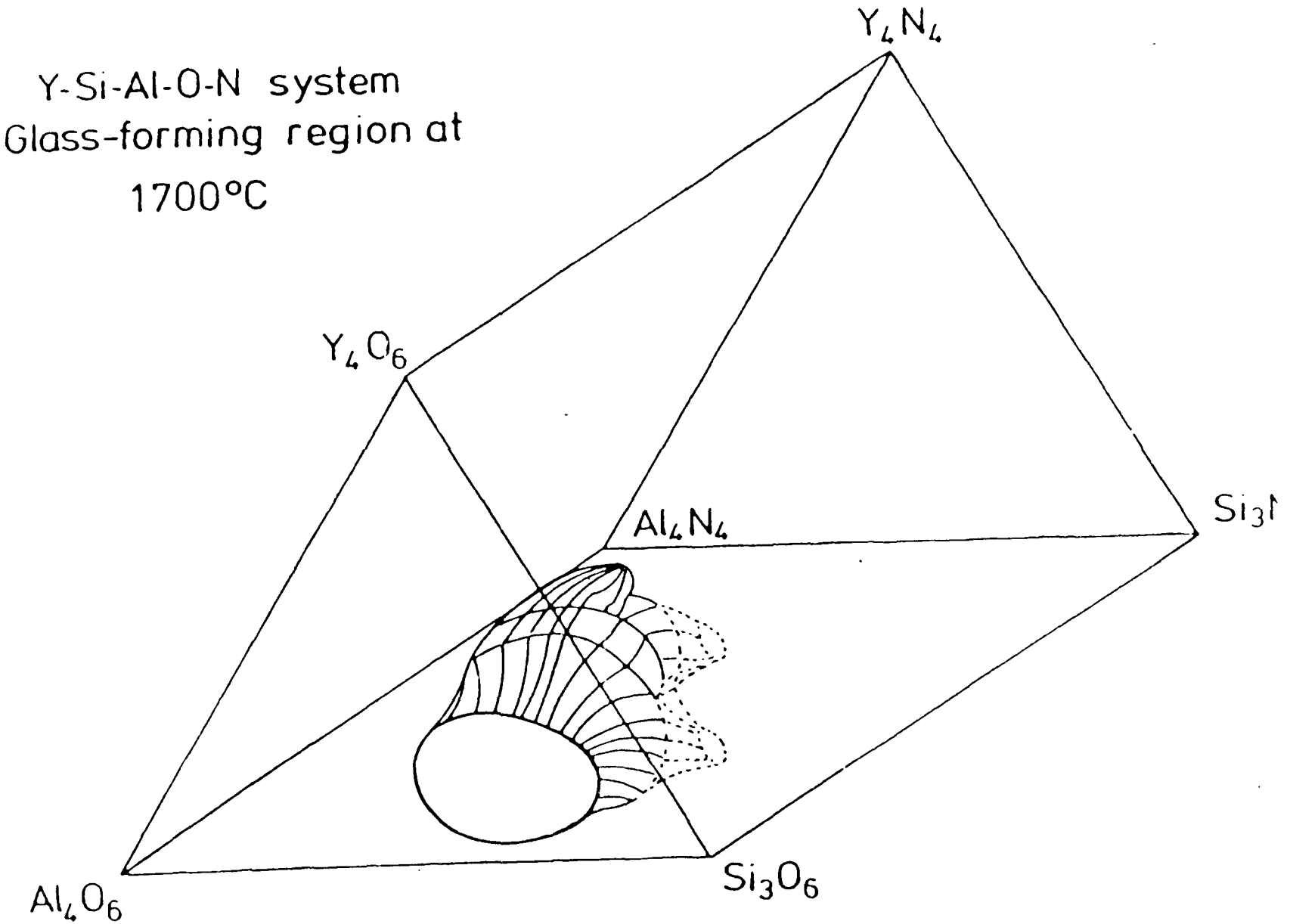

FIGURE 3 Glass formation region in the Y-Si-Al-O-N Janecke prism.

also that while MgO is a network modifier in oxide systems, in oxynitride glasses it appears to act as a network former. In the Y-Si-Al-O-N system (figure 3) the expansion away from the oxide face is less at 10e/oN but the maximum nitrogen solubility is much greater. Depending on the particular system it was found that a limit of 17-25e/o of the oxygen could be replaced by nitrogen. Drew et al (6,8,9) found that, for glasses with a constant cation ratio, incorporation of nitrogen resulted in increasing viscosity, Tg, resistance to devitrification, refractive index, dielectric constant and ac. conductivity, in all the Mg-, Ca-, Y- and Nd-sialon glasses. Drew et al. also showed that the corresponding M-Si-O-N systems displayed a much smaller glass-forming region, thus showing the ability of Al_2O_3 to extend the range of glass formation.

2.4 Nitrogen coordination in glasses

The resulting improvements in glass properties by substitution of nitrogen for oxygen was usually attributed to the replacement of a 2-coordinated bridging oxygen atom, by a nitrogen atom coordinated by 3 silicon ions. Thus, it was assumed that properties were improved due to an increase in the crosslinking of the silicate network due to the tri-coordinated nitrogen.

However, prior to 1984, there was no direct evidence for the presence of tri-coordinated nitrogen in oxynitride glasses and published IR data (4,26) only suggested the presence of Si-N bonds in the structure. Brow and Pantano (27) carried out more extensive studies on the coordination of nitrogen in oxynitride glasses by analysis using Fourier Transform Infrared Spectroscopy (FTIR) and X-ray Photoelectron Spectroscopy (XPS). At this point direct evidence of the formation of Si-N bonds and of the presence of tri-coordinated (nitride-like) nitrogen groups was obtained. It was concluded that nitrogen was present in the structural network because introduction of the nitrogen caused shifting of the position of the Si-O-Si stretching peak towards that of Si-N. If nitrogen existed as precipitated Si_3N_4 the position of the Si-O-Si peak would not be expected to change. Rand and Roberts (28) also observed a similar shift of the Si-O-Si stretching vibration, to lower wavelengths in nitrided silicon thin-films. XPS studies by Brow and Pantano also revealed that nitrogen is usually present in more than one form, and they proposed that non-bridging nitrogen ions may also be present, similar to the following:

(1) $\equiv Si - N^- - Si \equiv$

(2) $\equiv Si - N^{2-}$

They based the interpretation of XPS analysis on an analogous situation involving bridging and non-bridging ions in silicate glasses. They presumed that the local charge on the non-bridging nitrogen ions was balanced by the presence of interstitial metal ions in their vicinity. Thus, while it has not been proven beyond doubt that nitrogen is present in oxynitride glasses in a tri-coordinated state, all evidence indicates that this is the symmetry that it accepts and no theory to indicate that it is present in some other form has been put forward to date.

2.5 Nucleation and crystallization in oxynitride glasses

Reports of formation of various M-sialon glasses have been described with resultant changes in physical properties due to incorporation of nitrogen. After formation of these glasses, suitable heat-treatment results in formation of tiny nuclei, upon which crystals then grow. This process results in the formation of glass-ceramics which have superior properties to the parent glass. Using suitable heat treatments, properties of glass-ceramics can be tailored to particular requirements. Many glasses require the addition of a nucleating agent to promote the crystallisation process, but in general oxynitride glasses are self-nucleating. Inclusion of nitrogen also affects the crystallization process in oxynitride glasses.

Abromovici et al. (29) investigated the effect of nitrogen on nucleation and crystallisation in SiO_2-Al_2O_3-MgO and related glass forming systems. In the SiO_2-Al_2O_3-Li_2O system they found the presence of nitrogen to influence the phase composition of crystallized samples only to a limited extent. In the SiO_2-Al_2O_3-MgO system they reported that in samples with TiO_2 as a nucleating agent the addition of nitrogen leads to a more advanced and finer crystallization. They concluded from this that nitrogen promotes nucleation and in some cases advances crystallization, but they failed to give any explanation for this. Nitrogen is known to be an inhibitor of crystallization because it increases viscosity and a more probable explanation of their observation is that nitrogen does in fact inhibit growth of large crystals, but in some cases this may be compensated for by a more extensive growth of smaller crystals, where less matter transport would be required for their propagation.

The crystalline phases formed in glasses on heat-treatment and the extent of their formation will determine the properties of the particular material. The phases formed will depend on both the composition of the parent glass and the heat-treatment process.

Ahn and Thomas (30) carried out preliminary studies on crystallized Y-sialon glasses. They reported that appreciable crystallization was only effected after glasses were doped with up to 5w/o ZrO_2 which acted as a nucleating agent. They identified the main crystalline phase as $Y_2Si_2O_7$. Subsequent investigators and current work in this project has shown that Y-sialon glasses crystallise readily without the aid of nucleating agents. Winder et al. (31) carried out further work in this system and reported that low nitrogen:oxygen ratios again favour formation of yttrium disilicate ($Y_2Si_2O_7$) while the increased glass viscosity, associated with an increase in the nitrogen:oxygen ratio, favoured suppression of $Y_2Si_2O_7$ crystallization and preferential formation at higher temperatures of yttrogarnet ($Y_3Al_5O_{12}$).

More extensive studies of crystallization in Y-sialon glasses were carried out by Lewis et al (32). They reported that on heat-treatment at 1250°C the oxide glasses fully crystallized to yttrium disilicate, mullite and Al_2O_3. Again with increasing nitrogen content, they found that the disilicate phase was progressively replaced by yttrium aluminium garnet and nitrogen was mainly incorporated into Si_2N_2O. They also reported that heat-treatment of the nitrogen glasses at 1100°C produced partial crystallization involving intermediate phases related to nitrogen wollastonite. In further investigations, Lewis et al. (33) investigated crystallization in the Mg-sialon system and found that fosterite was the main crystallizing phase. They also identified secondary phases and these included a magnesium substituted β'-sialon, designated as β'' which was first reported by Drew et al (6). At higher temperature, this is replaced by a Mg-Si-Al-O-N petalite phase.

Extensive investigation of oxynitride glass formation and property evaluation has been carried out by several scientists. The desire to improve existing materials and to develop new and better materials necessitates continued research. The area of oxynitride glasses and glass-ceramics offers encouraging possibilities for developing improved materials, but more detailed property evaluation must be carried out before these materials can be exploited fully. While several investigators have demonstrated the benefits of nitrogen inclusion in oxide glasses, few have produced any detailed property measurements on the corresponding glass-ceramics. The possibility of developing quality oxynitride glass-ceramics by suitable heat-treatments makes the future of this field very attractive.

3. TECHNICAL OBJECTIVES

a) Exploration of glass forming compositions in M-Si-Al-O-N systems (where M = Y, Nd, Sm, La.)

b) Study of the effect of nitrogen on properties (viscosity, T_g, T_c, microhardness) of glasses.

c) Optimisation of suitable heat-treatment processes to produce fine grained glass-ceramics from selected glass compositions.

d) Evaluation of optical properties of selected glasses and comparison with the corresponding glass-ceramics.

4. MATERIALS AND EXPERIMENTAL METHODS

The following glass forming systems were investigated:

1. Mg - Si - Al - O - N
2. Y - Si - Al - O - N
3. Mg - Si - Y - O - N
4. Mg - Si - Nd - O - N
5. Nd - Si - Y - O - N
6. Mg - Si - Sm - O - N
7. Sm - Si - Al - O - N
8. Nd - Si - Al - O - N
9. La - Si - Al - O - N

4.1 Materials

Nitrogen was added to the glass compositions via silicon nitride, LC12 grade Si_3N_4, obtained from Hermann C. Starck, Goslar, FRG (α:β=95:5). Adjustments in compositional calculations were made to take into account the surface oxide, ie. 4w/o silica on the silicon nitride. Neodymium oxide (Nd_2O_3), samarium oxide (Sm_2O_3) lanthanum oxide (La_2O_3) and yttrium oxide (Y_2O_3) were obtained in 99.9% purity from Rare-Earth Products Ltd. (England). These oxides were calcined

at 800°C to remove volatiles, carbon dioxide and chemically absorbed water. Silica (SiO_2) was in the form of pulverised quartz, supplied by Fluka Chemicals. Laboratory grade aluminium oxide (Al_2O_3) and magnesium oxide (MgO) was used supplied by Hopkins and Williams.

4.2 Powder Mixing

Batches of between 60g and 100g were prepared in each case. Compositions were wet-mixed for ten minutes in isopropanol using a Janke and Kunkel Ultra-turrax T25 homogeniser. The alcohol was then evaporated off and this was followed by a further period of dry-mixing for 5 minutes.

4.3 Glass Melting

Glass melting was carried out in a high temperature Carbolite resistance furnace, fitted with Lanthanum Chromite elements. The hot zone was 6-9 cm long and graphite crucibles of up to 40mm internal diameter lined with boron nitride could be used, thus enabling quite large samples to be melted. Melting was carried out at between 1650°C and 1700°C under a constant flow of nitrogen. After one hour the crucible was then withdrawn rapidly from the hot zone of the furnace and, while still in a molten state, the glass was poured into a pre-heated graphite mould. This mould was normally heated to a temperature 50°C higher than the glass transition temperature of the sample being cast. The mould was then transferred to a muffle furnace for annealing. In this way internal stresses were removed and after maintaining the mould and cast at around the transition temperature of the glass for one hour, the furnace was then cooled slowly.

4.4 Phase analysis

X-ray powder diffraction methods were used to identify crystalline phases occurring during fusion or after devitrification. An Hagg-Guinier focusing camera was used with Cukα radiation and a potassium chloride internal standard.

4.5 Microscopic Analysis

Samples were mounted in cold setting epoxy resin or bakelite and polished with successive finer grades of SiC papers, with final polishing using alumina paste. Preliminary investigation of sample microstructure was carried out using optical microscopy. Further and more detailed analysis was carried out on samples after sputter coating with a gold alloy, using a Jeol JSM 840 scanning electron microscope, with auxiliary electron probe microanalysis.

4.6 Hardness Measurement

Hardness values for as-quenched and crystallised glasses were obtained using a Wilson Tukon Microhardness Tester. An indentation load of 200g was used with an indentation time of 15 seconds. A minimum of six measurements were taken from each sample and an average of these results obtained.

4.7 Density Measurement

Bulk density of samples was measured using a Mercury Displacement Balance. The sample is immersed in a mercury bath and the volume of mercury displaced is equal to the bulk volume of the sample. The weight required to immerse the sample plus the weight of the sample gives a direct measure of the upthrust of the mercury and from these parameters, sample bulk density can be calculated.

4.8 Viscosity Measurement

Comparative viscosity measurements were carried out on samples by measuring the height:diameter ratio of rapidly cooled beads.

More accurate high viscosity measurements were carried out using a method involving three point beam bending of a simple shaped test piece under an applied load and subsequent measurement of strain rate. Changes in viscosity were measured while the sample was being heated in a high-temperature deformation under load apparatus. The method is applicable in the 10^{8} - 10^{14} poise range. A plot of deformation vs. time was obtained as the samples were heated under a constant stress. Sometimes samples deformed sufficiently under their own weight so the additional stress was not required. Deformation is a function of strain and from the plot of deformation vs. time, viscosity at different temperatures can be calculated.

Test samples were machined to the required dimensions (<6mm x <12mm x >52mm - the length being greater than the distance between the sample supports), using a diamond grinding process. Further grinding and polishing was then carried out using SiC paper and alumina paste. All corners were rounded in the polishing process and, to remove all surface imperfections, samples were washed with 40%HF for a few seconds.

4.9 Differential Thermal Analysis (DTA)

Simultaneous differential thermal analysis/thermogravimet y was carried out on samples to detect both the glass transition

temperature (Tg), crystallisation temperature (Tc) and any detectable weight loss. The instrument used was a Stanton-Redcroft 780 series simultaneous Thermo-Gravimetric Differential Thermal Analyser. Small samples of glass were analysed in a flowing nitrogen atmosphere using platinum crucibles lined with a thin film of boron nitride to prevent any reaction with the sample. B.D.H. grade alumina was used as a reference material and samples were heated to a temperature above Tc in each case. A constant heating rate of 20°C/min was used throughout.

From DTA results, suitable heat treatment programmes were established for the production of glass-ceramics. The glass-ceramic process normally consists of a two-stage heat treatment during which (1) nucleation of crystals and (2) crystal growth occurs. The first stage is usually carried out at approximately 50°C above Tg and the second stage at the so-called crystallisation temperature, Tc. Heat-treatment of the glass was carried out in a horizontally mounted tube furnace under flowing nitrogen. The samples were placed on a bed of boron nitride in an alumina boat.

4.10 Optical Analysis (UV - visible)

The glass was cast, from the molten state, into cylindrical bars. These bars were then sliced into thin segments using a diamond wafering blade. These sections were then polished and mounted in a Varian DMS 100S UV-visible spectrophotometer with a scanning range from 190-900nm.

5. RESULTS AND DISCUSSION

5.1 Properties of glasses in Mg-Si-RE-O-N systems

A standard cation composition in equivalent %, namely 28% M_A, 56% Si, 16% M_B has been chosen to compare glasses from different systems and also the effects of nitrogen:oxygen ratio on glass properties.

Figure 4 shows the density after firing for the glasses in systems 1 to 5. The low values for some magnesium-containing glass compositions reflects the fact that some expansion occurs due to bubble formation. Weight losses in these glasses were of the order of 5-6%.

Figure 5 shows the variation of density after firing with nitrogen content for glasses in the Mg-Y-Si-O-N and

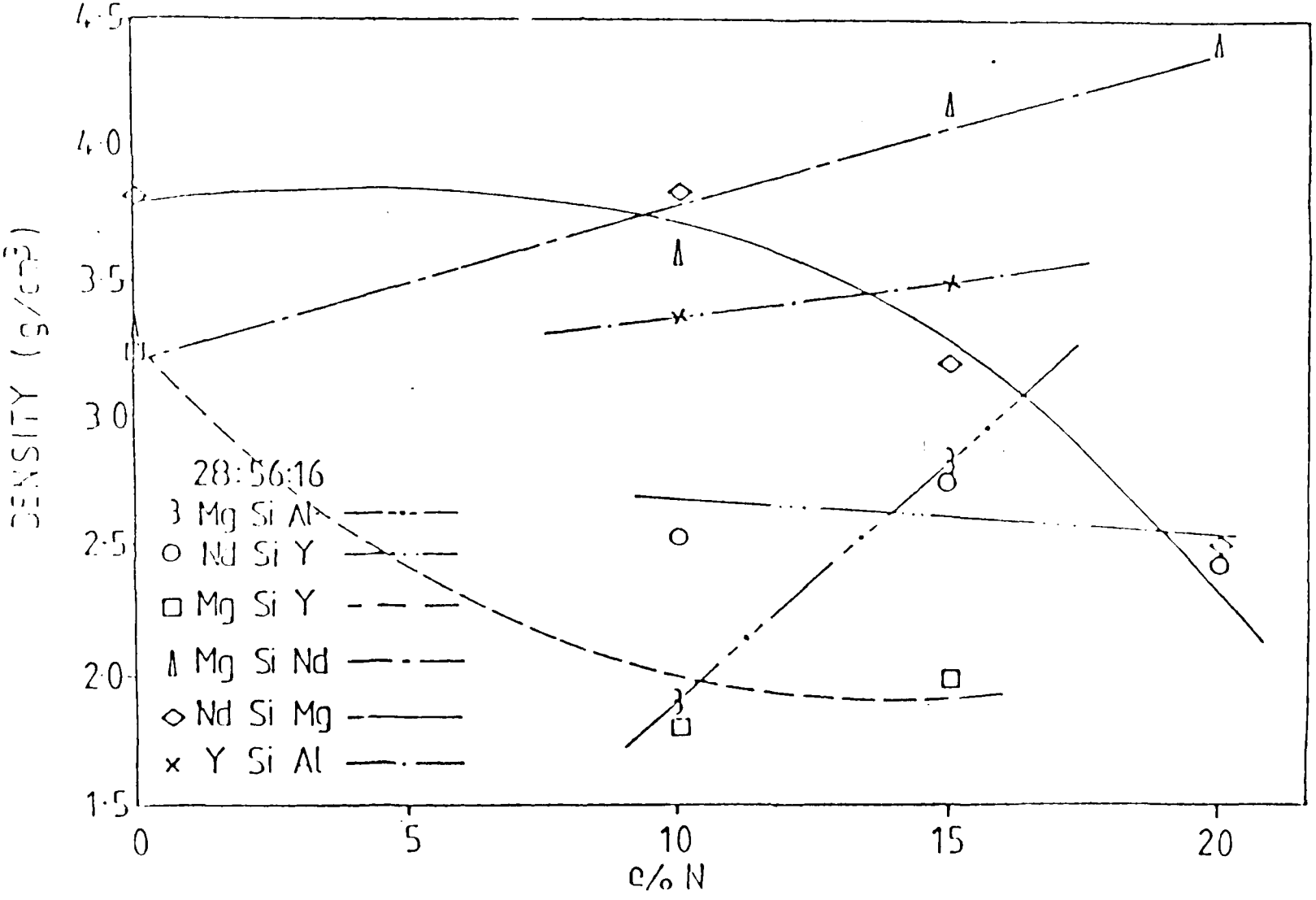

FIGURE 4 Variation of density after firing with nitrogen content for glasses in systems 1-5 (Mg-Si-Al-O-N, Y-Si-Al-O-N, Mg-Si-Y-O-N, Mg-Si-Nd-O-N, Nd-Si-Y-O-N).

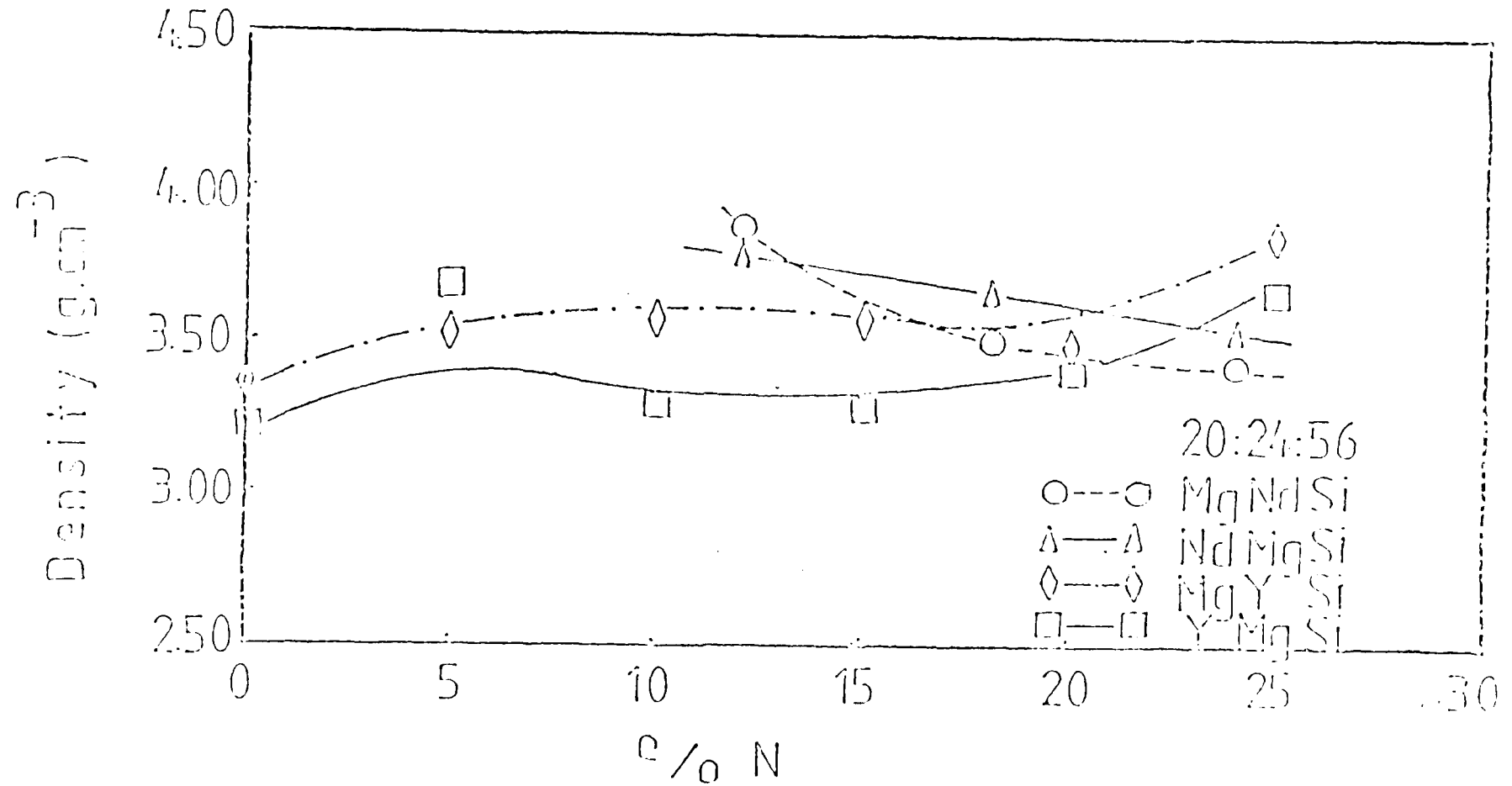

FIGURE 5 Variation of density after firing with nitrogen content for glasses in Mg-Y-Si-O-N and Mg-Nd-Si-O-N systems for two different cation ratios.

Mg-Nd-Si-O-N systems for two different cation ratios (24e/o Mg, 56e/o Si, 20e/o RE and 20e/o Mg, 56e/o Si, 24e/o RE where RE=Y or Nd). All the Y-containing glasses have densities of approximately 3.5 gcm^{-3} whereas Nd-containing glasses vary from 4.0 to 4.4 gcm^{-3} and decrease with increasing nitrogen content.

A simple qualitative comparison of viscosities was made by measuring the height/diameter ratio of the glass beads after firing. Results are shown in figure 6 for the standard cation composition glasses. In all systems, viscosity increases with increasing nitrogen content. The Mg-Si-Al-O-N glasses have the lowest viscosities and Y-Si-Al-O-N glasses appear to have the highest but the Mg-Si-Y-O-N and Nd-Si-Mg-O-N glasses both have viscosities of the same high order of magnitude.

Figure 7 shows the changes in relative viscosity after firing for the two non-standard cation compositions in each of the Mg-Si-RE-O-N systems. In all cases viscosity increases with increasing nitrogen concentration. The lowest viscosity is found for the high Mg content Nd-containing glasses. For a fixed oxygen nitrogen ratio Mg lovers the viscosity of glasses as might be predicted.

Surface tension comparisons were made by measuring the contact angle, Θ, for the glass beads after firing and results for the standard compositions are shown in figure 8. In all cases, Θ decreases with nitrogen content and Mg-Si-Al-O-N glasses have high Θ values. Results for the non-standard cation glasses are shown in figure 9. For the Mg-Si-Y-O-N system, Θ increases up to 10e/o N and then remains constant as nitrogen concentration increases further. For Mg-Si-Nd-O-N glasses, Θ increases with increasing nitrogen content.

Microhardness values for the standard cation glasses are shown in figure 10 and, as with viscosity, microhardness increases with nitrogen content for all systems. Y-containing glasses have slightly higher values than Nd-containing glasses. The changes in microhardness with nitrogen concentration for non-standard cation composition Mg-Si-RE-O-N glasses are shown in figure 11, microhardness increasing with nitrogen content for both systems.

Microhardness values for crystallized samples are shown in figure 12. In general, the values are lover than for non-crystallized glasses Microhardness after crystallization does not vary with nitrogen content except for M_A-Si-Al-O-N glasses. reflective of the fact that phase assemblages are similar in non-Al glasses (Apatite is a major crystallization product at all nitrogen levels). With the M_A-Si-Al-O-N glasses

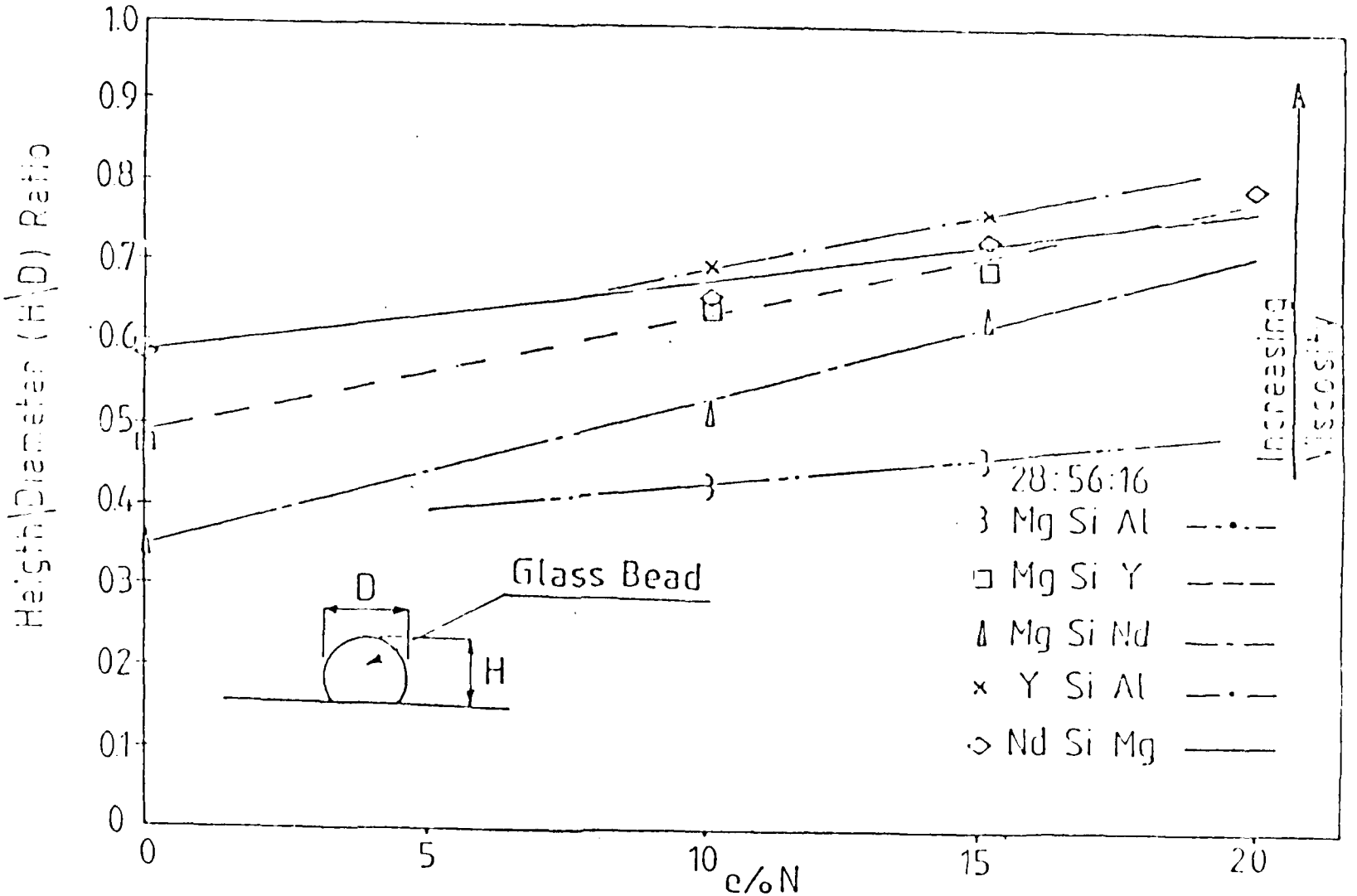

FIGURE 6 Changes in relative viscosity of glasses in systems 1-5.

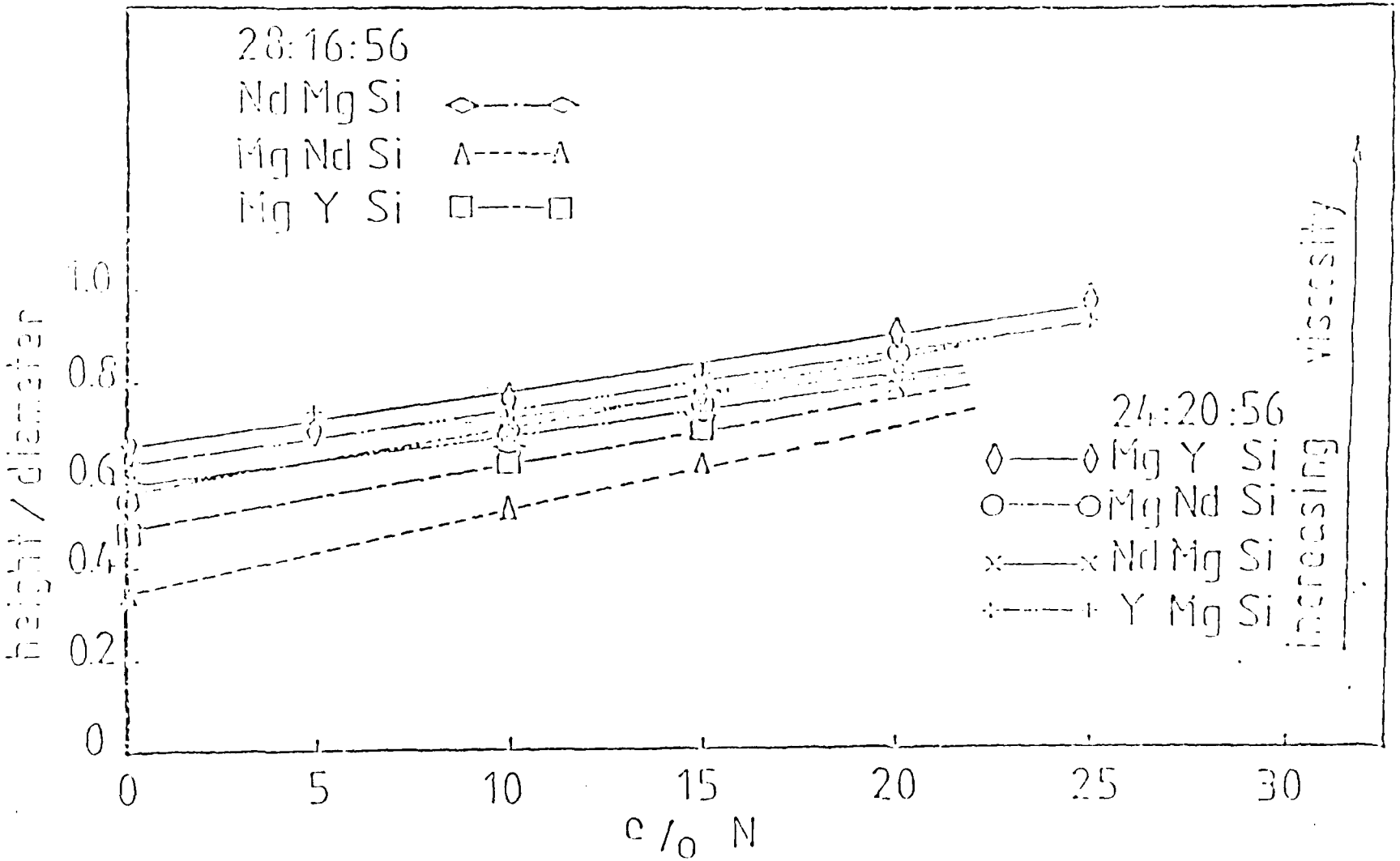

FIGURE 7 Changes in relative viscosity for the two non-standard cation compositions in the Mg-RE-Si-O-N systems.

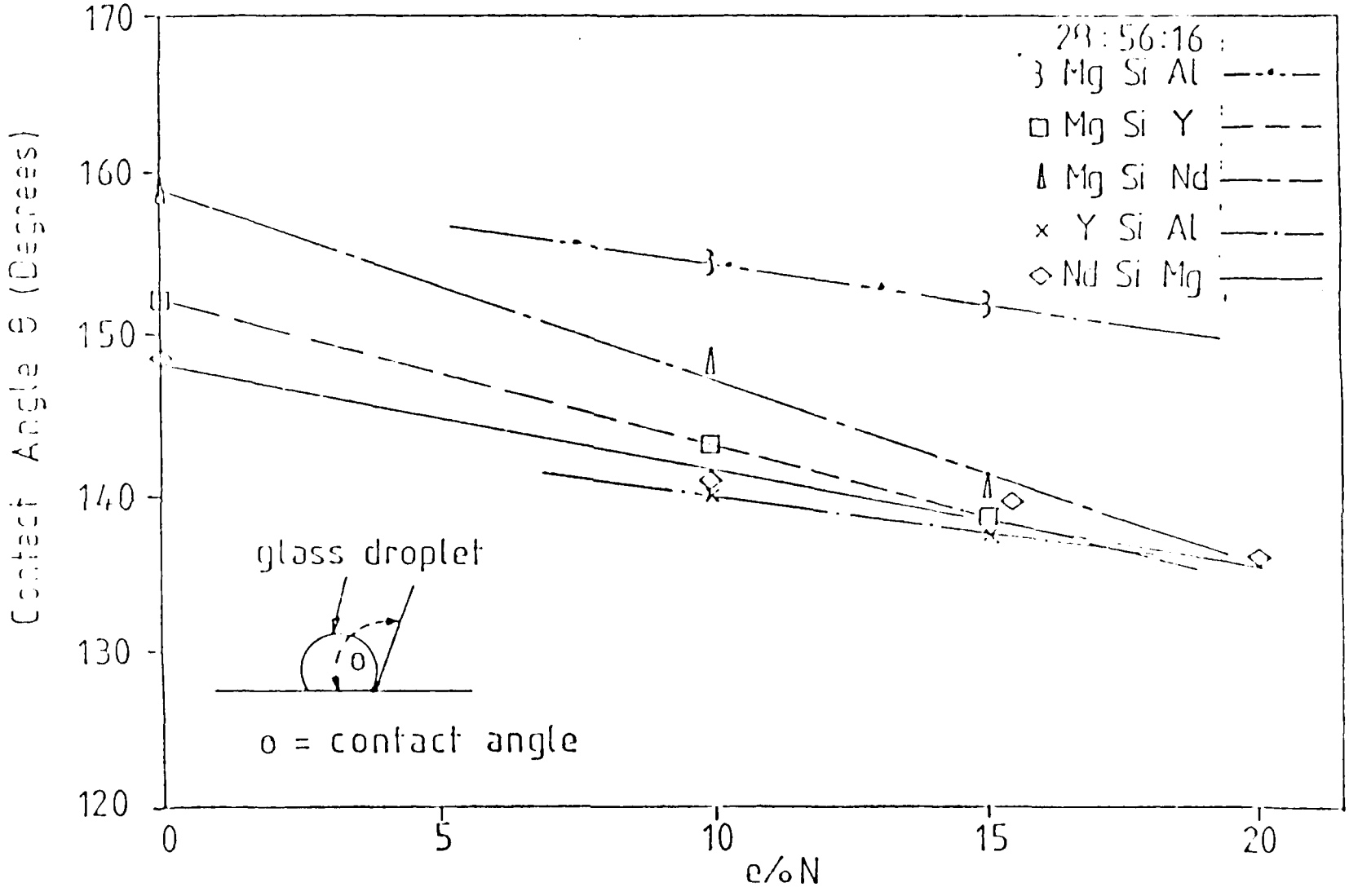

FIGURE 8 Variation of contact angle with nitrogen content after firing for the glass beads (standard compositions) in systems 1-5.

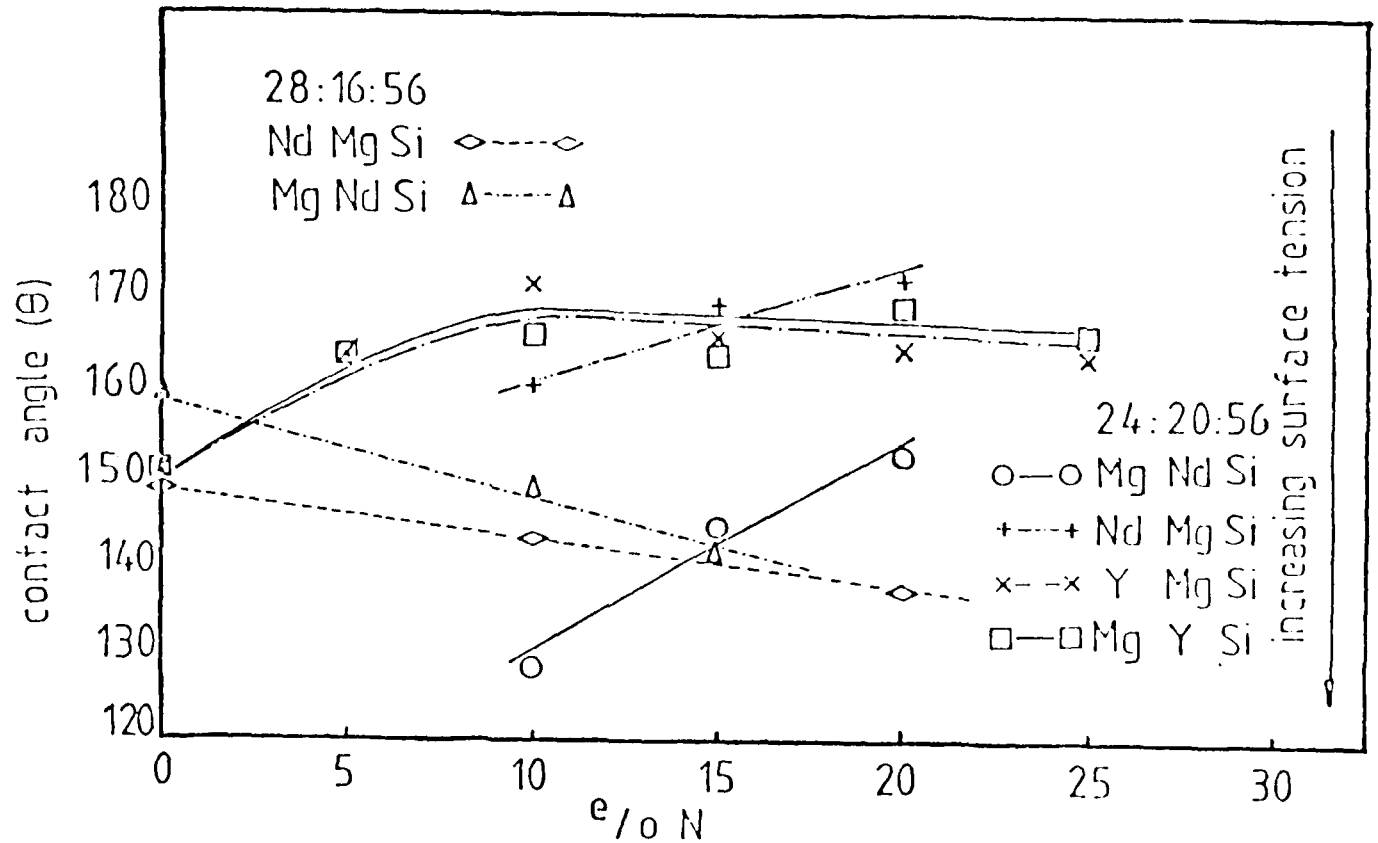

FIGURE 9 Variation of contact angle with nitrogen content after firing for the glass beads (non-standard compositions) in each of the Mg-Re-Si-O-N systems.

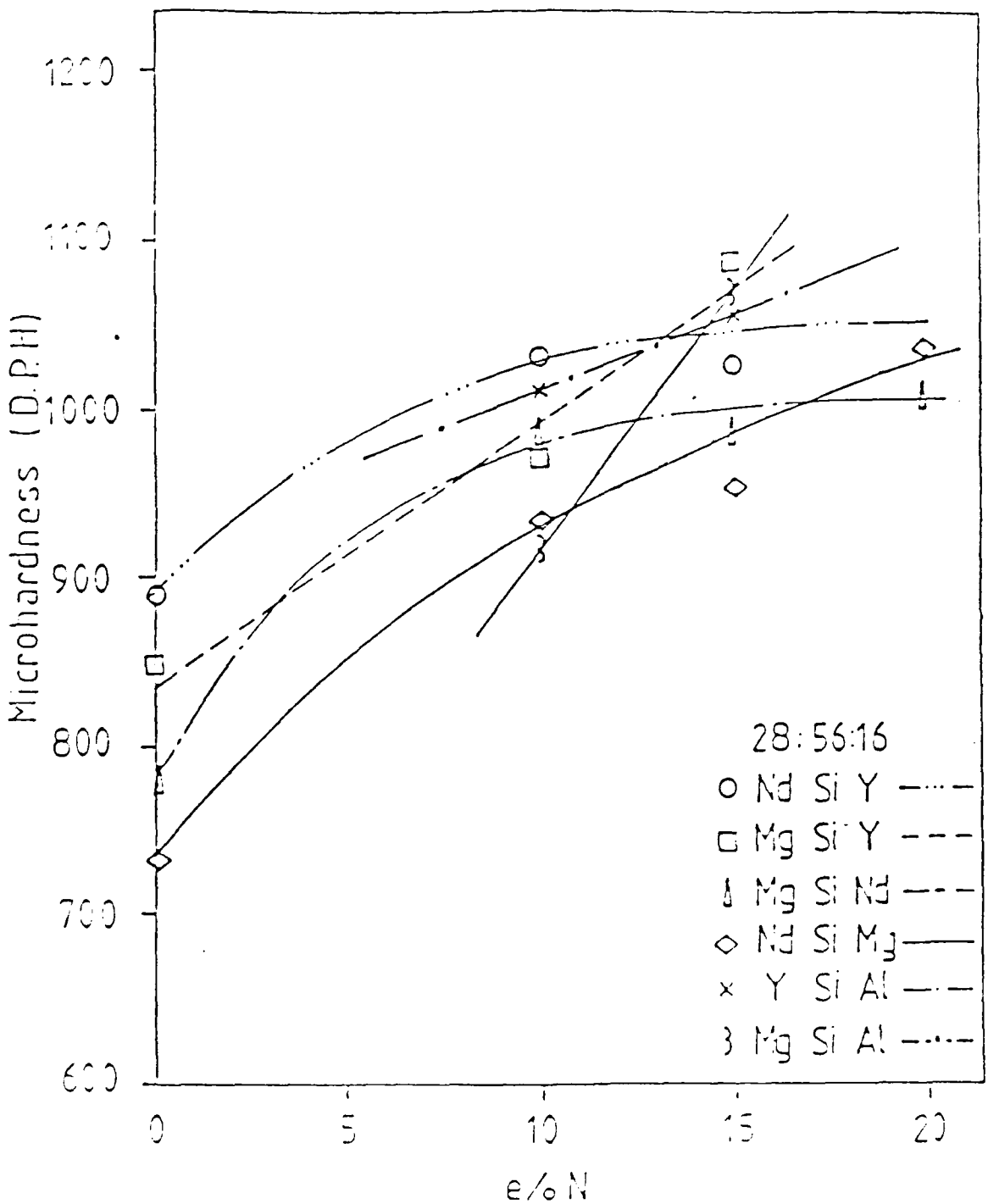

FIGURE 10 Changes in microhardness with nitrogen content for standard glass compositions in systems 1-5.

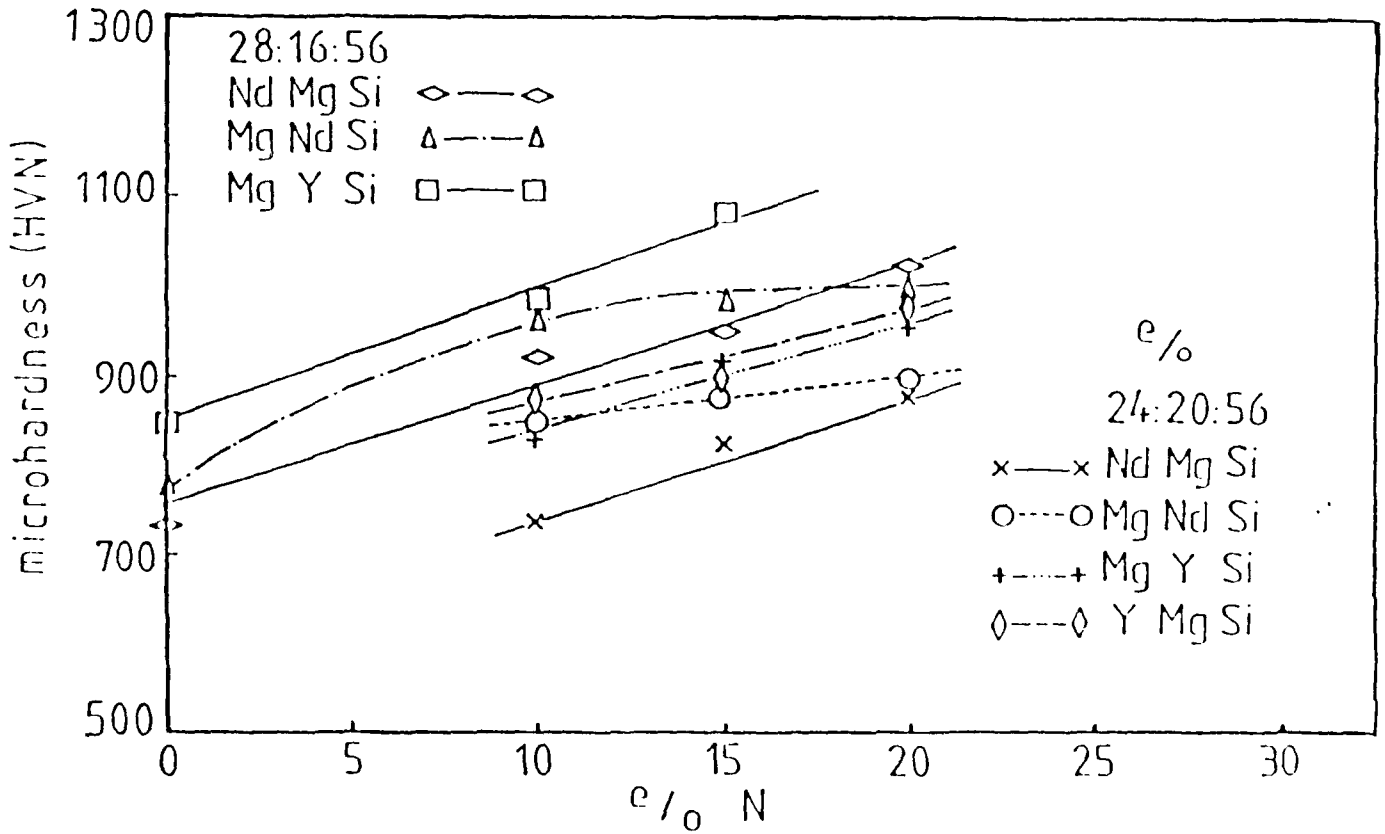

FIGURE 11 Changes in microhardness with nitrogen content for non-standard Mg-Re-Si-O-N glasses.

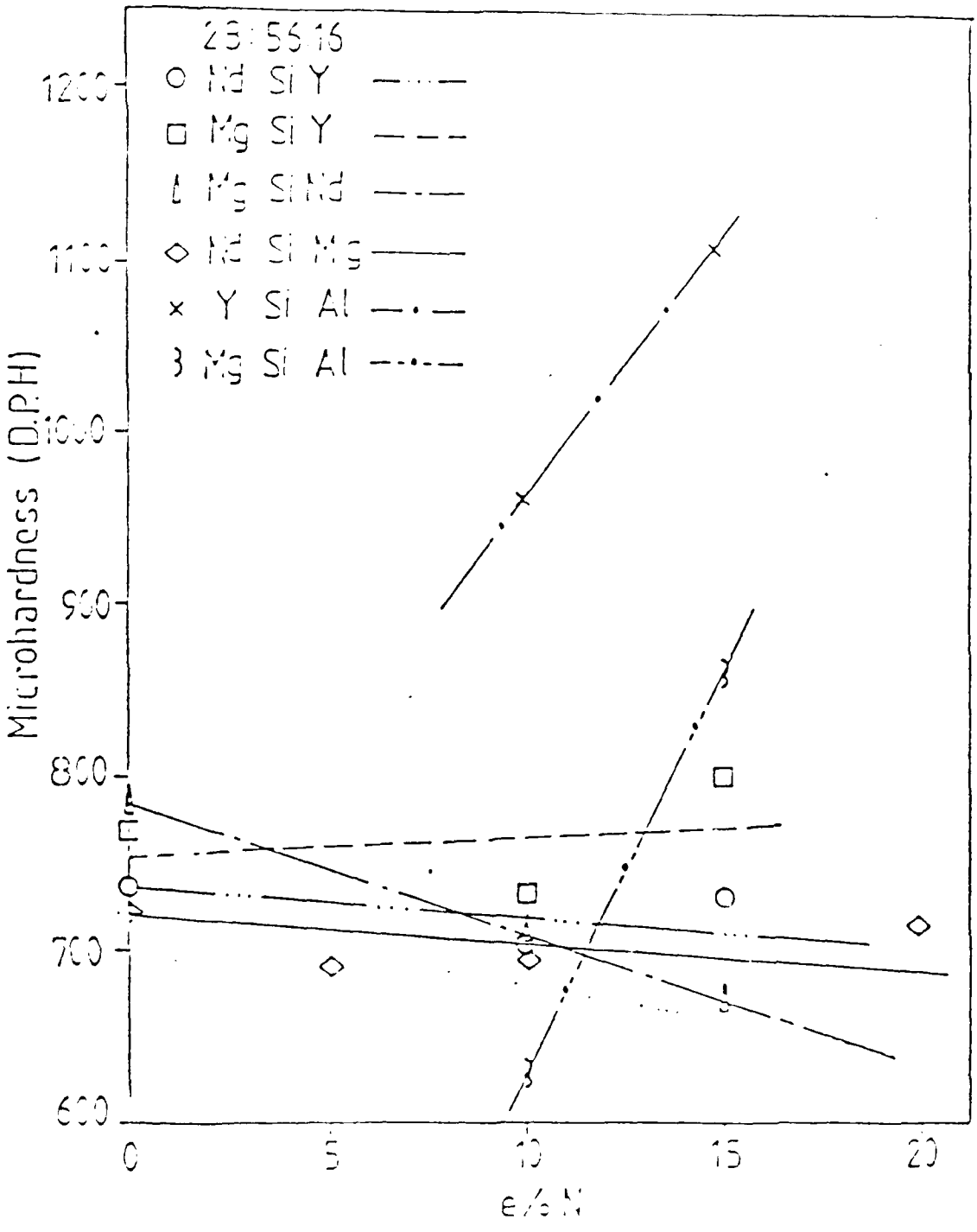

FIGURE 12 Changes in microhardness with nitrogen content for crystallized glasses in systems 1-5.

the phase assemblage after crystallization changes with nitrogen content.

All properties reported to date were assessed on samples which had been slow cooled (5°C min^{-1}) from the melting temperature. Inevitably, in some cases crystalline phases had begun to nucleate within the glasses.

Figure 13 shows a scanning electron micrograph of the composition: 24e/o Mg, 56e/o Si, 20e/o Nd / 90e/o O, 10 e/o N. This shows white, hexagonal shaped crystalloid groups with a dendritic morphology and also dark, hexagonal shaped crystals in a grey matrix.

5.2 Properties of glasses in M-Si-Al-O-N systems

Figure 14 shows the variation in density after firing with nitrogen content for glasses in M-Si-Al-O-N systems 1, 2, 7-9. The highest densities are obtained with glasses in the Nd-Si-Al-O-N system and the lowest for glasses in the Mg-Si-Al-O-N system. The oxide compositions (Oe/oN) in the Nd- and Sm-Si-Al-O-N systems have higher densities than the oxynitride glasses in these systems, the glasses decreasing in density as nitrogen content increases. In each of the Y- and La-Si-Al-O-N systems, there is a maximum in density at 17e/oN, both showing the same trend with La-containing glasses having higher densities.

Results of a qualitative comparison of viscosities for all the M-Si-Al-O-N glass compositions are shown in figure 15. The trends are similar to results reported previously, with viscosity increasing with nitrogen content for a fixed cation composition.

The variation of contact angle θ, with nitrogen content for the glass beads after firing is shown in figure 16. For Mg, Nd and Y-sialon glasses, θ decreases slightly with increase in nitrogen content whereas, for La- and Sm-sialon glasses, the contact angle increases with increasing nitrogen concentration. Microhardness values are shown in figure 17. For Mg, Nd and Y-sialon glasses, microhardness increases with nitrogen content whereas the values for the La- and Sm-sialon systems are much lower and remain constant at all nitrogen concentrations. Most of the samples in these two systems contain some crystalline phases, as a result of the slow cooling rates employed (5°C min^{-1}) allowing time for nucleation to occur. As found previously, the microhardness values are much lower than for non-crystallized glasses.

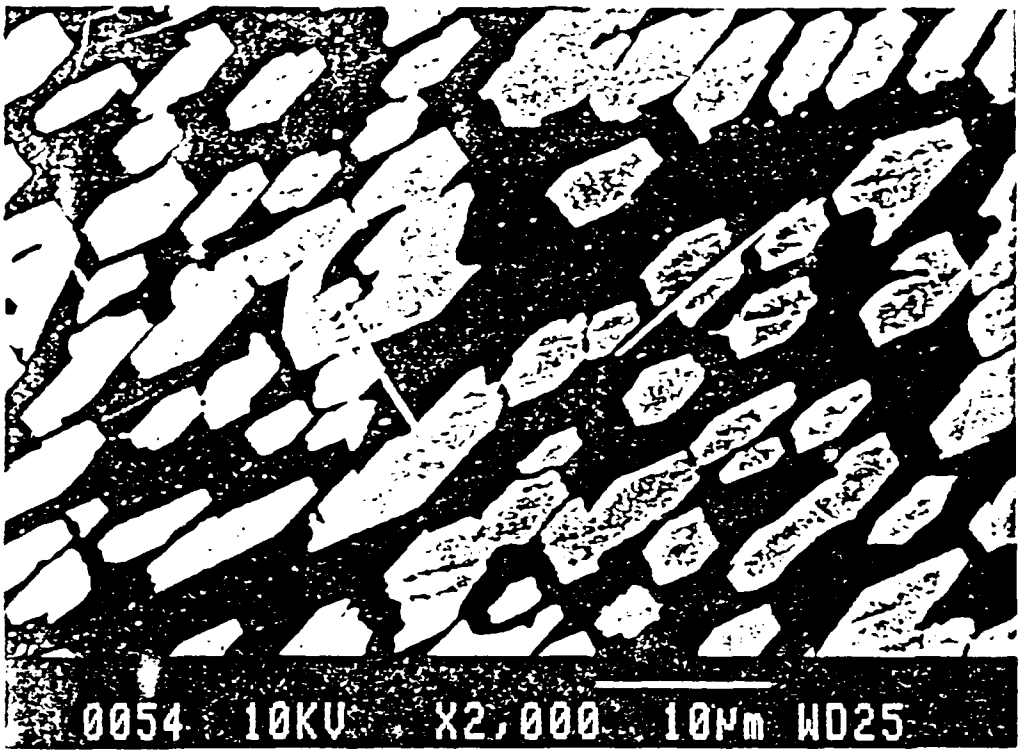

FIGURE 13 Scanning electron micrograph of the composition: (e/o) 24Mg 56Si 20Nd/90O 10N.

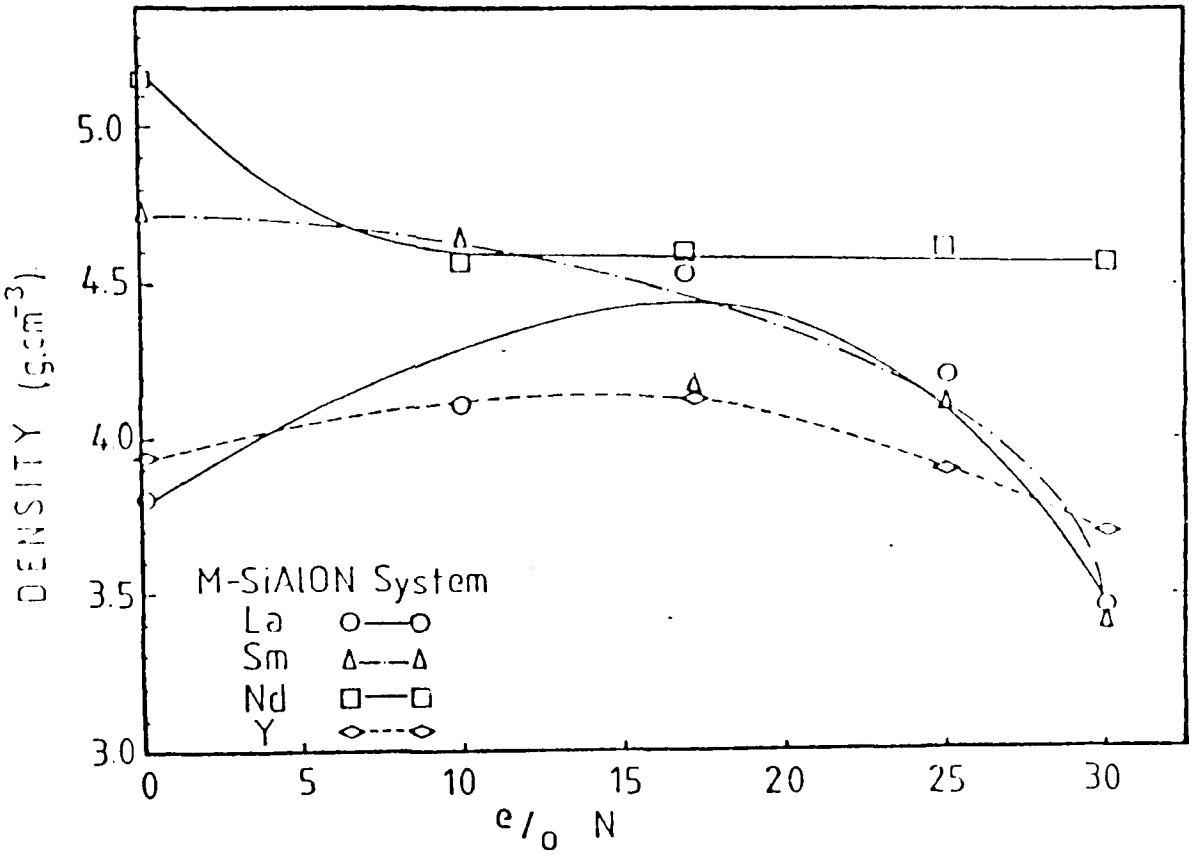

FIGURE 14 Variation of density after firing with nitrogen content for glasses in M-Si-Al-O-N systems (La, Sm, Nd and Y).

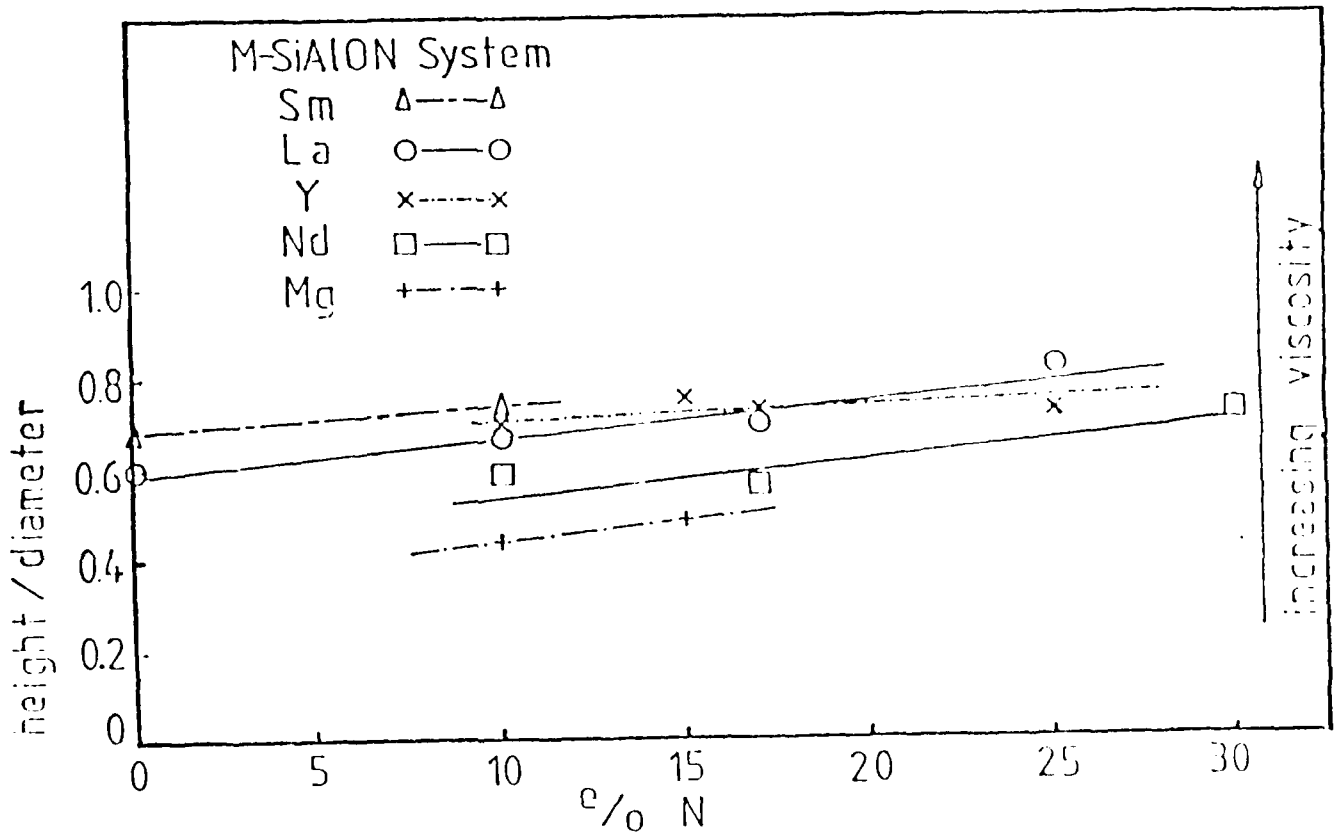

FIGURE 15 Changes in relative viscosity with nitrogen content for M-Si-Al-O-N glass compositions.

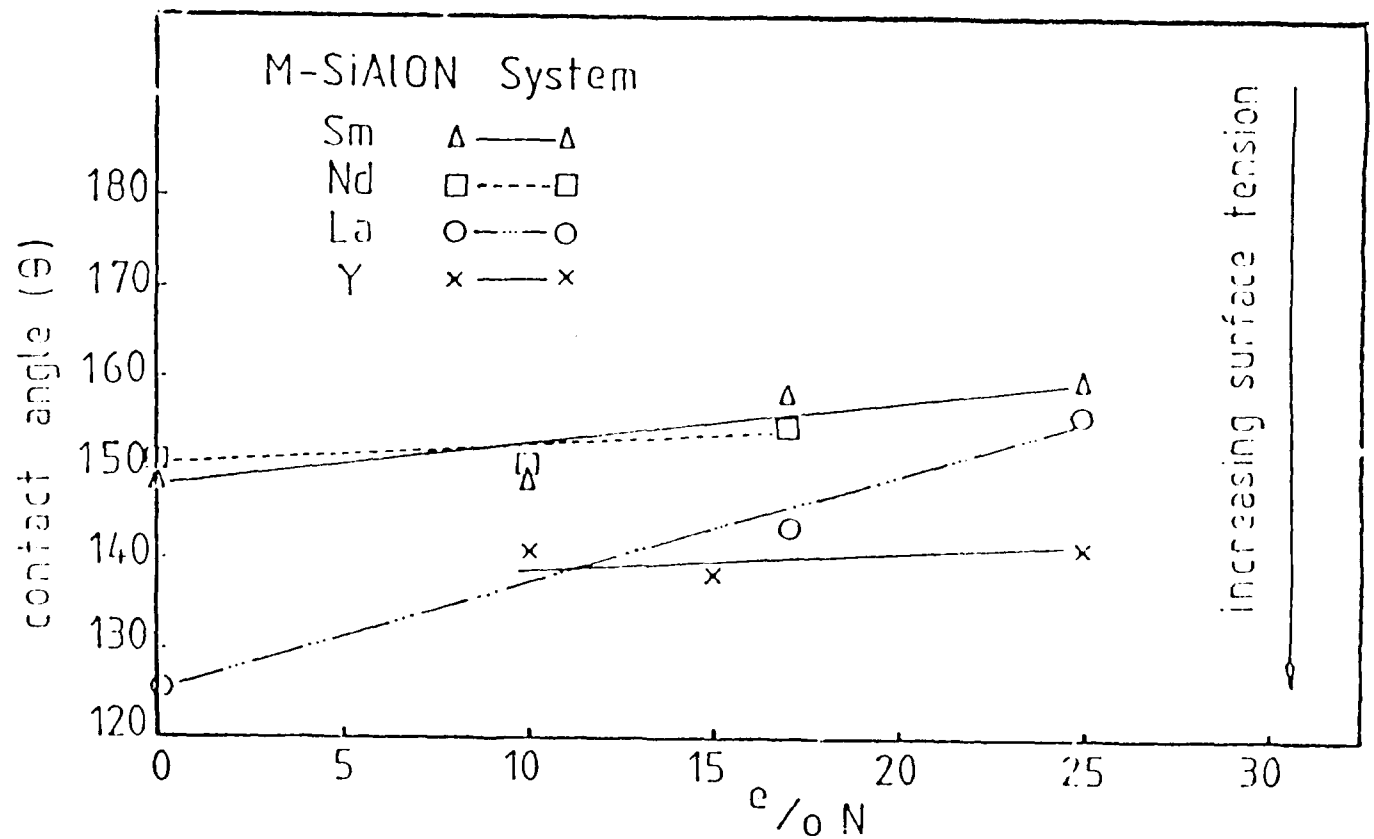

FIGURE 16 Variation of contact angle with nitrogen content after firing for the glass beads in M-Si-Al-O-N systems.

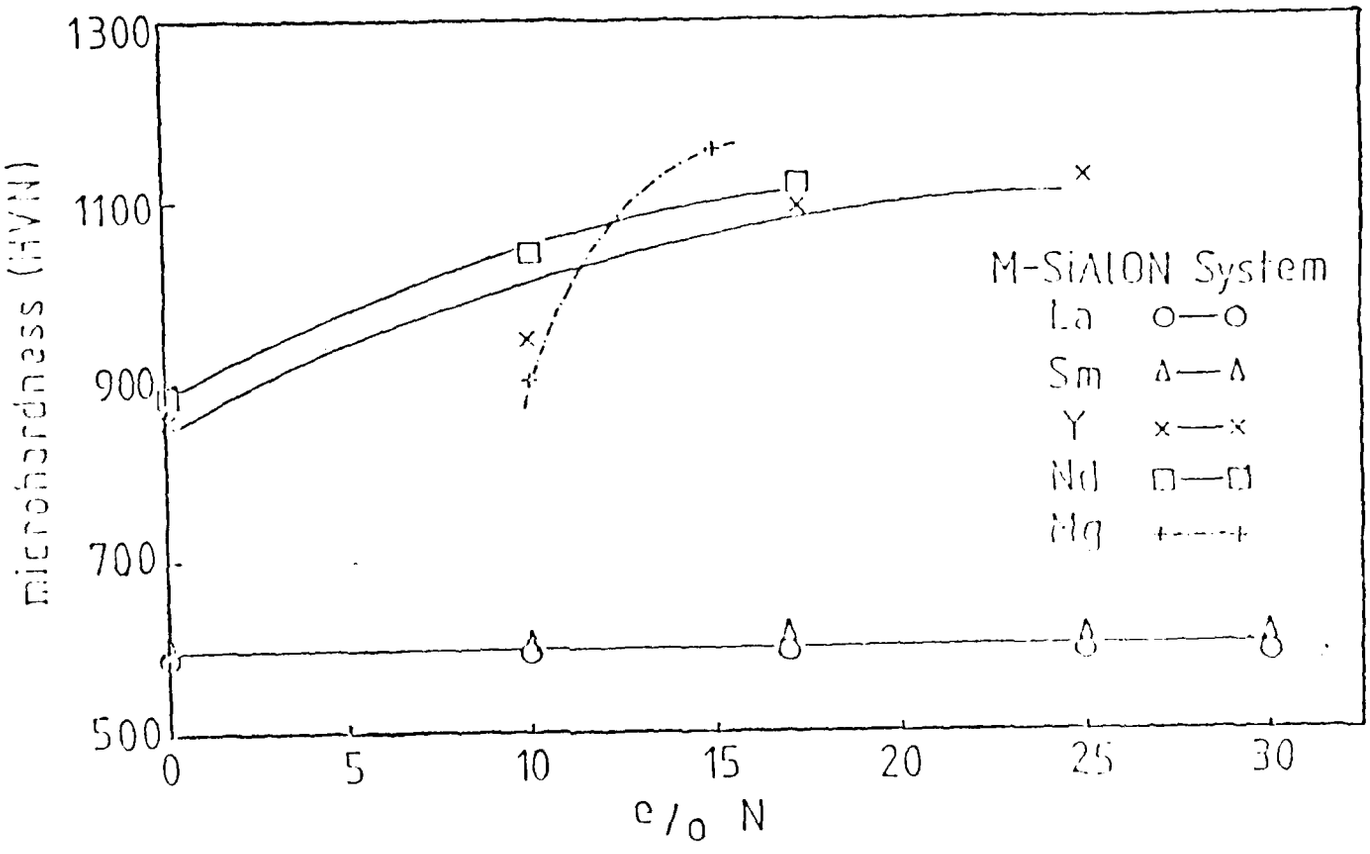

FIGURE 17 Changes in microhardness with nitrogen content for glass compositions in M-Si-Al-O-N systems.

5.3 Characterization of crystalline phases in M-Si-Al-O-N systems

Further characterization by scanning electron microscopy of crystalline phases in M_x-Si-Al-O-N glasses has been undertaken. In Sm and La-sialon glasses, apatite and YAM-type phases are observed. The apatite phase has a range of compositions from $RE_{4.67}Si_3O_{13}$ to $RE_5Si_3O_{12}N$ and the YAM-type phase has a range of composition from $RE_4Al_2O_9$ through RE_4AlSiO_8N to $RE_4Si_2O_7N_2$ (where RE=La, Sm, Nd or Y). Traces of these are also present in some Nd-sialon glasses along with Nd-N-wollastonite ($Nd_3Si_3O_6N_3$). Observations of La and Nd-sialon compositions reveal white, hexagonal shaped crystals in a grey matrix phase as shown in figure 18. and these white crystals become much finer as nitrogen content increases. Microprobe analysis has been carried out and the X-ray spectra for the Nd-sialon composition (28e/o Nd, 56e/o Si, 16e/o Al) containing 17e/o N are shown in figure 19. The white areas (crystals) contain Nd and Si with some Ca impurity while the grey areas (mostly amorphous) contain Nd, Si and Al. Thus, the white crystals are apatite ($Nd_5Si_3O_{12}N$ - $Nd_{4.67}Si_3O_{13}$) in a grey Nd-Si-Al-O-N glass matrix.

The X-ray spectra of the La-Si-Al-O-N compositions are similar and are shown in Figure 20 but the white crystals contain small amounts of Al and the glass phase contains some Ca. In the Sm-Si-Al-O-N system, the standard composition containing 0 e/o N has three different phases present; (1) white, elongated crystals containing Sm, Si and Ca, (2) light-grey spheroidal crystals containign Sm, Si, Al and a small amount of Ca, and (3) grey matrix containing Sm, Si, Al with very little Ca. The standard composition containing 10e/o N has course, white, hexagonal shaped crystals containing Sm, Si and some Ca within a grey amorphous Sm-Si-Al-O-N matrix. X-ray spectra for this composition are given in Figure 21.

5.4 Glass Transition and Crystallization Temperatures (Tg + Tc)

It has been established that abrupt changes in the properties of a glass occur at its transition temperature Tg. These include changes in properties such as thermal expansion coefficient, specific volume and specific heat. As a melt cools the glass transition is associated with a slowing down of rearrangement in the structure. Tg is related to viscosity and a glass has an approximate viscosity at 10^{13} poise at its transition temperature.

DTA curves for both the Y- and Nd-sialon glasses can be seen in figures 22 and 23 respectively. Tg is observed as an endothermic peak in each case, while the crystallization

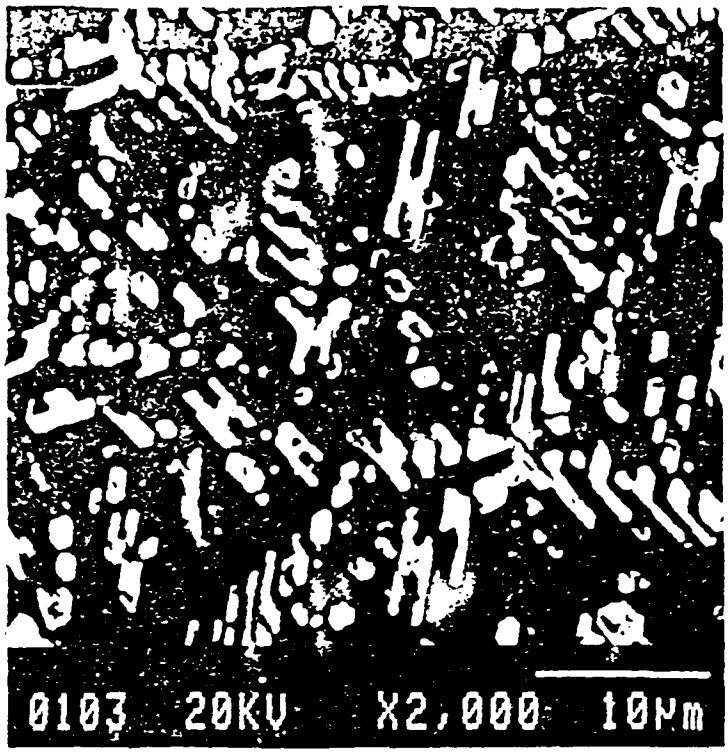

(a)

(b)

FIGURE 18 Scanning electron micrographs of (a) La-sialon and (b) Nd-sialon compositions.

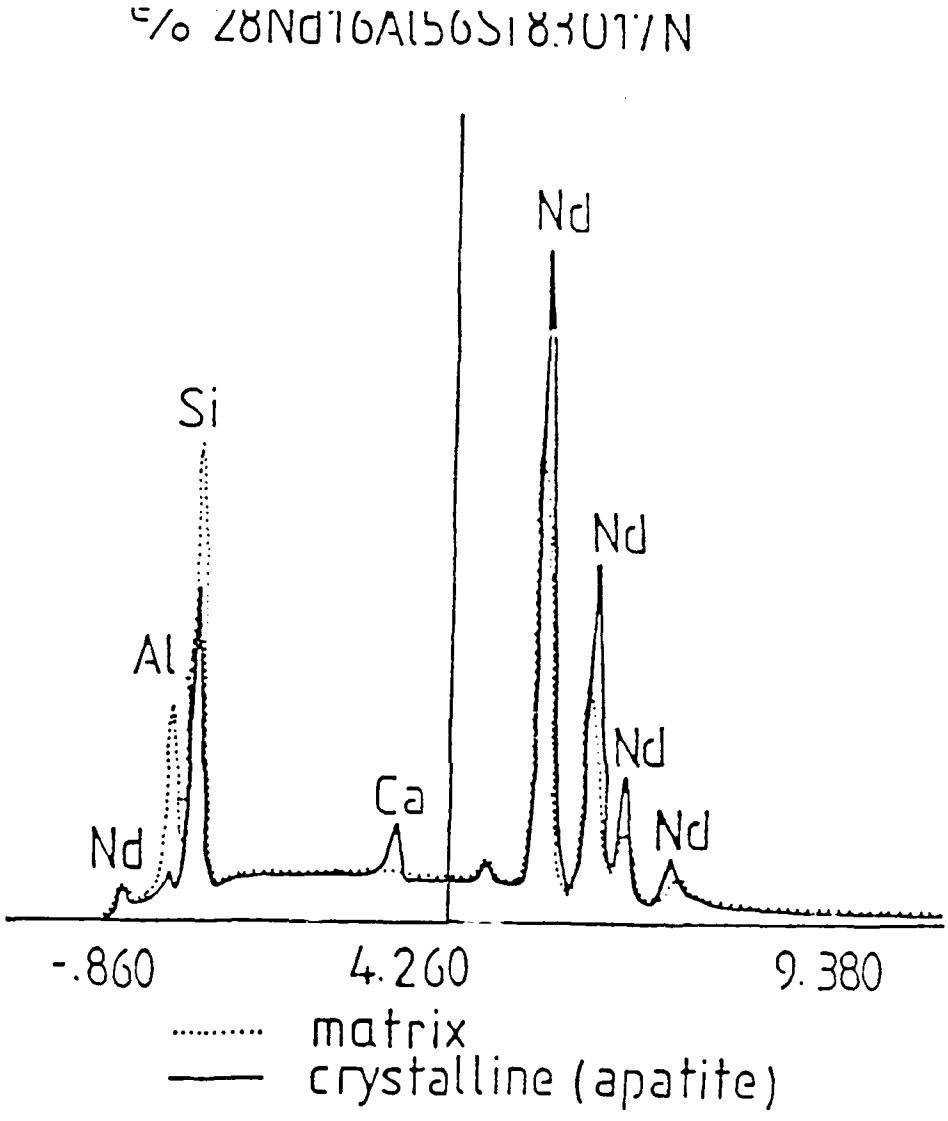

FIGURE 19 X-ray spectra for the Nd-sialon composition: (e/o) 28Nd 56Si 16Al/830 17N.

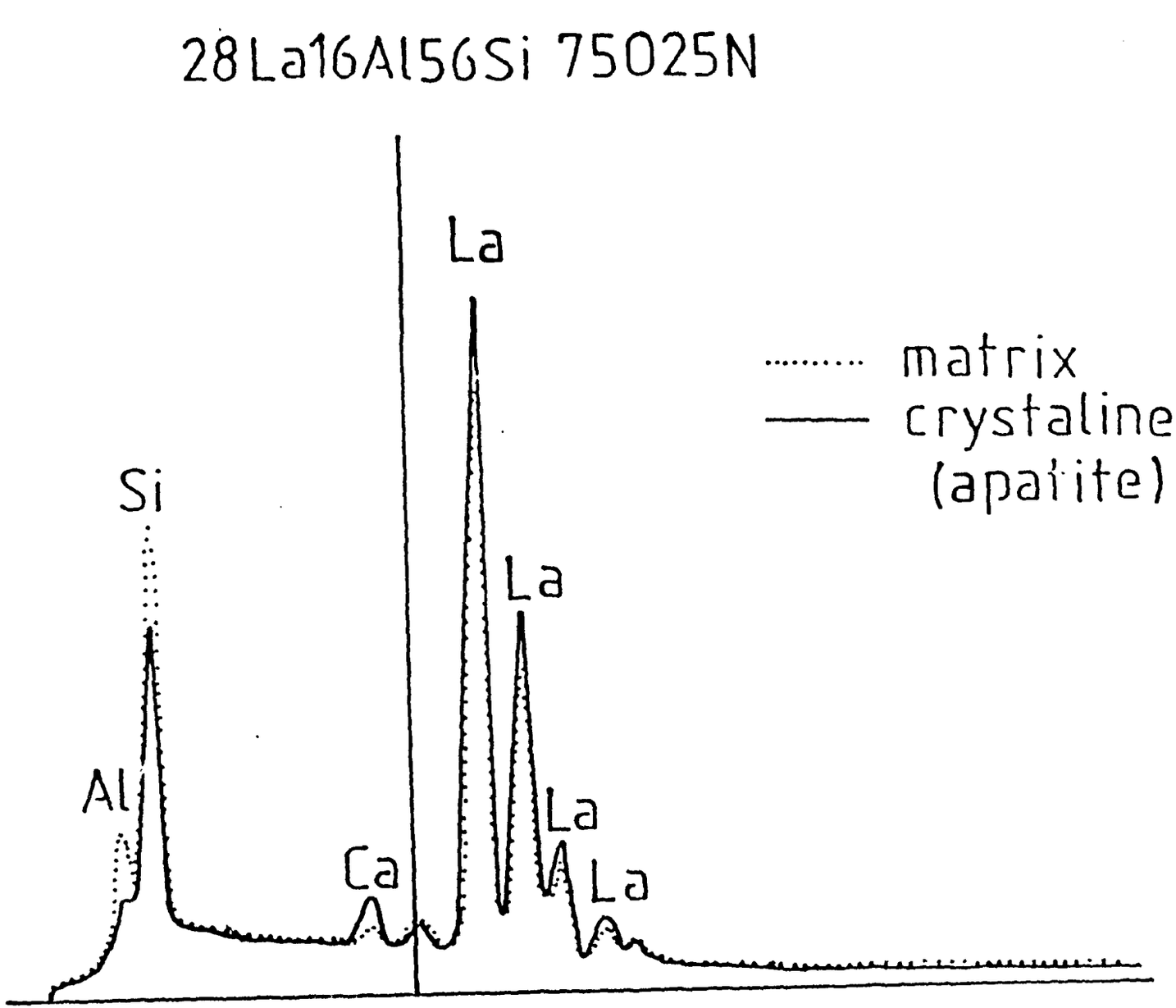

FIGURE 20 X-ray spectra for the La-sialon composition: (e/o) 28La 56Si 16Al/750 25N.

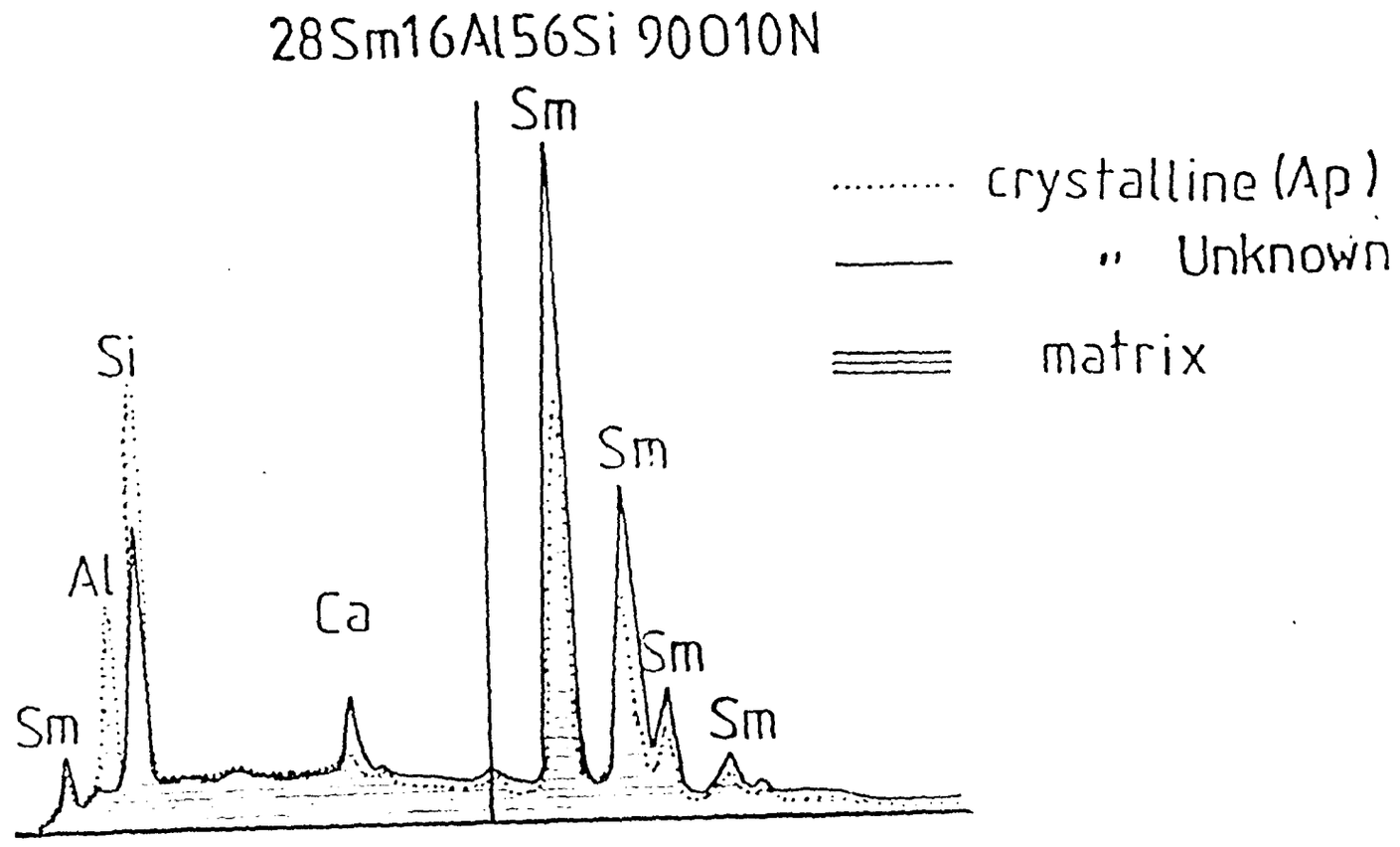

FIGURE 21 X-ray spectra for the Sm-sialon composition: (e/o) 28Sm 56Si 16Al/90O 10N.

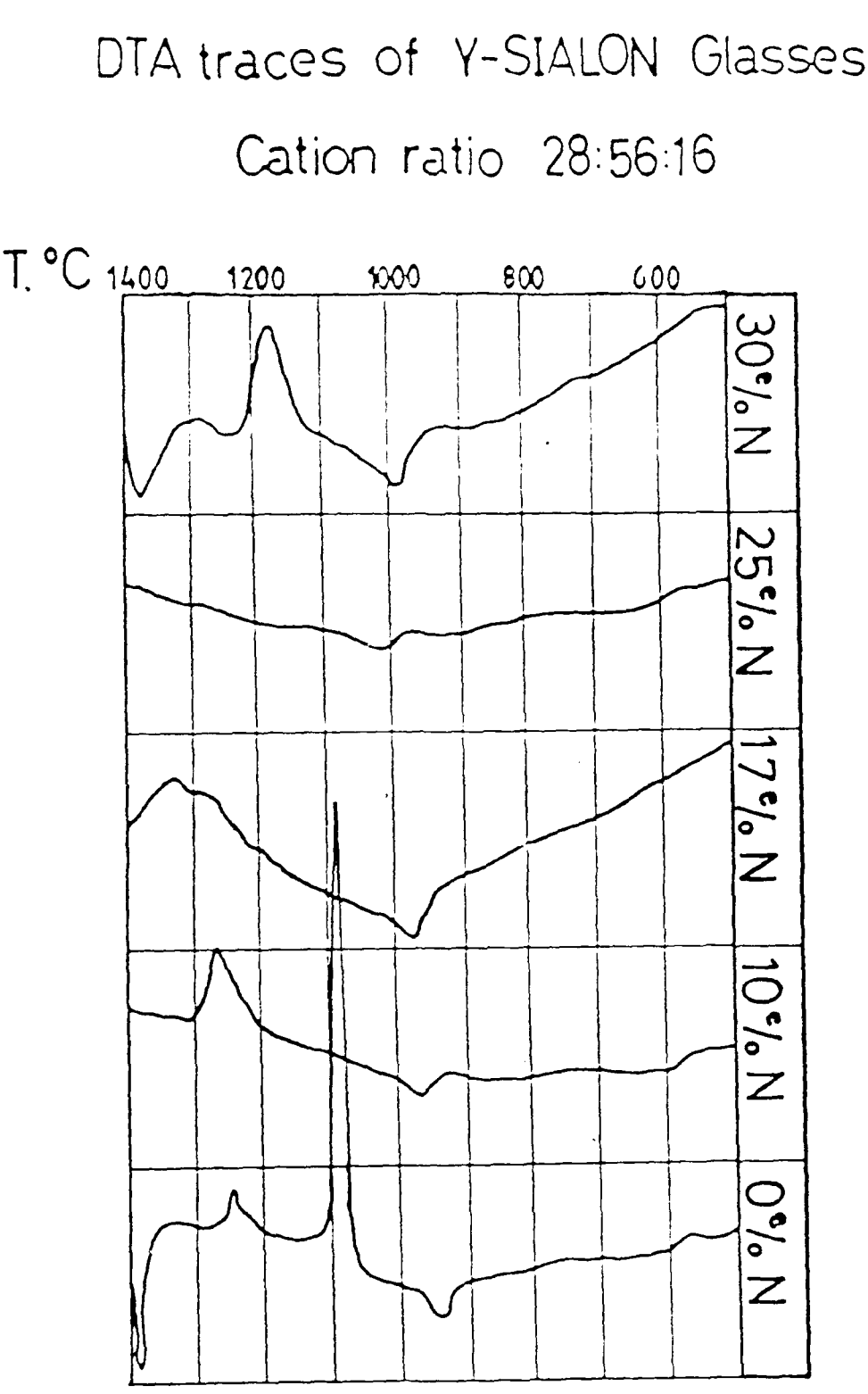

FIGURE 22 DTA traces for Y-sialon glasses (standard cation composition) showing effect of N on Tg and Tc.

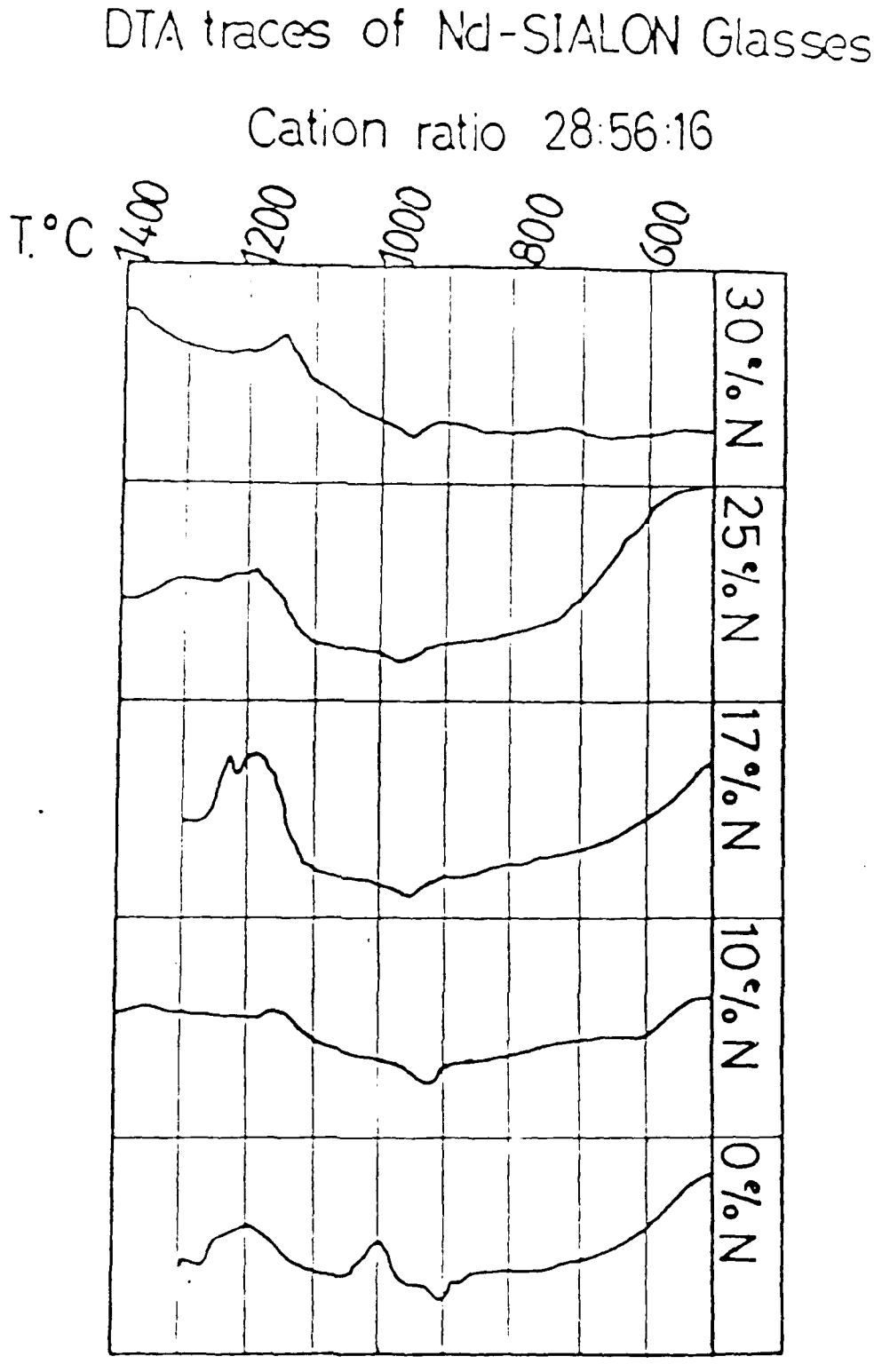

FIGURE 23 DTA traces for Nd-sialon glasses (standard cation composition) showing effect of N on Tg and Tc.

process is observed as an exothermic peak. In some instances, for example, in the 0e/o nitrogen sample in both systems, two crystallization peaks are observed indicating that more than one phase is being crystallized. In some instances it is difficult to specify a particular temperature for crystallization, e.g. in the traces for 17 and 25e/o nitrogen glasses where crystallization appears as a very broad drift rather than as a sharp exothermic peak. In all cases Tc has been taken as the highest point in the exotherm. In fact it is unclear whether optimum crystallization occurs at this temperature or not, as superior properties are developed in glasses heat-treated at temperatures below Tc. The further endothermic peak seen in the curve of the 0e/o nitrogen Y-glass in figure 22 represents melting of a crystalline phase.

The curves in figures 24 and 25 demonstrate the effect of nitrogen on these glasses. The change in Tg in both systems is shown more clearly in figure 24. The Tg values recorded are in very good agreement with those reported by Drew (34) and, for both systems, an approximately linear increase in Tg is observed as nitrogen content is increased from 0e/o to 25e/o nitrogen, after which Tg levels out. The increase observed is from 900°C at 0e/o nitrogen to 975°C at 25e/o nitrogen in the Nd-sialon system and from 940°C to 1000°C respectively in the Y-sialon system. From these trends the stabilising effect of nitrogen on the glasses is clearly demonstrated. In both systems the increase in Tg with nitrogen content is roughly parallel, with Tg values in the Y-sialon system being an average of 35°C higher, indicating that yttrium as an added cation tends to form more stable glasses.

Crystallization temperatures are plotted against nitrogen content for both systems in figure 25. Tc is seen to rise in the Nd sialon system from 1000°C at 0e/o nitrogen to 1170°C at 10e/o nitrogen and only a slight increase in Tc is then observed on further increasing the nitrogen content. In the Y-sialon system a sharp increase in Tc is observed from 1090°C at 0e/o nitrogen to 1325°C at 17e/o nitrogen, after which Tc decreases slightly. This increase in Tg and Tc reflects increasing resistance to any type of structural mobility, as the nitrogen content is increased.

The sharp distinctive crystallization peak observed on analysis of the Y-sialon (0%N) sample, which represents a rapid uninhibited crystallization process, is seen to disappear on introduction of nitrogen (figure 22). This is explained by the findings of Ahn of Thomas (30) when it was found that nitrogen decreases the tendency for crystallization to occur in Y-sialon glasses. Thus, in the absence of nitrogen, crystallization is

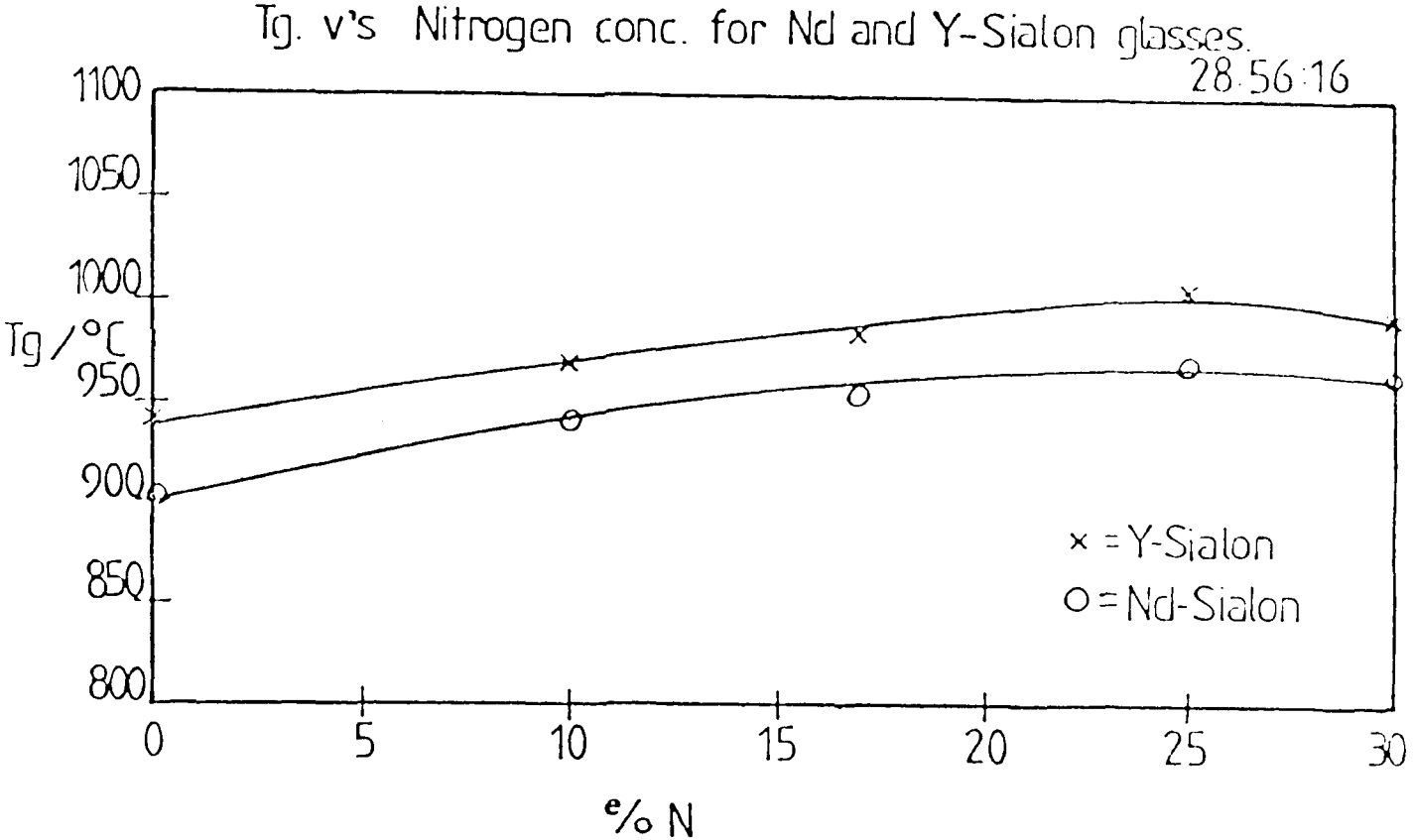

FIGURE 24 Variation of Tg with nitrogen content for Y-sialon and Nd-sialon glasses.

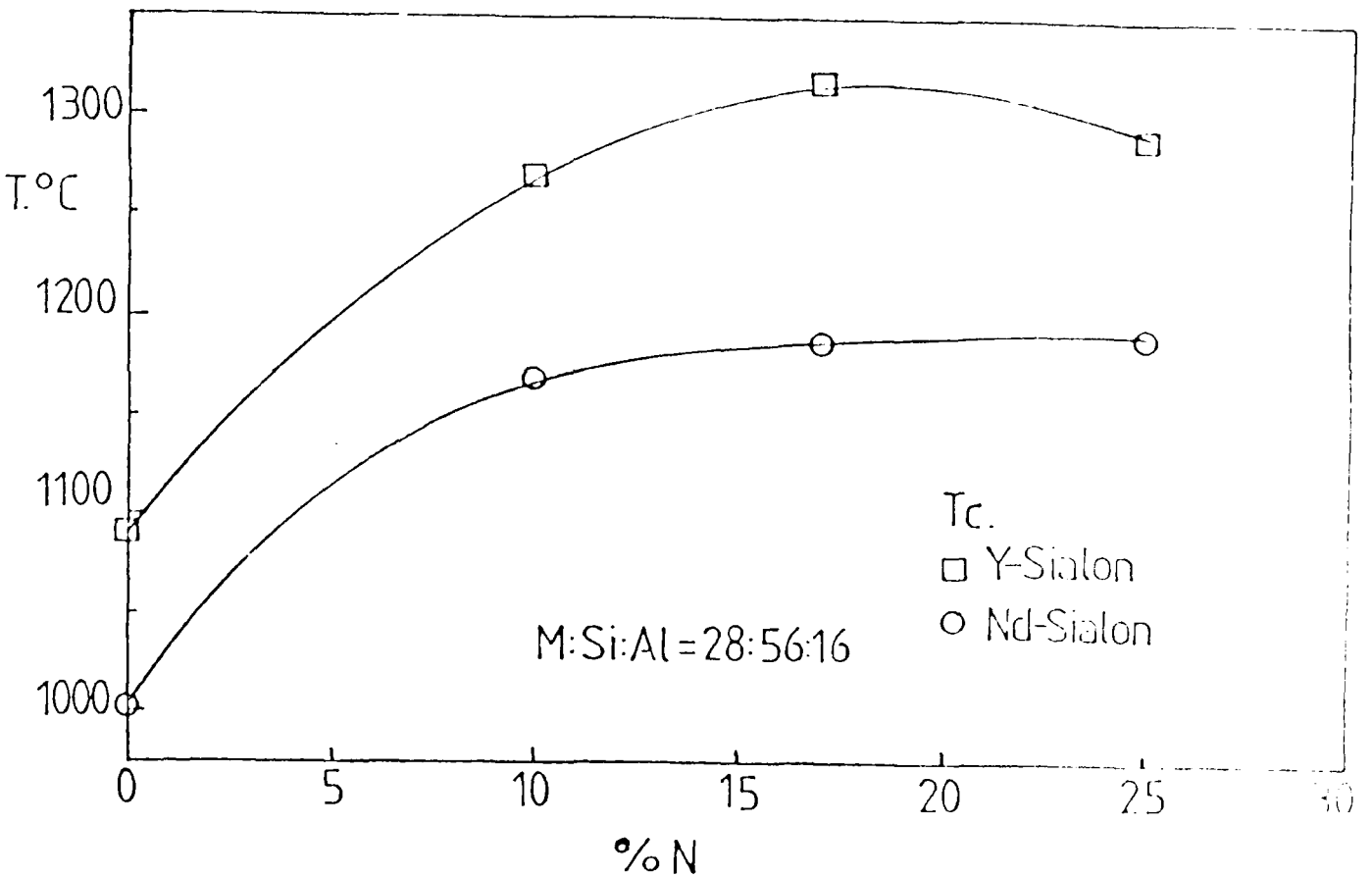

FIGURE 25 Variation of Tc with nitrogen content for Y-sialon and Nd-sialon glasses.

expected to take place more freely. This inhibiting effect of nitrogen on crystallization is observed clearly in figure 22 with crystallization peaks becoming broader and occurring at higher temperatures as the nitrogen level increases, reflecting an increasingly sluggish crystallization process. A sharper crystallization peak is observed in the 30e/o nitrogen sample and this occurs at a slightly lower temperature than samples with lower nitrogen contents. However, this sample is not fully amorphous and this peak probably represents crystallization of a glassy phase that is similar in composition to that of lower nitrogen content glasses.

One further observation from the DTA curves is that while Tc is seen to increase as nitrogen is incorporated into the samples, the onset of crystallization occurs at approximately the same temperature, in the 0, 10, 17 and 25e/o nitrogen samples in both systems (if the second crystallisation peak in the 0e/o nitrogen samples is considered). The particular crystalline phases formed corresponding to the Tc peaks in the DTA curves are listed in Table 1. The similarity in the compositions of the phases being crystallized leads to the onset of crystalliation at roughly the same temperature for different N-content samples, e.g. in the Y-sialon system, γ-$Y_2Si_2O_7$ is the main crystalline phase, while in the Nd-sialon system, $Nd_4Si_3O_{12}$ (apatite) is the primary phase.

The process of crystallization requires singificant structural rearrangement. Increases in Tc with nitrogen content, indicate that the structural rearrangement necessary for crystallization, which is itself related to viscosity, can take place only at higher temperatures, where the lower viscosity allows more structural mobility.

From the data on Tg and Tc, various heat-treatment schedules have been applied to a range of glasses and microhardness tests have been carried out on samples after heat-treatment at various temperatures in order to optimise the glass-ceramic process.

5.5 Heat treatments on Sm-Sialon glasses

The effects of heat-treatment on Sm-sialon glasses with standard cation composition and varying N contents has been investigated. Heat treatment was carried out over a range of temperature from Tg to Tc for 2.5 and 24 hours.

Figure 26 shows that, in general, microhardness appears to decrease with increasing annealing temperature. The decrease is associated with initial crystallization in these glasses

TABLE 1

Crystalline phases corresponding to Tc peaks in the Nd and Y-sialon systems $M_xSi_{12-(m+n)}Al_{(m+n)}O_nN_{16-n}$

Nitrogen Content	Crystalline Phase corresponding to Tc	
e/cN	Nd-sialon system	Y-sialon system
	Tc_1 Tc_2	Tc_1 Tc_2
Ce/c	Apatite + $Nd_2Si_2O_7$	y-$Y_2Si_2O_7$ + x
10	Apatite + $Nd_2Si_2O_7$	y-$Y_2Si_2O_7$
17	Apatite	y-$Y_2Si_2O_7$
25	Apatite	$Y_5N(SiO_4)_3$

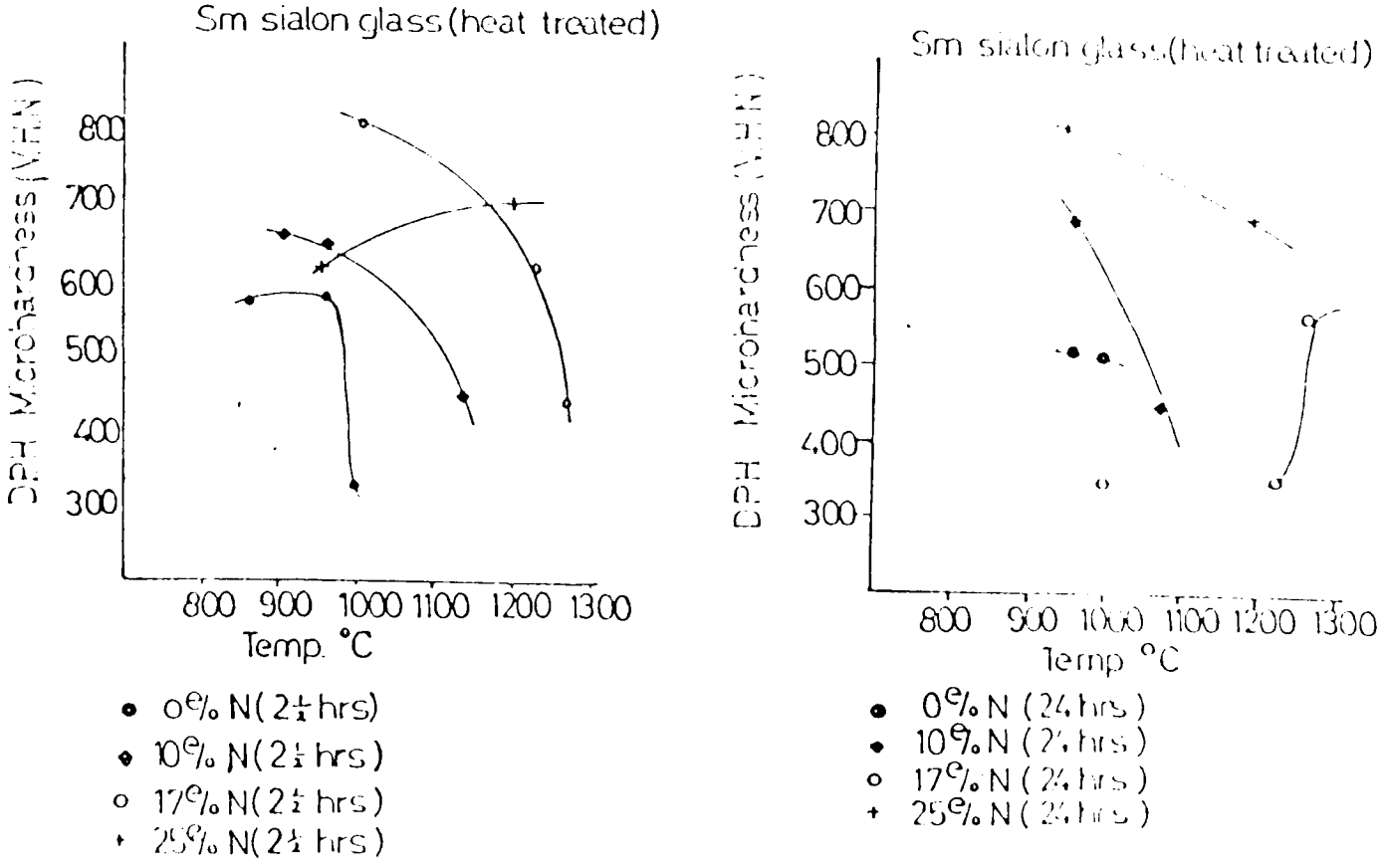

FIGURE 26 Effect of heat treatment temperature after (a) 2.5 hours, (b) 24 hours annealing on microhardness of Sm-sialon glasses (standard cation composition).

although there is no significant difference in values obtained from 2.5 and 24 hour treatment programmes except in the case of the 17 e/oN samples where microhardness values follow the general trend for 2.5 hour treatments but appear to increase when annealed above 1200°C for 24 hours. This may be due to the presence of a secondary phase of higher hardness. On X-ray analysis, an unknown phase is observed along with apatite ($Sm_4Si_3O_{12}$) in a sample heat-treated at Tc (1265°C) for 24 hours.

Scanning electron microscopy (see figure 27) shows two types of crystals present: (1) small black needle-like crystals and (2) larger white lath-like crystals. From the analysis, the black crystals are a form of samarium silicate, possibly apatite, while the white crystals contain much less Sm and Si by comparison.

Heat treatment of a Sm-glass containing no nitrogen at 998°C (Tc) for 24 hours resulted in an unusual colour effect with brown and red coloured bands observed across the sample. Figure 28 shows a scanning electron micrograph from the interface of two different coloured bands. In one region, much larger white crystals (up to 10μm length) are observed while in the adjoining region, they are much smaller. Only apatite was detected by X-ray analysis and, so far, compositional differences have not been determined between the two regions but this may account for the differences in crystal growth rates.

5.6 Optimization of heat-treatment schedules for Nd-sialon glass-ceramics

In both the Nd- and Y-sialon systems, glasses were heat-treated using single and double stage heat-treatments. Single stage heat-treatments of glasses in the Nd-sialon system, were carried out at temperatures between 900°C and 1185°C. Nucleation occurs above Tg and extensive crystallization takes place on heat-treatment below Tc.

Two parameters are variable during such heat-treatments, i.e. time and temperature. To investigate the effect of heat-treatment temperature, time was held constant at 2.5 hours. Therefore all single stage heat-treatments were carried out for 2.5 hours while double heat-treatments required a further period of 2.5 hours at a higher temperature. In a few cases longer heat-treatment times of up to 24 hours were used.

The resulting phase assemblages, determined by X-ray analysis of Nd-sialon samples subjected to single stage heat-treatments

FIGURE 27 Scanning electron micrograph of Sm-sialon standard composition (17e/oN) after heat-treatment for 24 hours at Tc (1265°C).

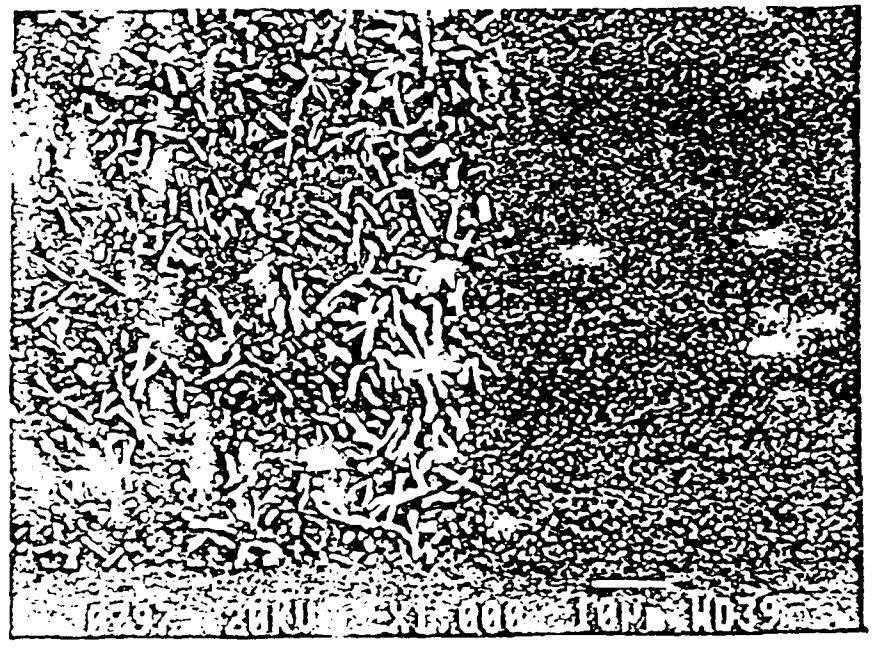

FIGURE 28 Scanning electron micrograph of Sm-sialon standard composition (0 e/oN) after heat-treatment for 24 hours at Tc (998°C).

at various temperatures, are shown in Table 2. The heat-treatment temperature is also shown. In almost all cases the apatite phase is present with $Nd_2Si_2O_7$ also formed in samples with lower nitrogen concentrations. Figure 29 shows variation of microhardness in these samples as the heat-treatment temperature is increased. It seems evident from this figure that single stage heat-treatment of Nd-sialon glasses, at any temperature, does little to improve properties. In samples containing 0, 10 and 17e/o nitrogen, hardness is seen to decrease as the heat-treatment temperature rises above 1100°C.

Characterisation of these heat-treated samples by SEM reveals white, often hexagonally shaped crystals in a grey matrix. Figure 30 shows a scanning electron micrograph of the Nd-Si-Al-O-N composition containing 0e/o N after heat treatment at 1155°C for 2.5 hours and it is evident that at this temperature the glass phase begins to soften and flow around the crystals.

Observations on the fast cooled Nd-Si-Al-O-N glass compositions, containing up to 25e/o N, by scanning electron microscopy show that very small crystals are nucleated but these are not detectable by X-ray diffraction. The scanning electron micrograph (a) and X-ray spectra (b) for the composition containing 25e/o N are shown in figure 31. As can be seen, phase separation is observed. The glass matrix is aluminium-rich while the phase separated regions contain Nd, Si and small amounts of Al and Ca. In contrast, scanning electron microscopy reveals, in the Nd-Si-Al-O-N composition containing 30e/o N, the presence of dark grey crystalline regions in a glassy grey matrix. The dark grey crystals are β-silicon nitride, which is the only crystalline phase detected by X-ray diffraction.

With 10e/o N content, no crystalline phases are observed in the as-quenched glass nor after heat treatment for 2.5 hours at Tg (940°C). However, at 960°C, apatite and $Nd_2Si_2O_7$ phases are detected and the amount of $Nd_2Si_2O_7$ increases as heat treatment temperature increases, until just above the crystallization temperature (Tc = 1170°C), Y-phase is also formed.

Figure 32 shows scanning electron micrographs of the Nd-Si-Al-O-N glass composition containing 10e/o N after heat treatment for 2.5 hours at (a) 1095°C, (b) 1155°C and (c) 1185°C.

At 1095°C, which is 55°C higher than the Tg point for this composition, nucleation of crystals has developed such that the average diameter is approximately 0.5μm and the length is approximately 15μm.

Table 2: Phase assemblages of Nd-Si-Al-O-N glass compositions as quenched and heat treated at various temperatures.

Nitrogen Content (e/o)	Heat Treatment Temperature (°C)	Heat Treatment Time(h)	Phase Assemblage
0	As quenched	-	-
	900°C (Tg)	2.5	Apatite (t)
	940°C	"	Apatite (m)
	980°C (Tc_1)	"	Apatite (M)+$Nd_2Si_2O_7$(t)
	1000°C	"	" +$Nd_2Si_2O_7$(t)
	1095°C	"	$Nd_2Si_2O_7$
	1155°C	"	$Nd_2Si_2O_7$
10	As quenched	-	X
	940°C (Tg)	2.5	-
	960°C	"	Apatite+$Nd_2Si_2O_7$(t)
	1095°C	"	Apatite+$Nd_2Si_2O_7$
	1155°C	"	Apatite+$Nd_2Si_2O_7$
	1170°C (Tc)	"	Apatite+$Nd_2Si_2O_7$
	1185°C	"	Apatite+$Nd_2Si_2O_7$
17	As Quenched	-	-
	960°C (Tg)	2.5	-
	980°C	"	
	1095°C	"	Apatite(m)
	1155°C	"	Apatite(m)
	1185°C (Tc)	"	Apatite(m)
25	As Quenched	-	-
	980°C (Tg)	2.5	Apatite(t)
	1095°C	"	Apatite(t)
	1155°C	"	Apatite(m)
	1185°C (Tc)	"	Apatite(m)

m = minor
t = trace
M = Major

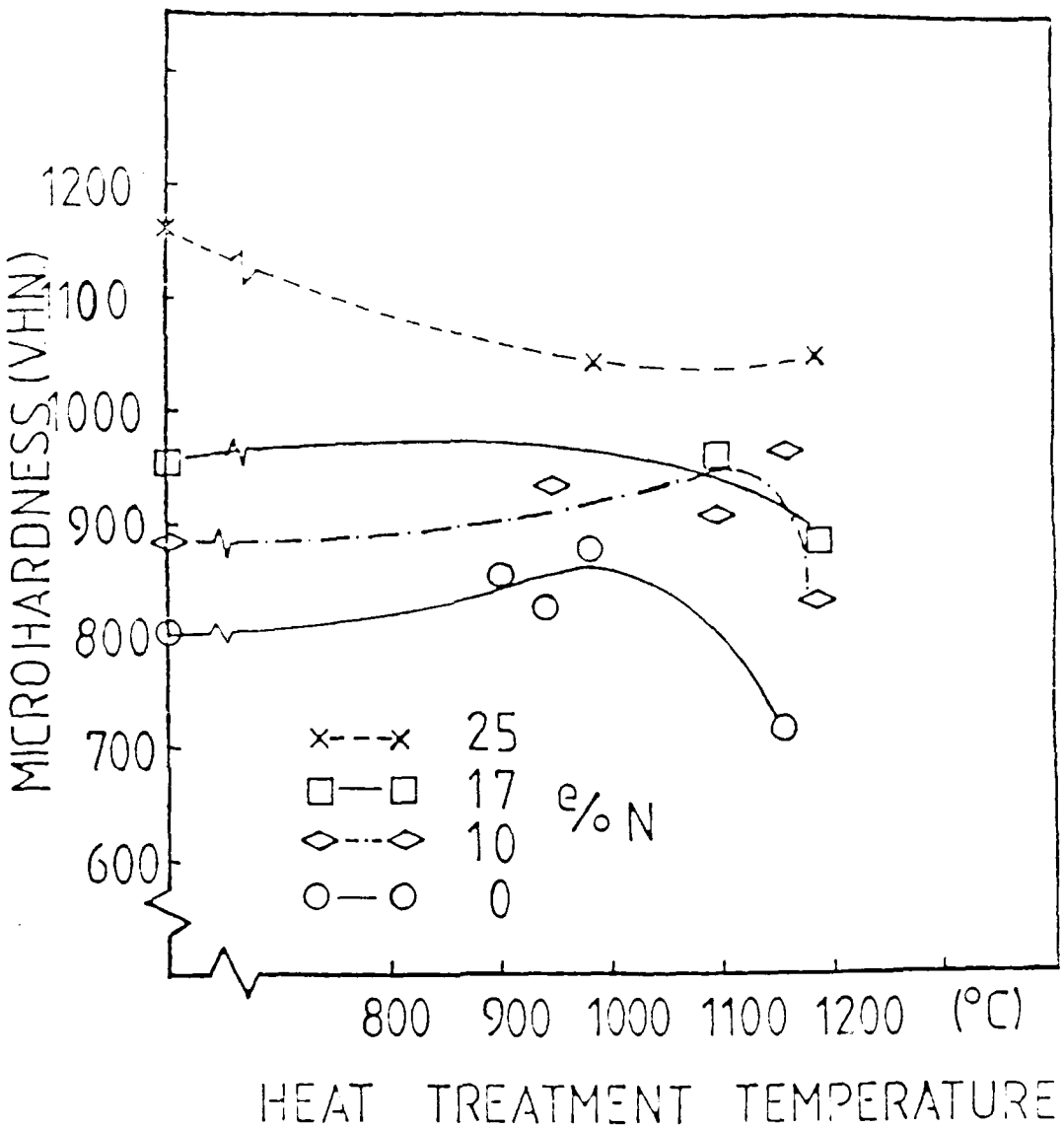

FIGURE 29 Effect of heat treatment temperature (2.5 hours anneal) on microhardness of Nd-sialon glasses (standard cation composition).

FIGURE 30 Scanning electron micrograph of Nd-sialon composition (0e/o N) after heat treatment at 1155°C for 2.5 hours.

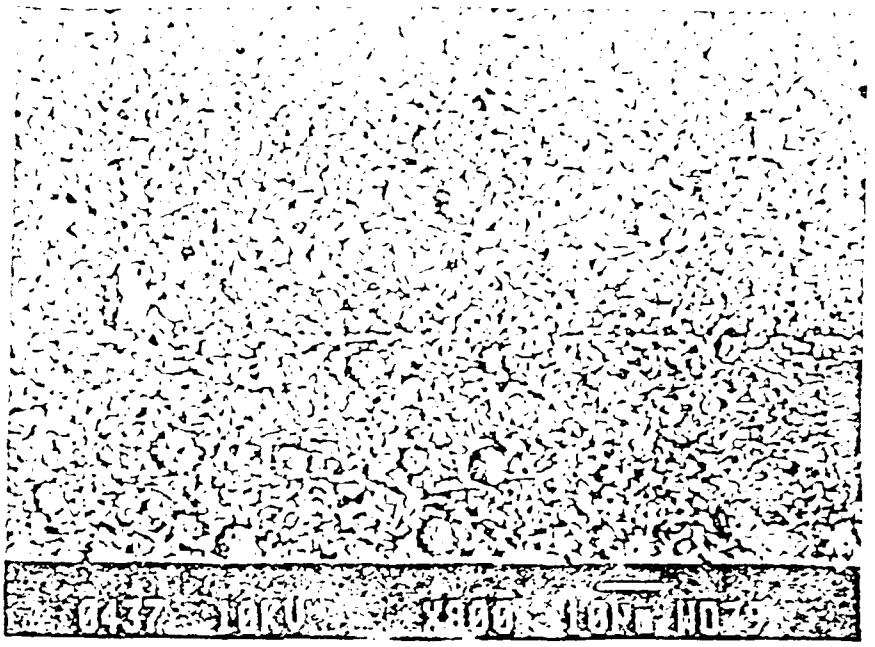

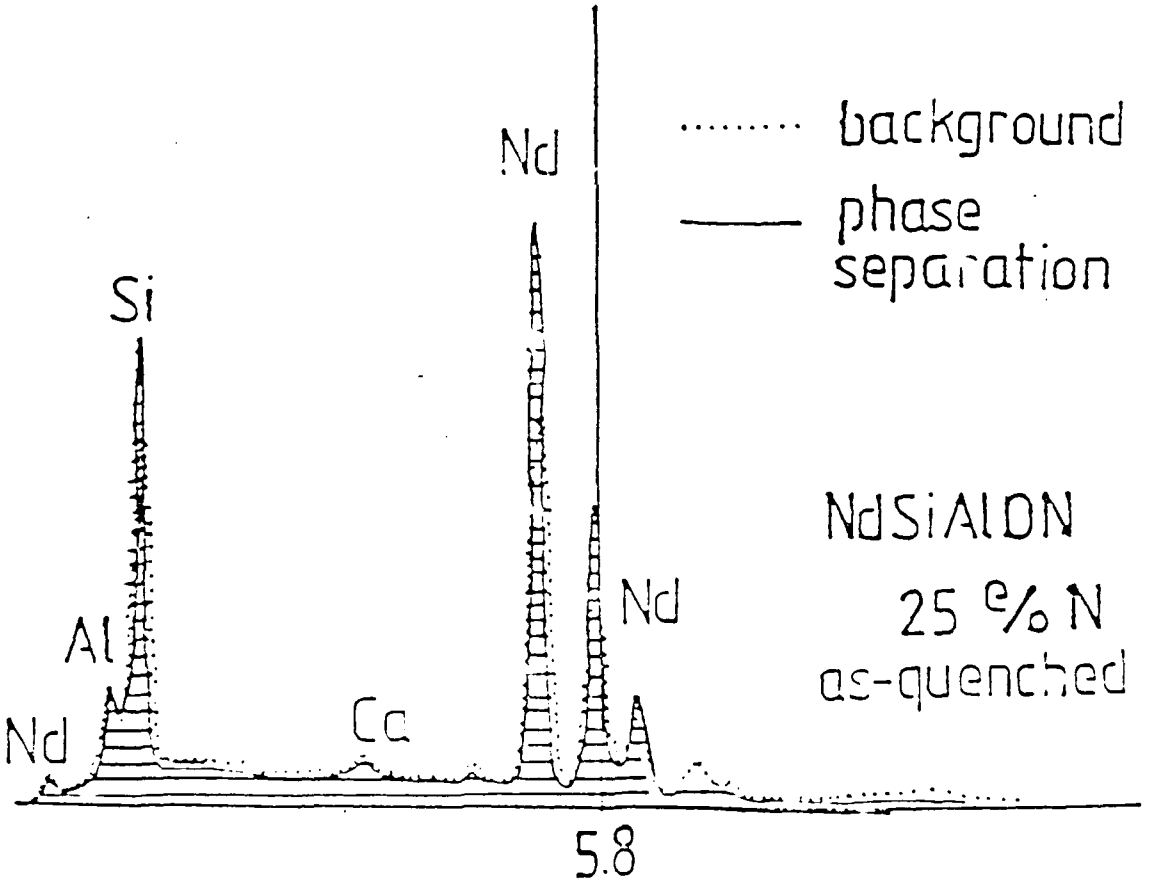

FIGURE 31 (a) Scanning electron micrograph and (b) X-ray spectra for the Nd-sialon glass composition (25e/o N) after firing.

At 1155°C (Figure 32b), before the Tc point (1170°C), two distinct crystallization areas are observed. The general background view consists of small hexagonal or circular cross-section, elongated crystals. The diameter of these fully formed crystals is in the range 0.5-1μm and their length varies from 5 to 8μm. The homogeneity of the background is interrupted by isolated islands which also contain some irregular shaped crystals. These crystals are quite directional forming in parallel rows approximately 2μm apart and extending to 80-90μm.

At 1185°C, which is above the temperature of the crystallisation peak, the general structural view (Figure 32c) is exactly the same as the previous crystallization sample (1155°C) and the scanning electron micrograph (lower magnification) shows a region of inhomogeneity, as observed at the lower heat treatment temperature, but the crystals are coarser and more hexagonal shaped rather than circular in cross-section with diameters of approximately 1.5-2μm. The large crystals in the separated regions are mainly neodymium silicate ($Nd_2Si_2O_7$).

Figure 33 compares the microstructures of Nd-Si-Al-O-N glass-ceramics containing (a) 10e/o, (b) 17e/o, and (c) 25e/o nitrogen after heat treatment at 1185°C for 2.5 hours. With 10e/o nitrogen content, the Nd-Si-Al-O-N glass-ceramic contains three different crystalline phases; apatite, $Nd_2Si_2O_7$ and Y-phase (YAM-type). The scanning electron micrograph (of figure 33a) shows the homogeneous region containing the apatite phase which forms hexagonal crystals of approximately 1 to 2μm cross-section. The other crystalline phases are located in the phase separated regions.

With 17e/o nitrogen content, the Nd-Si-Al-O-N glass-ceramics form only apatite phase after heat treatment and the crystals are 4-5μm in diameter with large regions of residual glass phase.

Above 10e/o nitrogen, apatite is the only crystalline phase detected. Observations by scanning electron microscopy of the Nd-Si-Al-O-N composition containing 17 and 25e/o nitrogen show only elongated, hexagonal crystals of apatite and the amount of this phase increases as the heat treatment temperature increases.

With 25e/o nitrogen content, the Nd-Si-Al-O-N glass-ceramics again form only apatite phase with crystal diameters of 0.4-0.6μm and lengths of 4-6.5μm and much less residual glass phase.

fig (a)

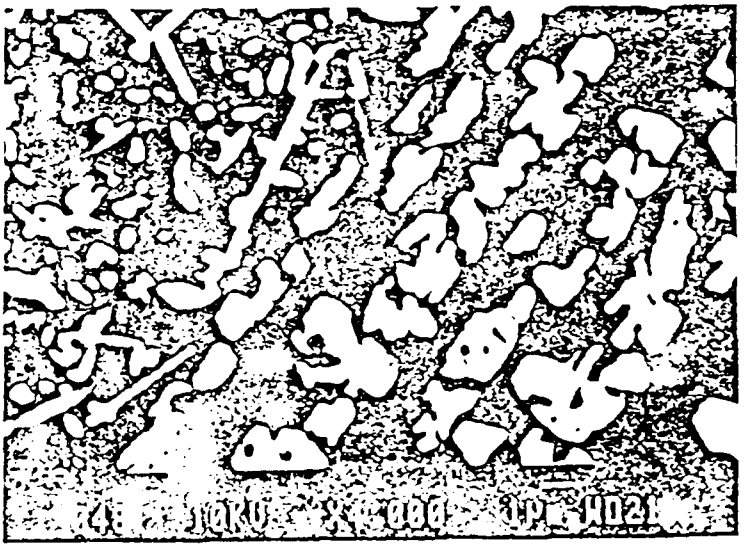

fig (b)

FIGURE 32 Scanning electron micrographs of Nd-sialon composition (10e/o N) after heat treatment for 2.5 hours at (a) 1095°C, (b) 1155°C and (c) 1185°C.

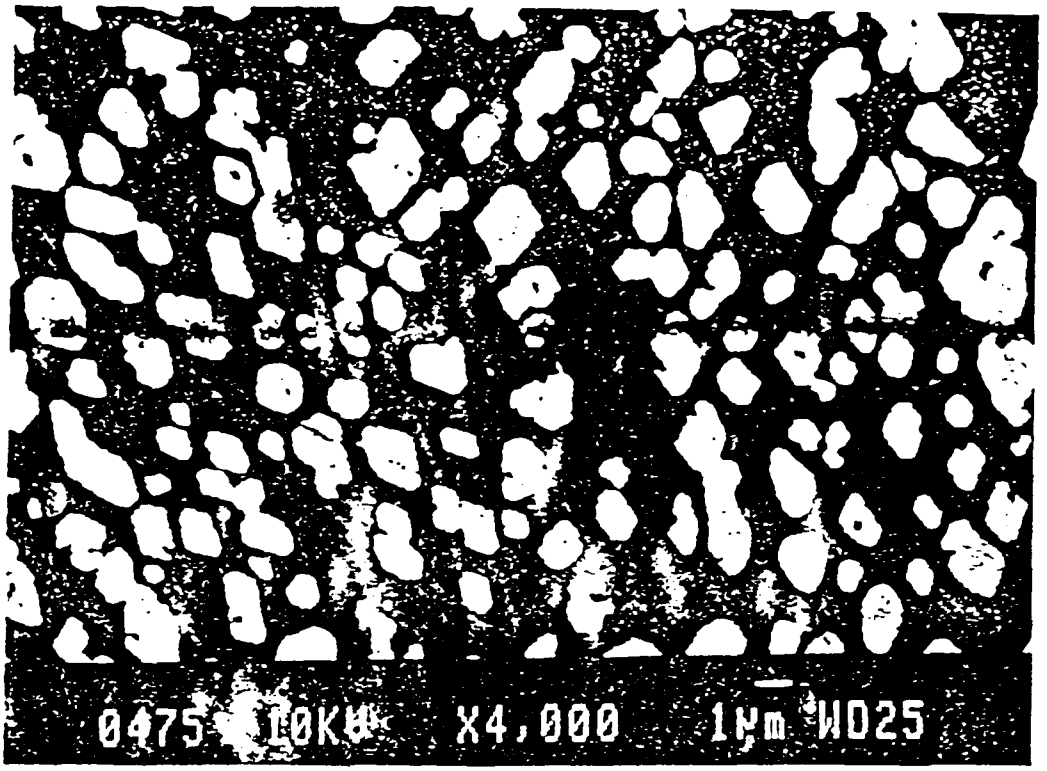

fig. 3(c)

FIGURE 32 Scanning electron micrographs of Nd-sialon composition (10e/o N) after heat treatment for 2.5 hours at (a) 1095°C, (b) 1155°C and (c) 1185°C.

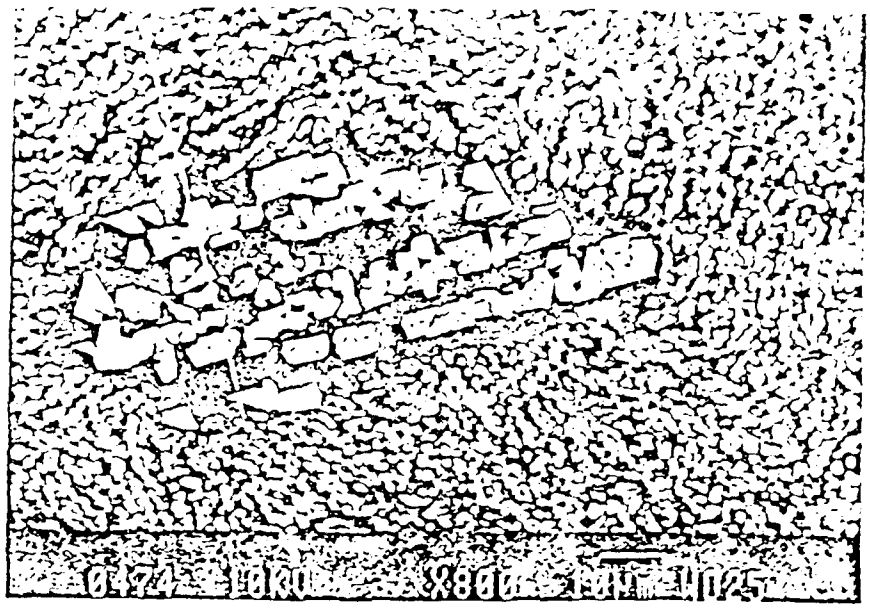

fig. (a)

fig. (b)

FIGURE 33 Scanning electron micrographs of Nd-sialon glass-ceramics containing (a) 10e/o (b) 17e/o and (c) 25e/o N after heat-treatment at 1185°C for 2.5 hours.

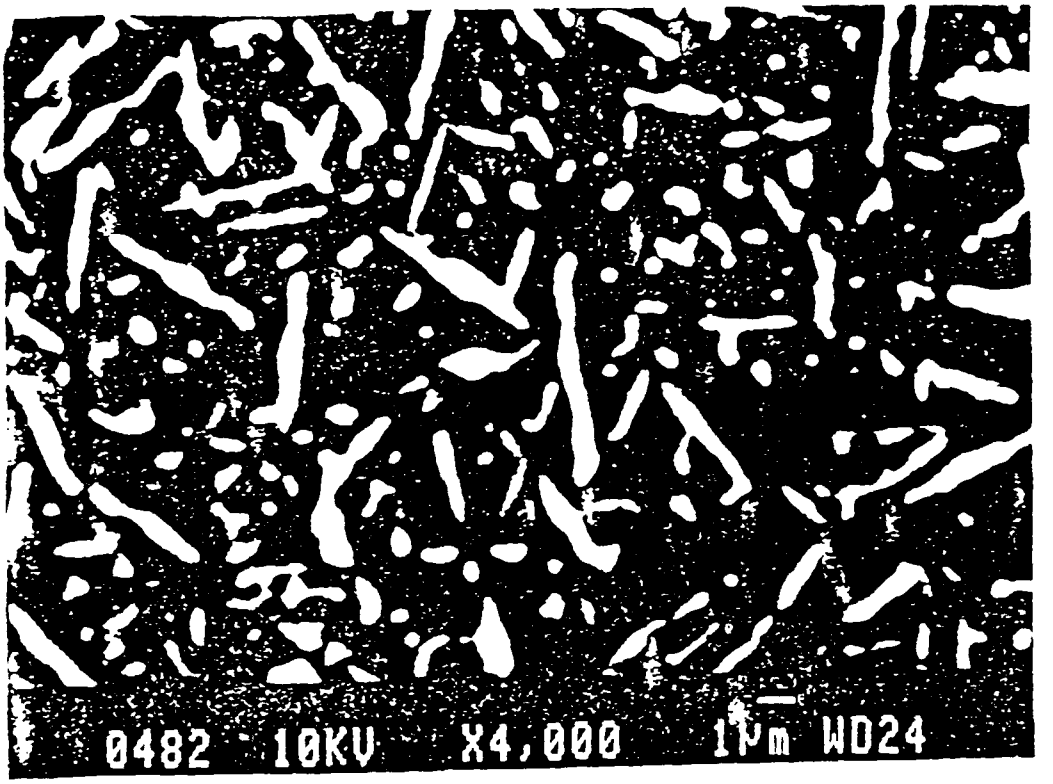

fig. (c)

FIGURE 33 Scanning electron micrographs of Nd-sialon glass-ceramics containing (a) 10e/o (b) 17e/o and (c) 25e/o N after heat-treatment at 1185°C for 2.5 hours.

Single stage heat-treatments of Nd-sialon glasses do not appear to have any beneficial effect on mechanical properties probably because the crystallization process is incomplete, indicating that samples in this system require an initial nucleation stage in the crystallization process before crystal growth leads to property improvement.

Results of X-ray analysis of samples in the Nd-sialon system, subjected to double stage heat-treatments are presented in Table 3. Results of samples subjected to longer term heat-treatments are also included in the table. Apatite is the only crystalline phase found in all samples that have had two-stage heat-treatments for extended periods.

The temperatures used in the double heat-treatment process were chosen such that the first temperature was a set interval eg. 50 or 90°C higher than Tg, which should be suitable for nucleation to occur, and the second temperature was a temperature related to Tc, which should allow crystal growth. The temperatures used and their relationship to Tg and Tc are presented in Table 4. Variations in microhardness after double heat treatments of samples in the Nd sialon system are shown in figure 34. This figure shows that significant improvements in microhardness are obtained but the first obvious trend is that while hardness does improve substantially in the nitrogen containing samples, only a very small improvement in hardness is observed in the samples with 0% nitrogen. Only five of the seven double heat-treatments were used for this sample, as in two cases the nucleation temperature of Tg+90 is higher than the crystallization temperature of Tc-60. Scanning electron microscopical analysis of these samples revealed that little or no crystal growth had occurred.

In the nitrogen-containing samples hardness increases substantially The most significant increase in hardness is seen in the sample containing 10e/o nitrogen where hardness increases from 850D.P.H in the as-quenched sample to 1030D.P.H. when heat-treated for 2.5 hours at Tg+50°C followed by a further 2.5 hours at Tc-40°C. This particular heat-treatment also produces the maximum hardness in the 17e/o nitrogen sample and also a good improvement in the 25e/o nitrogen sample.

The double heat-treatments are in two groups. In the first group of 3, the nucleation temperature is held constant at Tg+50, while the crystallization temperature is varied from 60°C below Tc (Tc-60) to Tc itself. In the second group the nucleation temperature is again held constant but at a higher temperature of Tg+90°C, while the crystallization temperature is again varied from 60°C below Tc to 50°C above Tc. This

TABLE 3

Crystalline Phases detected in Nd-sialon glasses after heat treatment at various temperatures.

Nitrogen Content e/o	Heat-Treatment Temp. (°C)	Heat Treatment Time (h)	Crystalline Phase detected
0	- (as quenched)	-	-
0	980°C	2.5	Apatite (t)
10	1185°C	2.5	$Nd_2Si_2O_7$
17	940 + 1170	2.5+2.5	$Nd_4Si_3O_{12}$ (apatite)
	960 + 1185	2.5+2.5	$Nd_4Si_3O_{12}$
	1000 + 1185	2.5+2.5	$Nd_4Si_3O_{12}$
	960 + 1185	12+12	$Nd_4Si_3O_{12}$
	1185	25	$Nd_4Si_3O_{12}$
25	1000 + 1185	21 + 2	$Nd_4Si_3O_{12}$
	1020	25	$Nd_4Si_3O_{12}$

TABLE 7

Relationship between Tg, Tc and the heat-treatment temperatures used during 2-stage heat treatments of Nd-sialon glasses.

Code	Relationship to Tg and Tc	Heat-treatment temperatures (°C) 0e/0N	10e/0N	17e/0N	25e/0N
A	Tg+50, Tc-60	950+ 950	995+1110	1005+1125	1025+1125
B	Tg+50, Tc-40	950+ 990	995+1130	1005+1145	1025+1145
C	Tg+50, Tc	950+1000	995+1170	1005+1185	1025+1185
D	Tg+90, Tc-60	-	1035+1110	1045+1125	1065+1125
E	Tg+90, Tc-40	-	1035+1130	1045+1145	1065+1185
F	Tg+90, Tc	990+1000	1035+1170	1045+1185	1065+1185
G	Tg+90, Tc+50	990+1050	1035+1220	1045+1235	1065+1235

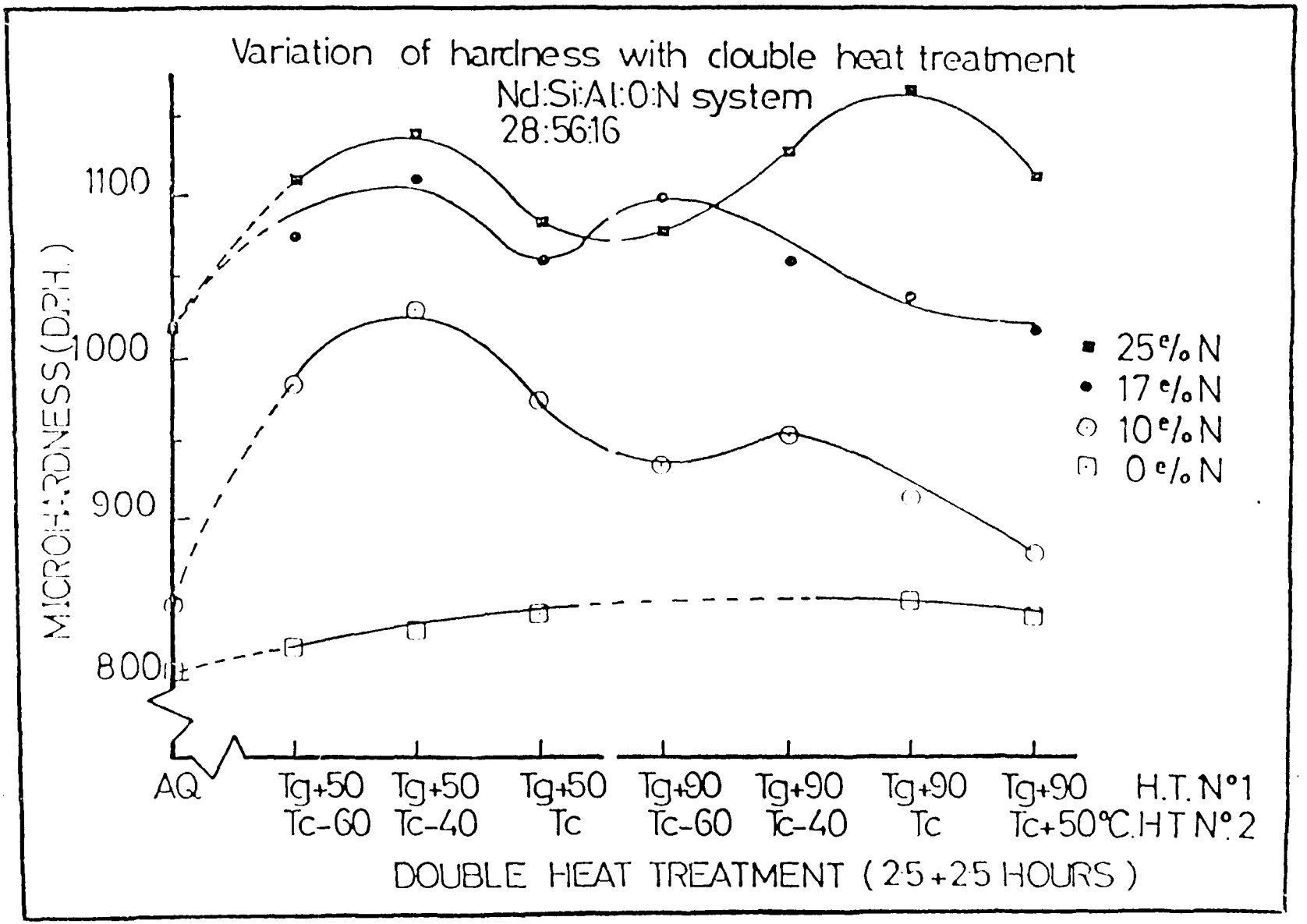

FIGURE 34 Effect of double stage heat-treatments on microhardness of Nd-sialon glasses (standard cation composition).

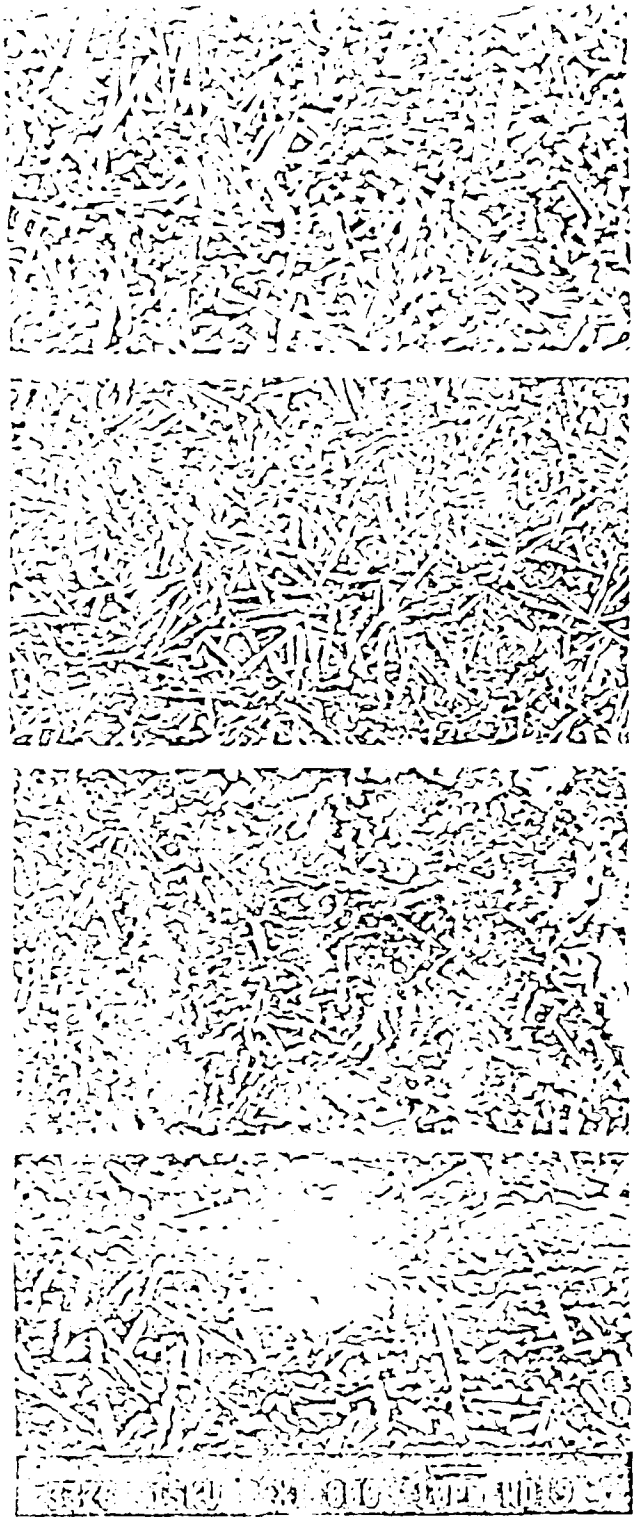

FIGURE 35 Scanning electron micrographs of Nd-sialon glasses (10e/oN) after 2-stage heat-treatments (2 x 2.5 hours) at (a) Tg+50 and Tc-60, (b) Tg+50 and Tc-40, (c) Tg+50 and Tc, (d) Tg-90 and Tc-40.

allows the effect of both the nucleation and crystallization temperatures to be observed. It appears that the lower nucleation temperature of Tg+50, as opposed to the higher temperature of Tg+90, leads to development of superior properties in most glasses. This indicates that if the nucleation temperature is too high, crystal growth occurs prematurely, without allowing time for sufficient nucleatiion.

Figure 35 shows scanning electron micrographs of 10e/o nitrogen samples after different heat-treatments. Figures a,b and c are from samples that have had the same nucleation temperature but increasing crystallization temperature as follows:

- (a) Tg+50 & Tc-60,
- (b) Tg+50 & Tc-40,
- (c) Tg+50 & Tc,
- (d) Tg+90 &Tc-40 (higher nucleation temperature).

Apatite is the only crystalline phase developed as evidence by X-ray analysis. Figure 35a shows an interlocking network of elongated crystals which are all of the same type and with lengths <20μm. Figure 35b shows a similar microstructure but with an even more tightly interlocked network of crystals which are longer and show appearances of dendritic growth in places. This improved microstructure has observed the maximum hardness value observed in this system. Crystallization at a higher temperature gives microstructure c, where the crystals are no longer closely interlocked, but are dispersed and more irregular in shape. This is reflected in a decreased microhardness value for this sample. Finally, figure 35d shows a micrograph of the same sample heat-treated at Tg+90 & Tc-40, i.e. with a higher nucleation temperature. Here, crystal growth is good but the number of crystals is smaller indicating insufficient nucleation. Again, microhardness of this sample is lower.

5.7 Optimization of heat-treatment schedules for Y-sialon glass-ceramics

Both single and double heat-treatments were carried out on Y-sialon glasses and microhardness of the resulting glass-ceramics were measured.

Results of X-ray analysis of Y-sialon glasses, after single-stage heat-treatments at various temperatures, are given in table 5. The most common crystalline phase is yttrium

TABLE 5

Phase assemblage of Y-sialon glass-ceramics after single stage heat treatments for 2.5 hours of various temperatures.

e/cN	Heat-Treatment Temperature(°C)	Time (h)	Crystalline Phases detected
0	950	2.5	- (all glass)
"	1050	"	γ-$Y_2Si_2O_7$+X
"	1200	"	Y_2O_3
10	1000	2.5	γ-$Y_2Si_2O_7$(t)
"	1200	"	γ-$Y_2Si_2O_7$+X
"	1400	"	Keivilite + $Y_5N(SiO_4)_3$
17	1000	2.5	-
"	1100	"	-
"	1200	"	$Y_2Si_2O_7$+$Y_4Si_2N_2O_7$
"	1250	"	$Y_2Si_2O_7$ + $Y_4Si_2N_2O_7$
"	1400	"	
25	1050	2.5	$Y_5N(SiO_4)_3$(t)
"	1400	"	$Y_{4.67}(SiO_4)_3O$+$Y_5N(SiO_4)_3$

Keivilite = β-$Y_2Si_2O_7$ x = unknown (t) = trace

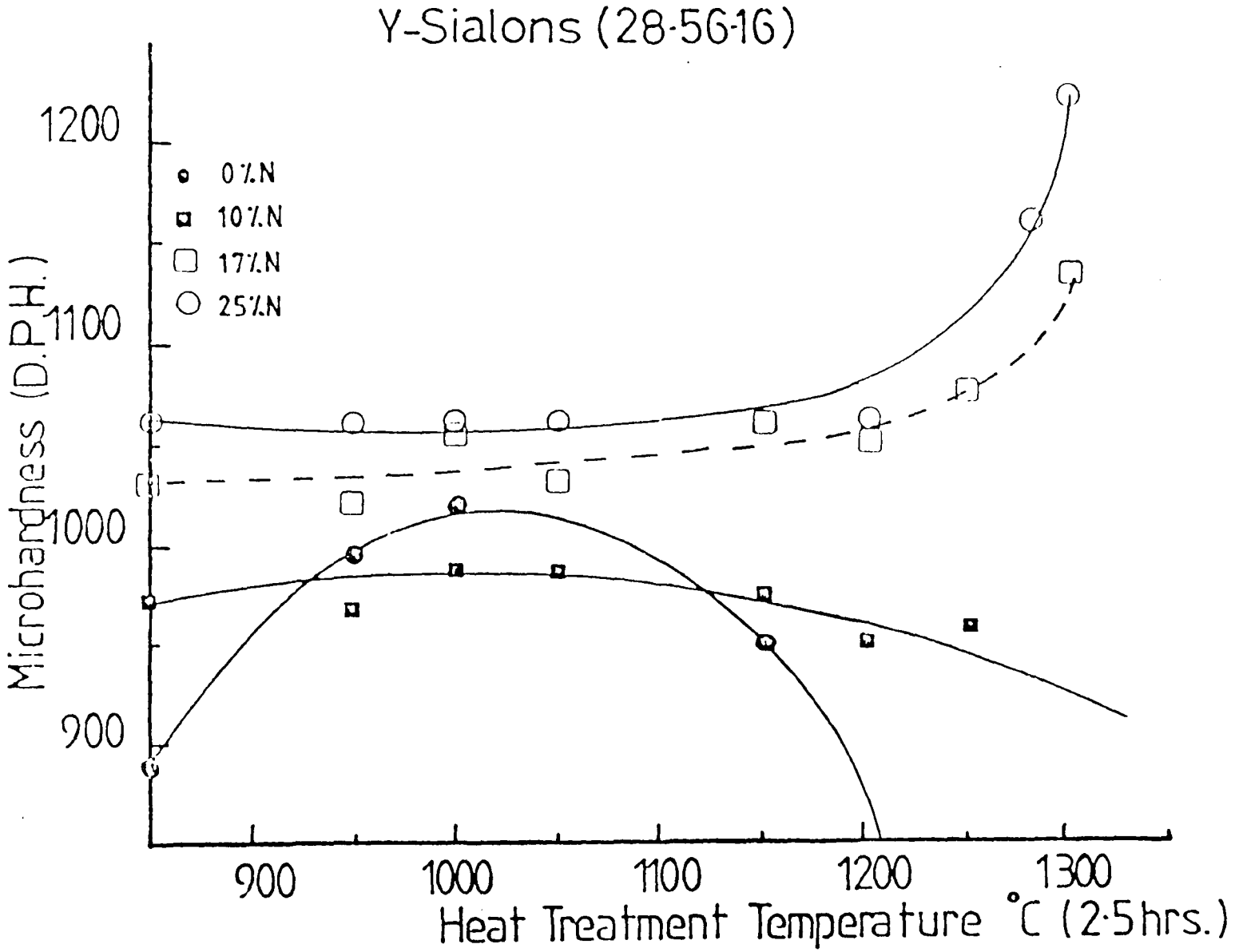

FIGURE 36 Effect of heat treatment temperature (2.5 hours annealing) on microhardness of Y-sialon glasses (standard cation composition).

silicate ($Y_2Si_2O_7$) with N-YAM phase ($Y_4Si_2N_2O_7$) appearing at higher nitrogen levels. Variation of microhardness after single-stage heat-treatment is shown in figure 36 where more positive trends are evident than those obtained in the Nd-sialon system after single-stage heat-treatments.

The first obvious trend is that hardness increases significantly in the 0%N samples after single-stage heat-treatment at 950°C and 1000°C. No result is shown for heat-treatment between 1000°C and 1150°C where hardness again decreases. The reason why this increase was not observed in the Nd-glasses with 0e/o nitrogen may be explained by referring to the DTA traces for glasses in both systems (figures 22 and 23). Crystallization is seen to take place very rapidly below 1100°C in the Y-glass with 0e/oN as evidenced by the sharp, highly-exothermic peak (figure 22). This glass displays a marked tendency to crystallize and this same tendency is not evident in the Nd-glass with 0%N, as indicated from the DTA trace (figure 23) and the absence of any increase in hardness (figure 29). Figure 37 shows a scanning electron micrograph of this glass after annealing at 1050°C for 2.5 hours. The densely-packed small crystals observed are γ-$Y_2Si_2O_7$.

Although a higher value of hardness is expected in heat-treated samples containing nitrogen, because of the formation of a more rigid glass network, crystallization in nitrogen-containing glasses is also inhibited because of the presence of nitrogen. Thus, the expected hardness increase in these samples may take longer to develop compared with oxide samples. The improved hardness values for the oxide samples are superior to those of samples containing 10e/o nitrogen that have been subjected to similar single-stage heat-treatments. However, when a nitrogen level of 17e/o is reached, property improvements due to the more tightly bonded structure ensure that the minimum hardness values for these samples are always greater than those of oxide samples after single-stage heat-treatments.

Single stage heat-treatments of samples containing 17 and 25e/o nitrogen result in only small improvements in hardness when the heat-treatment temperature is below 1200°C. However, after heat-treatment above this temperature, hardness in the 17e/o nitrogen samples is seen to increase from 1050 to 1135 DPH when heat-treated at 1300°C (30°C below Tc). The 25e/o nitrogen samples show an even more significant increase from 1060 to 1220 DPH when heat-treated at 1300°C.

Scanning electron micrographs of the 17e/oN samples with improved properties are shown in figure 38. Figure 38(a) shows the microstructure of a 17e/o nitrogen sample heat-treated at 1280°C for 2.5 hours. Two types of crystals are apparent in a

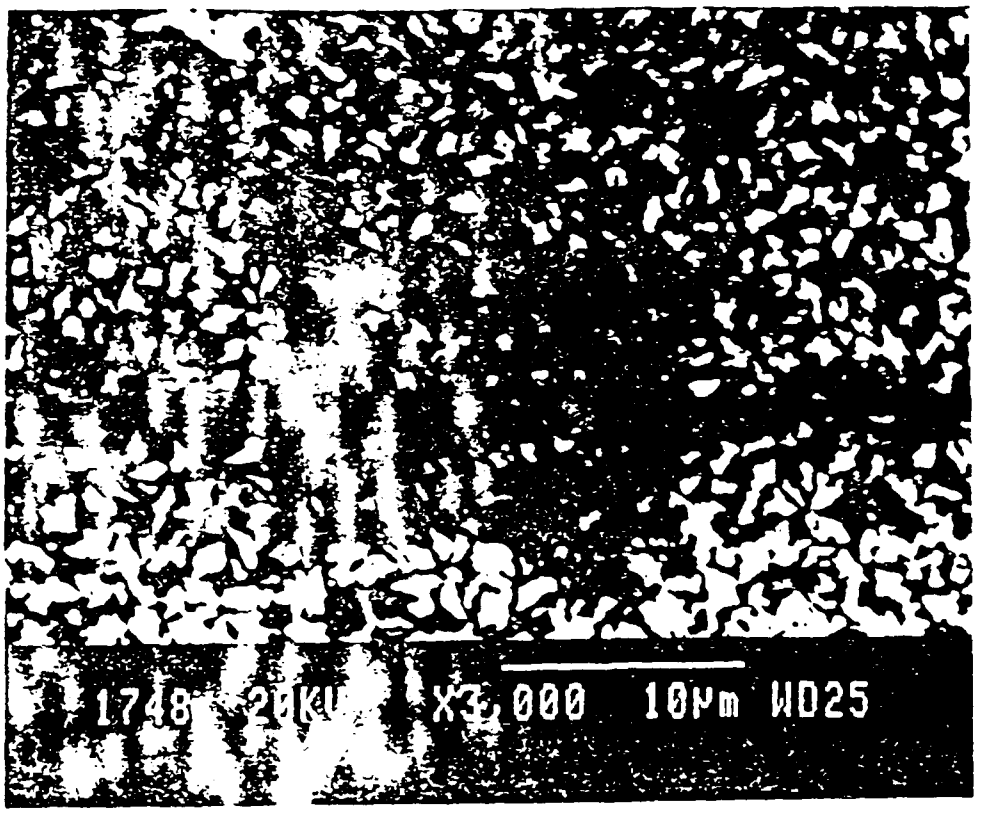

FIGURE 37 Scanning electron micrograph of Y-sialon standard composition (0 e/cN) after heat-treatment for 2.5 hours at 1050°C.

glassy background. The larger white crystals are $Y_2Si_2O_7$ and the smaller needle like black crystals which are just about visible are probably silicon oxynitride (Si_2N_2O). Figure 38(b) shows a micrograph of the same sample heat-treated at 20°C higher ie 1300°C for 2.5 hours and here more extensive crystal formationis apparent with the crystals of $Y_2Si_2O_7$ becoming more elongated and appearing to have a certain orientation. Figure 38(c) is a micrograph of a sample containing 25e/o nitrogen after heat-treatment at 1300°C. Tightly packed crystals, which may be N-apatite ($Y_5N(SiO_4)_3$), are seen against a dark background which may be a secondary glassy phase.

Subjecting the Y-sialon glasses to two-stage heat-treatments of 2 x 2.5 hours resulted in samples with much improved properties. Results of X-ray analysis of samples after 2-stage and long term heat-treatments are listed in table 6. Again the main crystalline phase detected is $Y_2Si_2O_7$ in different polymorphic forms. Variation of hardness in these samples after double heat-treatment is shown in figure 39. Again samples were subjected to similar double heat-treatments to those used on Nd-sialon samples and the relationship between Tg, Tc and all of the heat-treatment temperatures used, for samples of different nitrogen contents, are shown in table 7.

Again, in this system, significant improvements in microhardness are observed after double heat-treatments and in every case, hardness values increase well above those recorded for the as-quenched glasses. In the 0%N sample the nucleation temperature of Tg + 50 produces an improved microhardness at all crystallization temperatures, with a distinct maximum when crystallization at Tc itself. The sharp crystallization peak characteristic of this sample indicates very rapid crystallization which is not observed in nitrogen-containing glasses. A nucleation temperature of Tg +90 does not produce any further improvements in properties in these samples. It should be noted also that the maximum hardness value achieved by double heat-treatment of this oxide glass is far superior to the maximum value achieved through single-stage heat-treatment. This is also the case for all of the nitrogen containing glasses, thus, demonstrating the advantages of double stage heat-treatments.

The maximum hardness value obtained in the 10e/oN samples occurs after heat-treatment at Tg+50 followed by Tc-40, and this maximum is more than equaled by the maximum hardness value achieved in the 0e/oN samples. Thus, the improvement in properties due to increased cross-linking as a result of nitrogen incorporation, does not compensate for the slower development of properties due to inhibited crystallization,

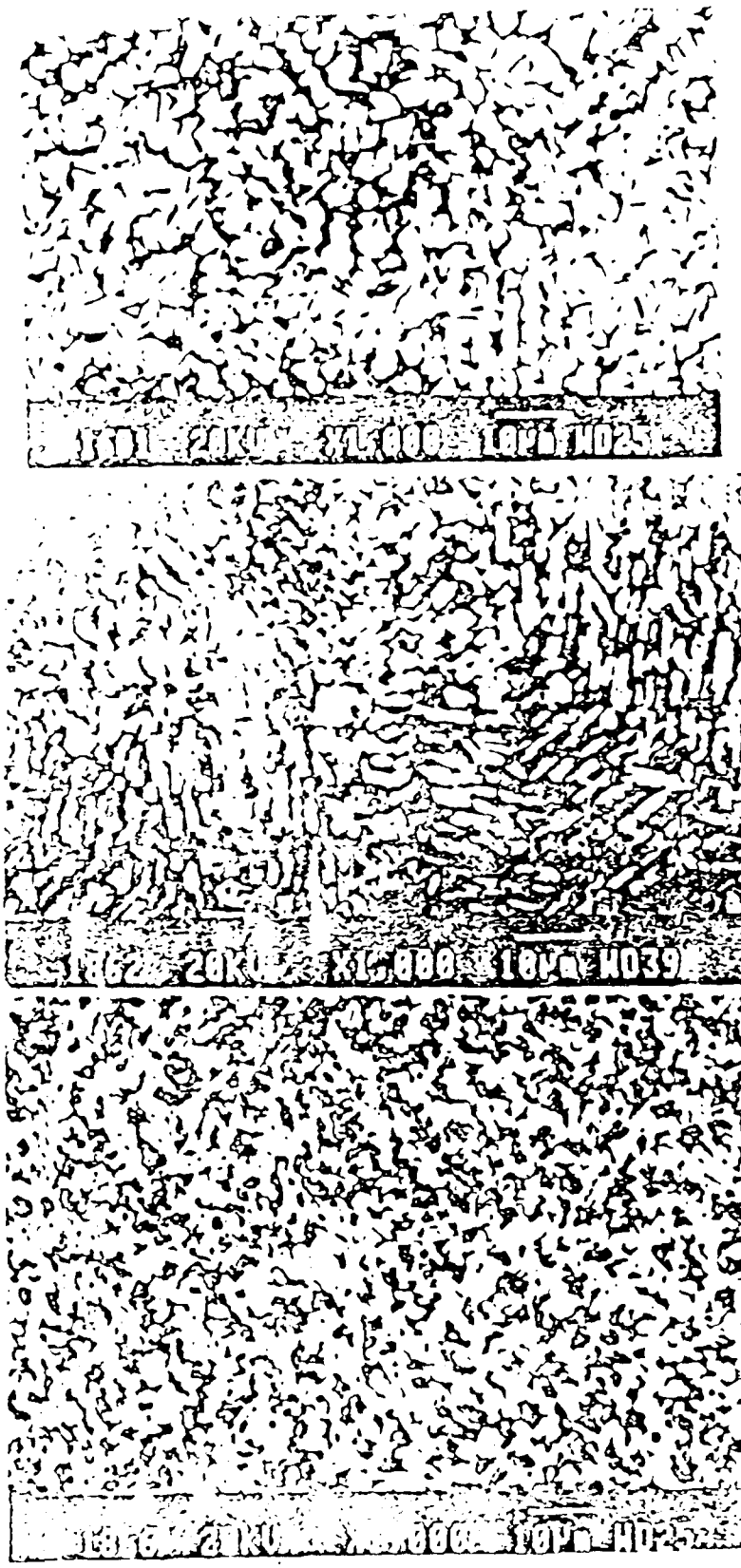

(a)

(b)

(c)

FIGURE 38 Scanning electron micrographs of Y-sialon glasses (standard composition) after heat-treatment for 2.5 hours (a) 17e/oN at 1280°C, (b) 17e/oN at 1300°C, (c) 25e/oN at 1300°C.

TABLE 9

Phase assemblages of Y-sialon glass-ceramics after double-stage heat treatments (2.5 hours + 2.5 hours) at various temperatures.

e/o Nitrogen	Heat Treatment Temperatures (°C) 1	2	Times (h)	Crystalline Phases detected
0	990	1030	2.5+2.5	γ-$Y_2Si_2O_7$
0	1000	1185	2.5+2.5	Keivilite
0	1000	1260		γ-$Y_2Si_2O_7$+$Y_8Si_4N_4O_{11}$
10	1000	1280	2.5+2.5	Keivilite
	1000	1185	" "	δ-$Y_2Si_2O_7$
	1020	1210	" "	γ-$Y_2Si_2O_7$
	1050		24	γ-$Y_2Si_2O_7$
17	1000	1185	2.5+2.5	γ-$Y_2Si_2O_7$
	1000	1280	" "	γ-$Y_2Si_2O_7$+
	1035	1265	" "	δ-$Y_2Si_2O_7$+SiO_2
	1075	1285	" "	Keivilite+ -$Y_2Si_2O_7$+SiO_2
	1300		24	Keivilite
25	1055	1200	2.5+2.5	γ-$Y_2Si_2O_7$
	1300		24	γ-$Y_2Si_2O_7$+$Al_5Y_3O_{12}$

Keivilite - β-$Y_2Si_2O_7$

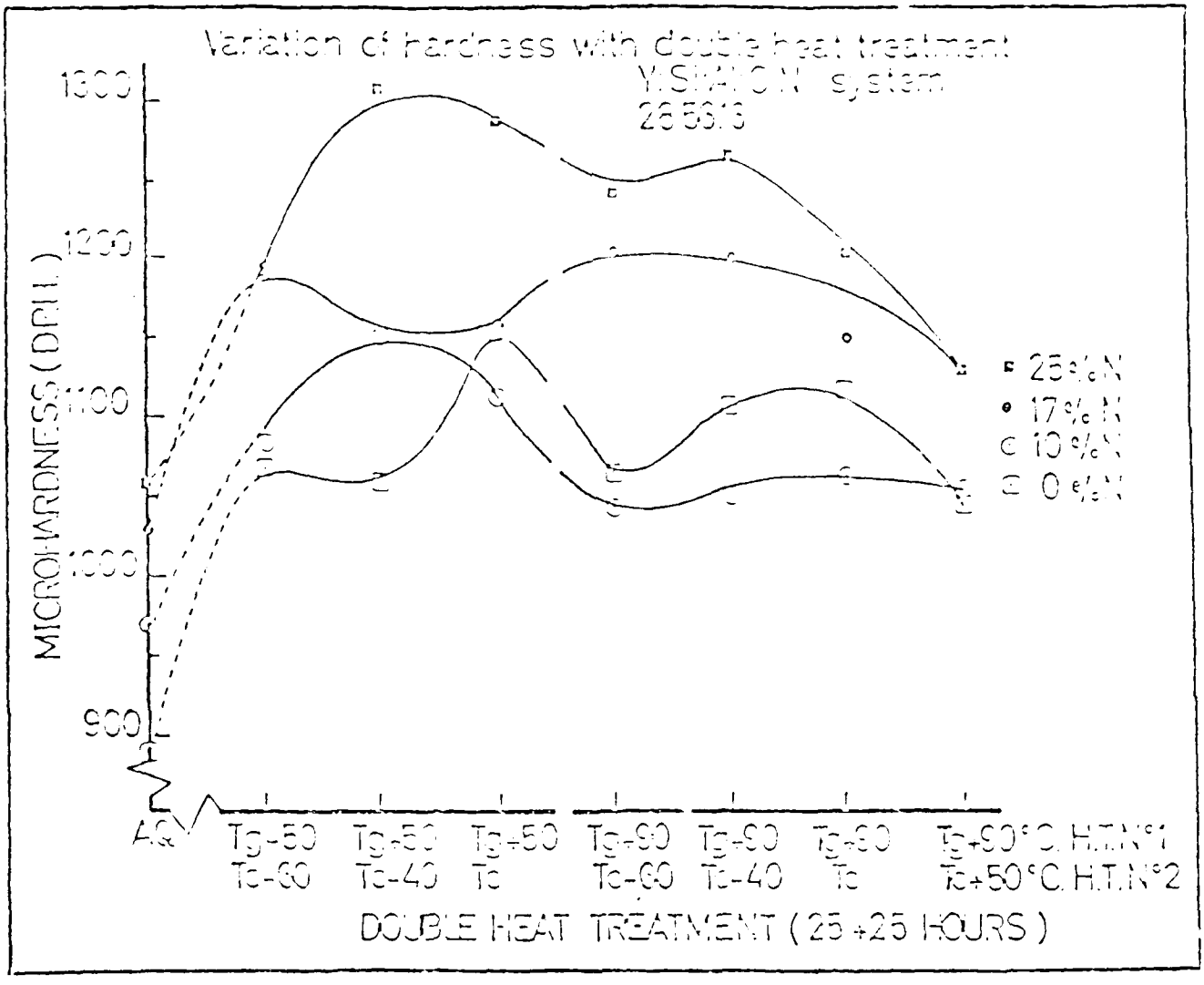

FIGURE 39 Effect of double-stage heat-treatments on microhardness of Y-sialon glasses (standard cation composition).

TABLE 7

Relationship between Tg, Tc and the heat-treatment temperatures used during 2-stage heat-treatments of Y-sialon glasses.

Code	Relationship to Tg and Tc	Heat-Treatment Temperatures (°C) 0e/cN	10e/cN	17e/cN	25e/cN
A	Tg+50, Tc-60	990÷1030	1020÷1190	1035÷1265	1055÷1180
B	Tg+50, Tc-40	990÷1050	1020÷1210	1035÷1285	1055÷1200
C	Tg+50, Tc	990÷1090	1020÷1250	1035÷1325	1055÷1240
D	Tg+90, Tc-60	1030÷1030	1060÷1190	1075÷1265	1095÷1180
E	Tg+90, Tc-40	1030÷1050	1060÷1210	1075÷1285	1095÷1200
F	Tg+90, Tc	1030÷1090	1060÷1250	1075÷1325	1095÷1240
G	Tg+90, Tc+50	1030÷1140	1060÷1300	1075÷1375	1095÷1300

until over 10e/o nitrogen is incorporated into glasses in this system. In the 17e/o nitrogen samples, highest hardness values are recorded following heat-treatment at Tg+90 and Tc-60 & Tc-40, which is a higher nucleation temperature than expected. In samples containing 25e/o nitrogen the highest hardness value recorded is following the same heat-treatment schedule as used for the 10e/o nitrogen sample to obtain maximum hardness, i.e. at Tg+50 followed by Tc-40. Thus, as in the Nd-sialon system, a double heat-treatment of 2.5 hours at Tg+50 followed by another 2.5 hours at Tc-40, appears to be the optimum heat-treatment process to produce highest hardness glass-ceramics.

Figures 40(a-c) shows scanning electron micrographs of Y-sialon-glass-ceramics containing 17e/o nitrogen after two-stage heat treatments. Figure 40(a) shows the sample after heat-treatment at Tg+50 and Tc-60, and reveals the typical microstructure of the 17e/o nitrogen-containing samples, after heat-treatment. In this sample a good distribution of white crystals of $Y_2Si_2O_7$ is seen in a grey background matrix. Dark needle-like crystals are also seen which are probably of SiO_2. Electron probe microanalysis of the crystals aided in their identification and figures 41 and 42 show results of crystal microanalysis. The white crystals are high in Si and Y content while containing little or no Al. Thsi confirms X-ray diffraction analysis which indicates that $Y_2Si_2O_7$ is the main crystallizing phase. Microanalysis of the black needle-like crystals was more difficult because of their size but they appear to contain mainly Si, with the Al peak probably from the background. Thus, it can be concluded that these crystals are Si_2N_2O with possible substitution of Si by Al. Figure 40(b) shows a micrograph of the 17e/o nitrogen sample after heat-treatment at a higher crystallization temperature. In this case while crystal numbers are lower, crystal growth is more advanced and more of the softer background glass matrix remains uncrystallized. Again in figure 40(c) which shows the microstructure of a sample with the same composition, heat-treated at a higher crystallization temperature, it is obvious that the crystals of both species are much fewer and that their size is much greater with much of the background remaining uncrystallized. This leads to an undesirable microstructure with a lower than desirable hardness. From these observations it can be concluded that controlled crystallization of the $Y_2Si_2O_7$ phase leads to improved properties and that samples having large areas of uncrystallized matrix do not exhibit optimum properties.

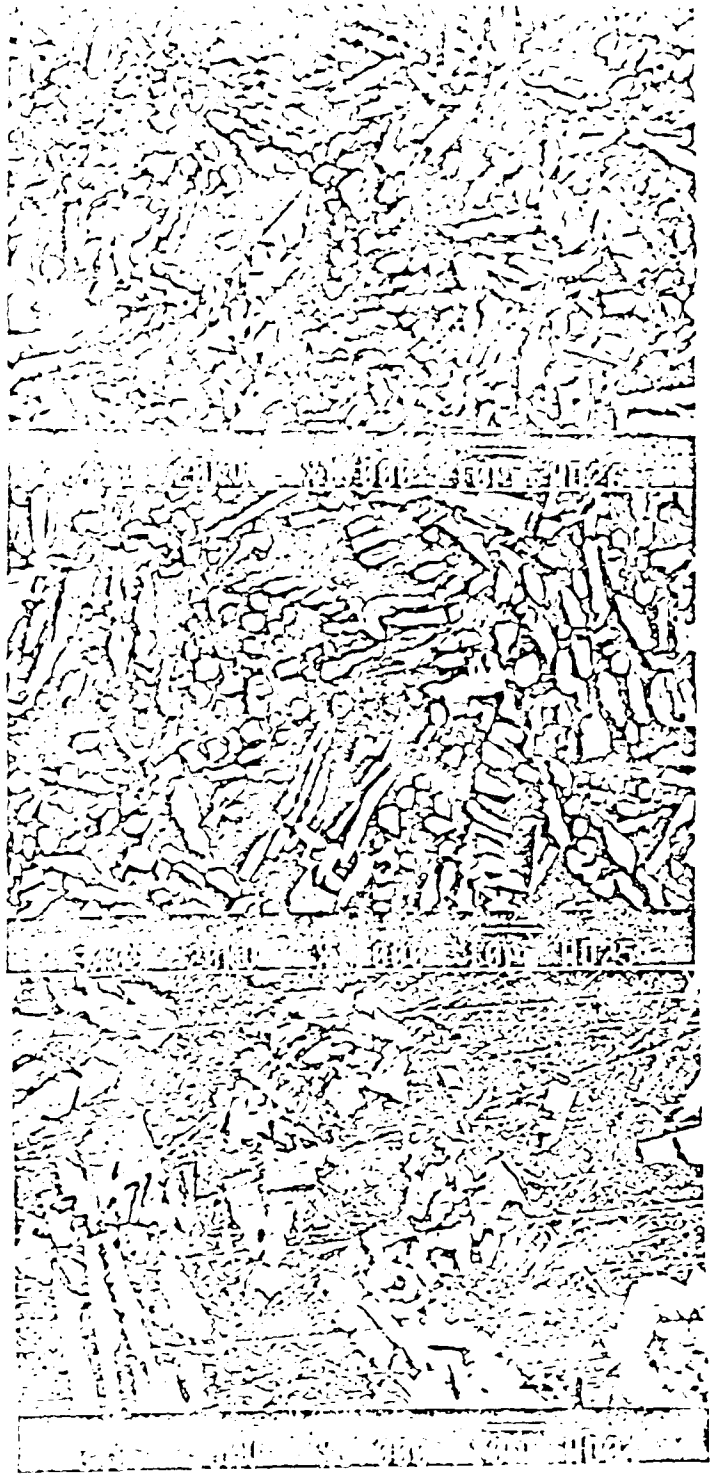

FIGURE 10 Scanning electron micrographs of Y-sialon glass-ceramics containing 17e/oN after 2-stage heat-treatment (2.5 + 2.5 hours) at (a) Tg+50 and Tc-60, (b) Tg+50 and Tc-40, (c) Tg-50 and Tc.

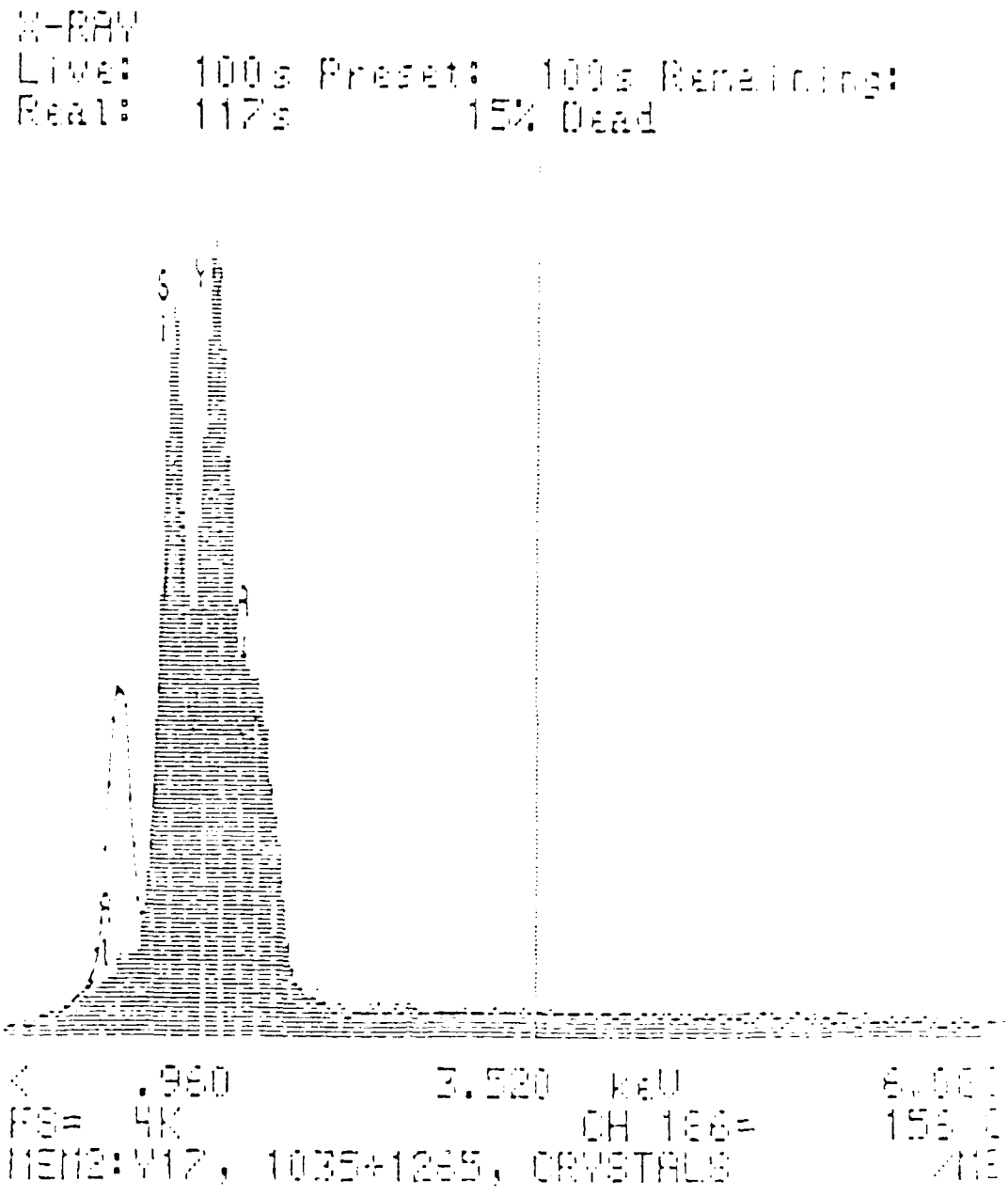

FIGURE 41 X-ray probe analysis of white crystals in Y-station glass-ceramic (17e/cN) heat-treated at 1035°C + 1265°C (2.5 hrs. + 2.5 hrs.).

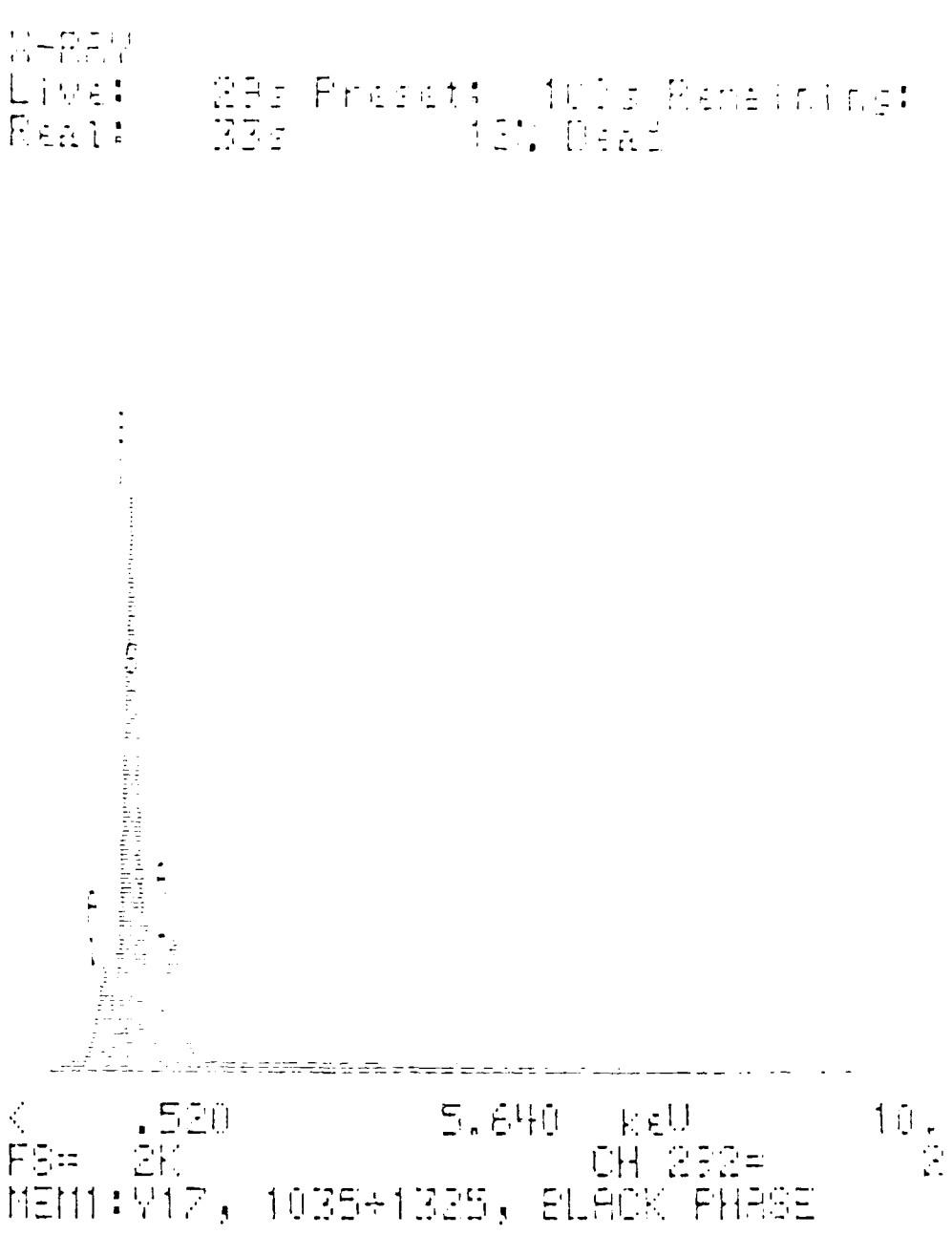

FIGURE 42 X-ray probe analysis of dark needle-like crystals in Y-sialon glass-ceramic (17e/oN) heat-treated at 1035°C + 1325°C (2.5 hrs. + 2.5 hrs.).

Figure 43 shows a scanning electron micrograph of the same sample containing 17e/o nitrogen after heat treatment at Tg+90 followed by Tc-60. This shows clusters of small $Y_2Si_2O_7$ crystals and crystals of Si_2N_2O (possibly O'-sialon) giving a well crystallised matrix and a better hardness value for this sample.

5.8 Effect of Nd-dopant on properties of Y-sialon glasses

Figure 44 shows the results of differential thermal analysis (DTA) on Y-Nd-sialon glasses of standard composition where the three upper curves show the effects of substituting Nd for Y at a constant 17e/oN. The two lower curves are for glasses with 5e/o Nd and 23e/o Y and show the effect of nitrogen substitution in the glasses. As observed previously, with 0e/oN, both Tg and Tc are at lower temperatures and the crystallization peak is sharper and more intense than for glasses containing nitrogen.

Optical absorption characteristics for these glasses have been investigated in the range 190-900 nm (UV-visible). Figure 45 compares the absorption spectrum for a Y-sialon glass doped with 0.2 e/oNd with a soda-lime-silicate glass and with quartz SiO_2 glass. With the Y-sialon glass, the absorption edge occurs at a lower wavelength (245nm) than the silicate glass. Figure 46 shows the effect of Nd doping on absorption in Y-sialon glasses. As Nd content increases (constant N content), the absorption peaks across the spectrum increase in intensity and the UV absorption edge shifts to higher wavelength (370 nm).

Figure 47 shows the effects of heat treatments at 900°C and 1000°C on absorption characteristics of the low-doped glass (17e/oN, standard composition with 0.2e/o Nd). Although no crystalline phases are observed, the glasses appear darker as heat-treatment temperature is increased and this is reflected in an increase in absorptivity as annealing temperature is increased.

6. CONCLUSIONS

Fully amorphous glasses can be prepared easily in large batches in Mg-Si-RE-O-N and RE-Si-Al-O-N systems with a range of nitrogen contents. For constant cation ratio glasses, nitrogen increases the glass transition, microhardness and viscosity and also inhibits crystallization. Single state (2.5 hours) and double-stage (2.5 + 2.5 hours) heat-treatments have been

FIGURE 43 Scanning electron micrograph of Y-sialon glass-ceramic containing 17e/oN after 2-stage heat treatment at Tg+90 and Tc-60 (2.5 + 2.5 hours).

DTA traces of Nd:Y:SIALON glasses

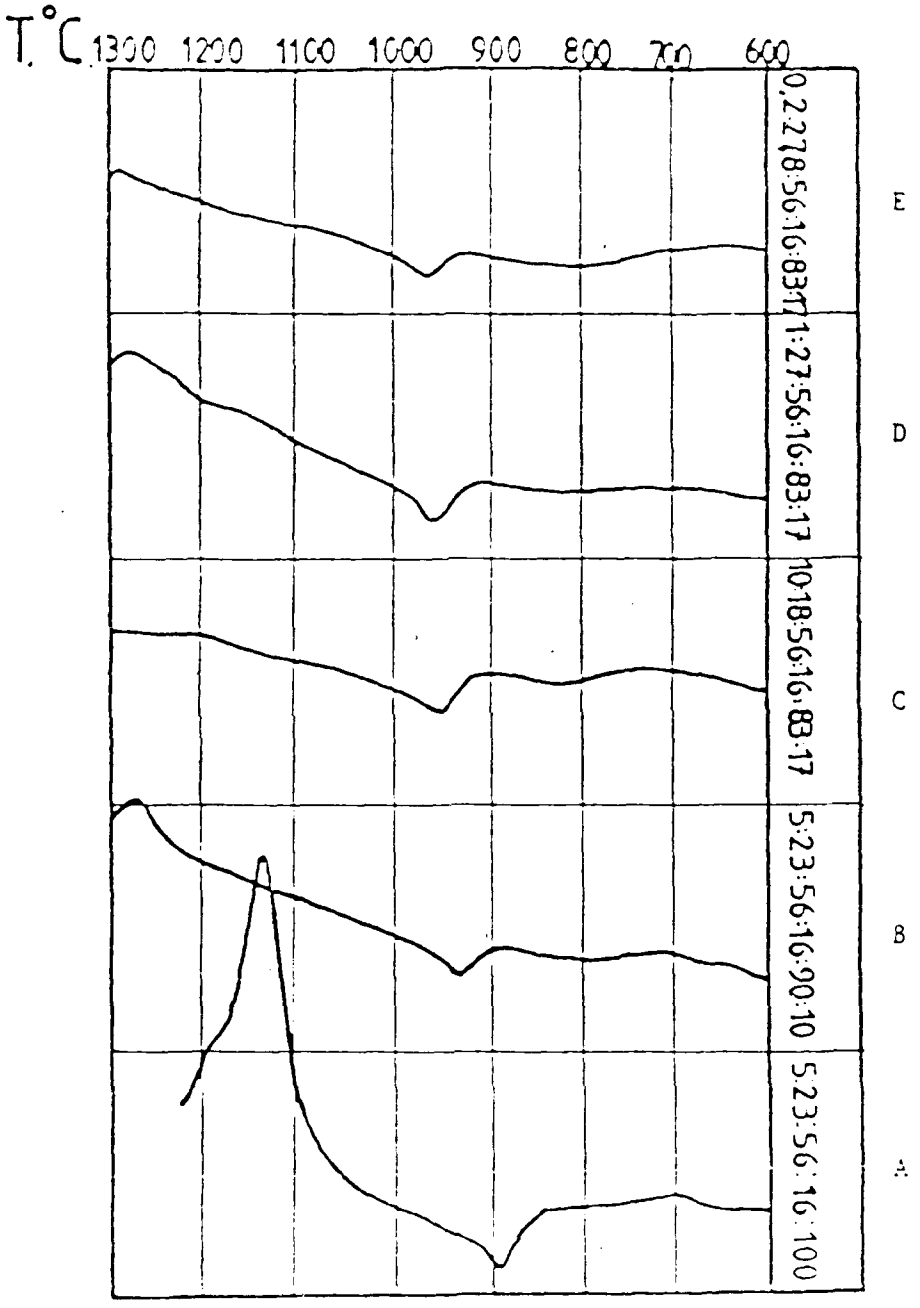

FIGURE 44 DTA traces for Y-Nd-sialon glasses showing effect of Nd dopant and N on Tg and Tc.

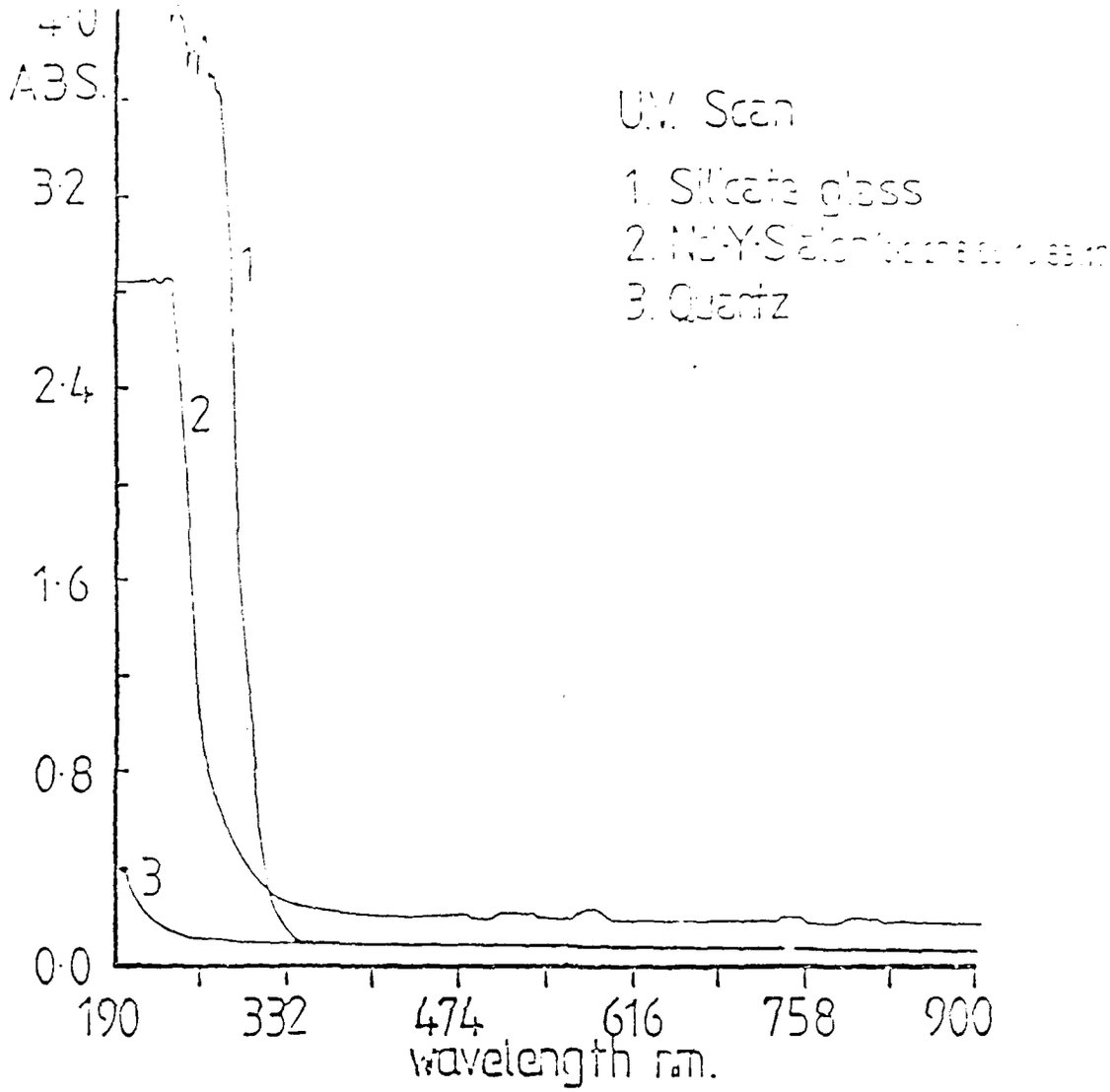

FIGURE 45 Absorption spectra (UV-vis.) for Y-sialon glass (0.2e/o'd) compared with silicate and quartz glasses.

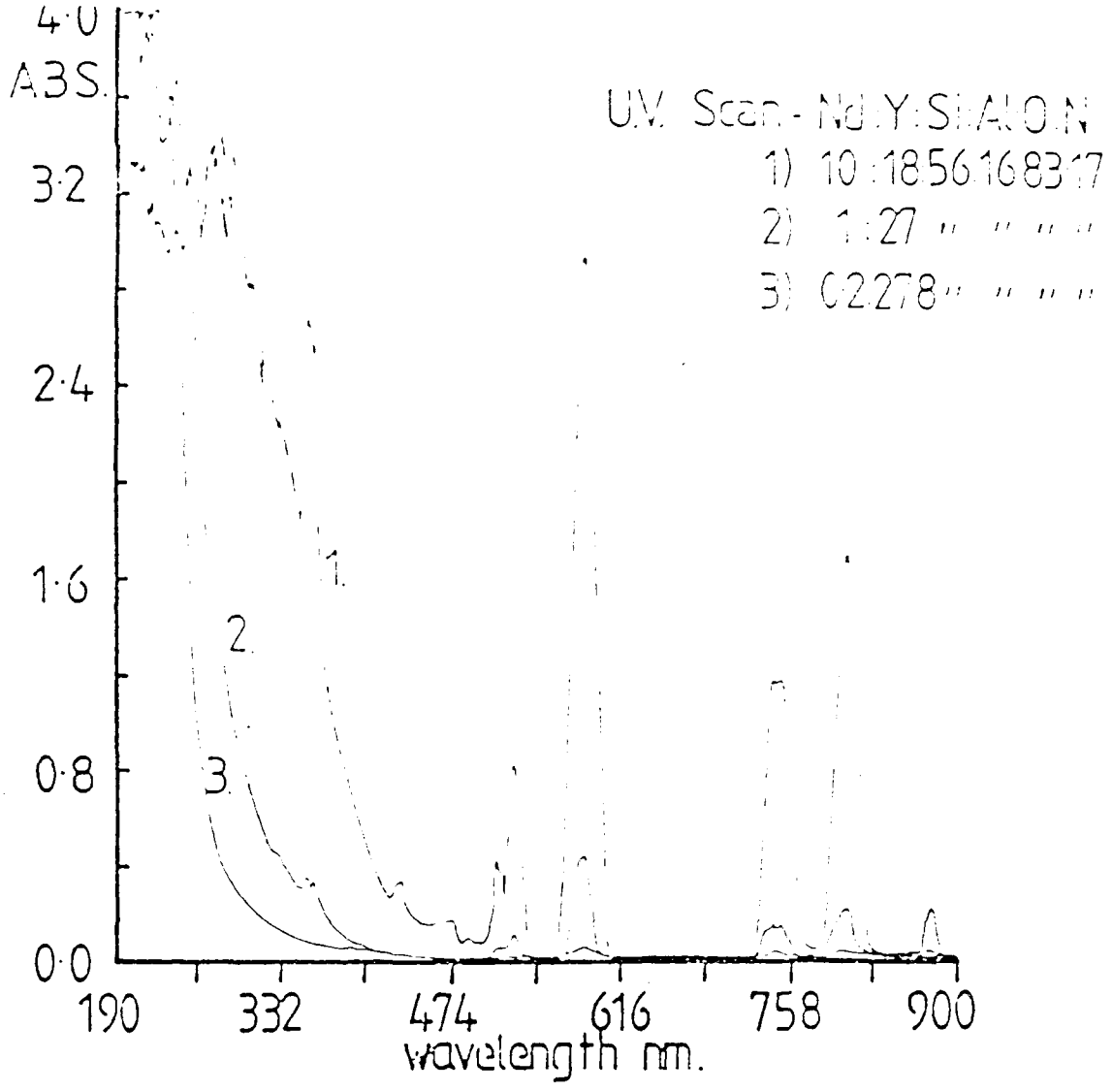

FIGURE 46 Effect of Nd-doping on UV-vis. absorption characteristics of Y-sialon glasses (standard composition, 17e/oN).

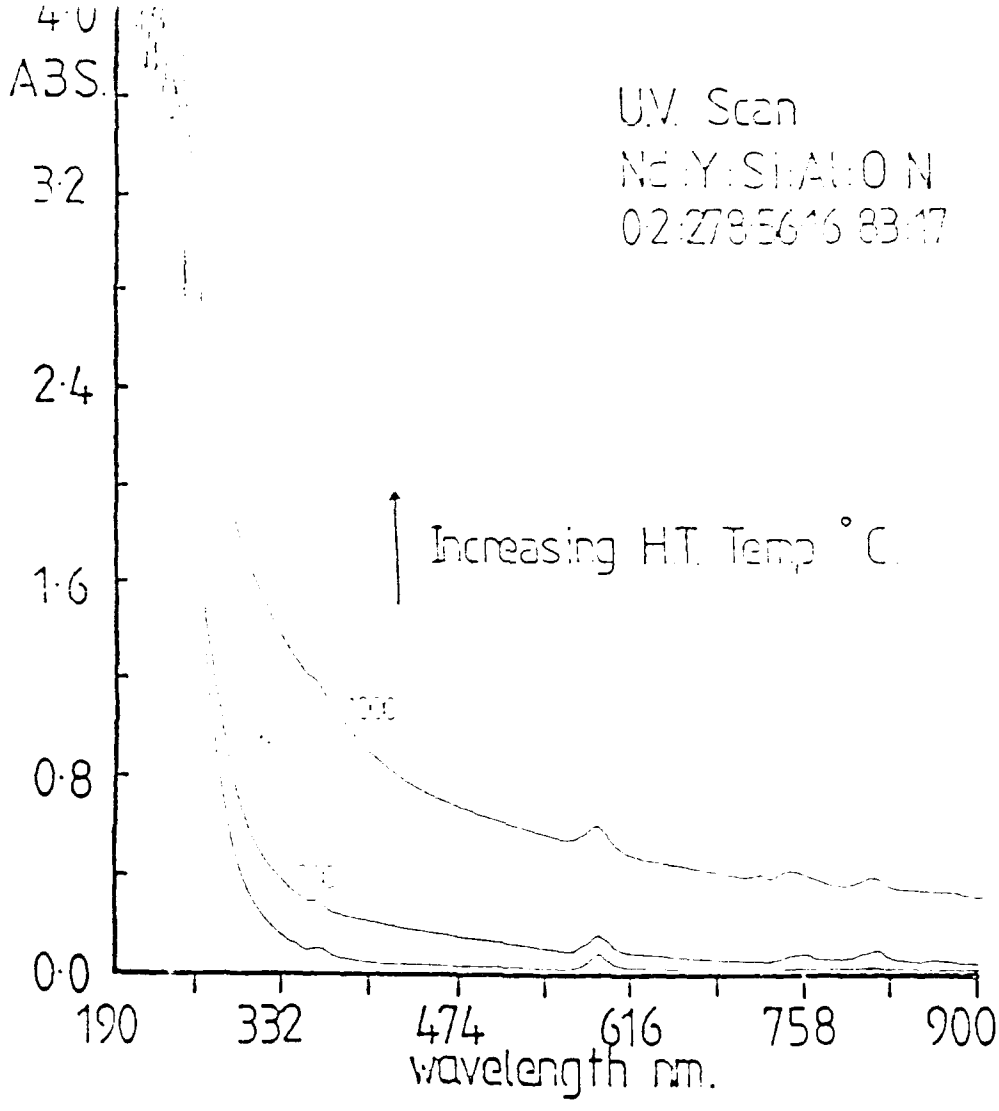

FIGURE 47 Effect of heat-treatment temperature on UV-vis. absorption characteristics of Y-sialon glass (17e/oN, standard composition with 0.2 e/oNd).

carried out on Nd- and Y-sialon glasses to transform them into fine-grained glass-ceramics. As evidenced by microhardness measurements, single stage heat-treatments of Nd-sialon glasses do not improve properties, while in the case of Y-sialon glasses, property improvements were observed in the oxide glass, when heat-treatment temperatures less than 1150°C were used, and in the 17e/o and 25e/o nitrogen samples when heat-treatment temperatures between 1250 and 1300°C were used.

Double stage heat-treatments produced improved properties in all samples in both the Nd- and Y-sialon systems. In nitrogen-containing samples of the Nd-sialon system the optimum heat-treatment schedule as evidenced by increases in microhardness and SEM analysis is 2.5 hours each at Tg+50 and Tc-40. This schedule was also found to be the optimum for both the 10e/o N and 25e/o N samples, in the Y-sialon system. In the case of Y-sialon samples containing 17e/o N the optimum heat-treatment was found to be Tg+90 folowed by Tc-60.

Glasses doped with Nd ions show a series of distinct absorption peaks in the visible region of the UV/Visible spectrum. The intensity of these peaks varies in proportion to the level of Nd ions present. Subjecting these glasses to different heat-treatments also varies absorption intensity. Nitrogen and Nd ion concentration and heat-treatment also affect the position of the UV absorption edge in the spectra of these glasses.

7. LITERATURE CITED

1. Jack, K.H., J. Mater. Sci. (1976) 11, 1135.
2. Jack, K.H., "Nitrogen Ceramics", ed. Riley F.L., Noordhoff, Leyden, (1977) p. 257.
3. Shillito, K.R., Wills, R.R. and Bennett, R.E., J. Am. Ceram. Soc. (1978) 61, 537.
4. Loehman, R.E., J. Am. Ceram. Soc. (1979) 62, 491.
5. Loehman, R.E., J. Non-cryst. Solids (1980) 42, 433.
6. Drew, R.A.L., Hampshire, S. and Jack, K.H. "Special Ceramics 7", ed. Taylor, D.E. and Popper, P., Proc. Brit. Ceram. Soc. (1981) 31, 119.
7. Messier D.R. and Broz, A., J. Am. Ceram. Soc. (1982) 65, C-124.
8. Drew, R.A.L., Hampshire, S. and Jack, K.H. "Progress in Nitrogen Ceramics" ed. Riley, F.L., Martinus Nijhoff, The Hague (1983) p. 323.
9. Drew, R.A.L., Hampshire, S. and Jack, K.H. "Ceramic Components for Engines", ed. Somiya, S., Kanai, E and Ando, K., Reidel Pub. Co. dordrecht (1984) p.394.
10. Hampshire, S., Drew, R.A.L. and Jack, K.H., J. Am. Ceram. Soc. (1984) 67, C46.
11. Elmer, T.H. and Nordberg, M.E., J. Am. Ceram. Soc. (1967) 50, 275.
12. Harding, F.L. and Ryder, R.J., Glass Tech. (1970) 11, 54.
13. Shaw, T.M. and Thomas, G.R. "Progress in Nitrogen Ceramics", ed. Riley, F.L., Martinus Nijhoff, The Hague (1983) p. 331.
14. Chyung, K. and Wusirika, R.R., U.S. Patent 4,070,198, Jan. 1978.
15. Mulfinger, H.O., J. Am. Ceram. Soc. (1966) 49, 462.
16. Kelen, T. and Mulfinger, H.O., Glasstechn. Ber. (1968) 41, 230.
17. Davies, M.W. and Meherali, S.G., Metall. Trans. (1971) 2, 2729.
18. Dancy, E.A. & Janssen, D., Canad. Met. Quart. (1976) 15, (2) 103.
19. Drew, P. & Lewis, M.H. J. Mater. Sci. (1974) 9, 261.
20. Lewis, M.H., Powell, B.D., Drew, P., Lumby, R.J., North, B., & Taylor, A.J. J. Mater. Sci. (1977) 12, 61.
21. Rae, A.W.J.M., Thompson, D.P. & Jack, K.H. "Ceramics for high performance applications II", ed. Burke, J.J., Lence, E.N. & Katz, R.N., Proc. 5th Army. Mat. Tech. Conf., Brook Hill Pub. Co., Chestnut Hill, Mass. (1977) p. 1039.
22. Hampshire, S. and Jack, K.H. "Special Ceramics 7", ed. Taylor, D.E. and Popper, P , Proc. Brit. Ceram. Soc. (1981) 31, 38.
23. Jack, K.H., "Non-oxide Technical and Engineering Ceramics", ed. Hampshire, S. Elsevier - Applied Science, Barking, England (1986) p.1.
24. Janecke, E., Z. Anorg. Chem. (1907) 53, 319.
25. Hampshire, S., Drew, R.A.L. and Jack, K.H., Phys. & Chem. Glass. (1985) 26, (5).
26. Schrimp, C. and Frischat, G.H., J. Non-Cryst. Sol., (1983) 56, (1-3) 153.

27. Brow, R.K., and Pantano, G.G., J. Am. Ceram. Soc. (1984) 67, (4) C72.
28. Rand, M.J. & Roberts, J.F., J. Electro-chem. Soc. (1973) 120 (3) 446.
29. Abromovici, R, Ish-Shalom, M., Ind. Eng. Chem. Prod. Res. Dev. (1985) 24, 586.
30. Ahn, C.C. and Thomas G., J. Am. Ceram. Soc., (1982) 65, (11), C185.
31. Winder, S.M. and Lewis, M.H., J. Mater. Sci. Lett. (1985) 4, 241.
32. Lewis, M.H., and Leng-Ward, G., Mater. Sci. Eng. (1985) 71, 101.
33. Lewis, M.H., Leng-Ward, G. and Wild, S., J. Mater. Sci. (1986) 21, 1647.
34. Drew, R.A.L. Research Reports in Materials Science, (ed. Evans, P.) Series one, No. 2, Parthenon Press, England. (1986).

END